Investigation of exotic bound systems with WASA-at-COSY and SIDDHARTA-2 facilities

Magdalena Skurzok

Jagiellonian University in Cracow

Seminar of the Institute of Physics UW, Warsaw
21.11.2024

Istituto Nazionale di Fisica Nucleare
Laboratori Nazionali di Frascati

JÜLICH Forschungszentrum

UNIWERSYTET JAGIELLOŃSKI W KRAKOWIE

Introduction – exotic systems

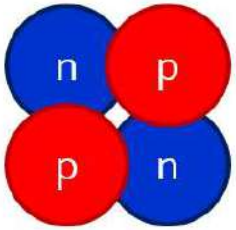

Classical nucleus
bound system of nucleons

„Exotic" systems

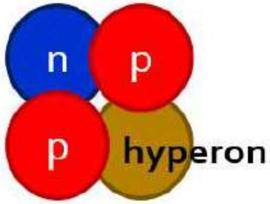

Hypernucleus
bound system of nucleons and hyperon (Λ,Σ)

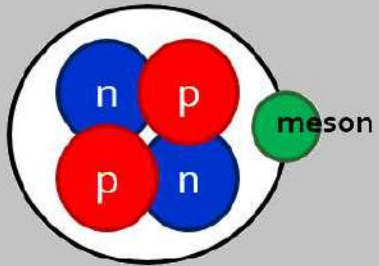

Mesic atom
charged meson orbiting around the nucleus (π)

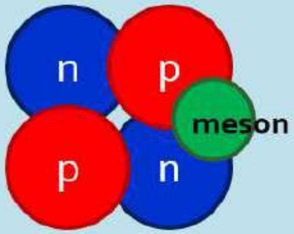

Mesic nucleus
bound system of nucleons and meson (K,η,η',ω,...)

Exotic systems - discovery

Hipernucleus

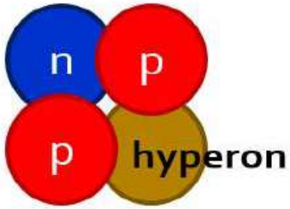

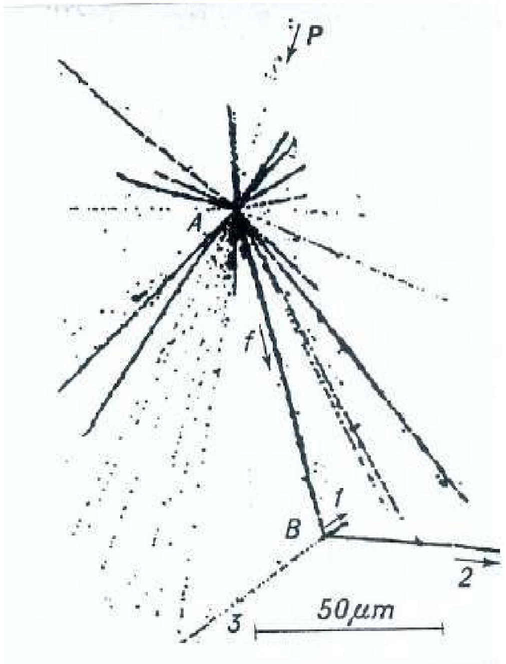

$\Lambda(uds)$, $\Sigma^-(dds)$
$t_\Lambda \backsim 10^{-10}s$
$\Lambda \rightarrow p\pi^-$
$\Lambda N \rightarrow NN$

M. Danysz and J. Pniewski. Phil. Mag. 44, 348 (1953)

Mesic atom

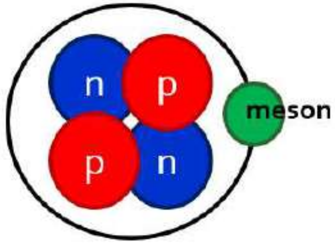

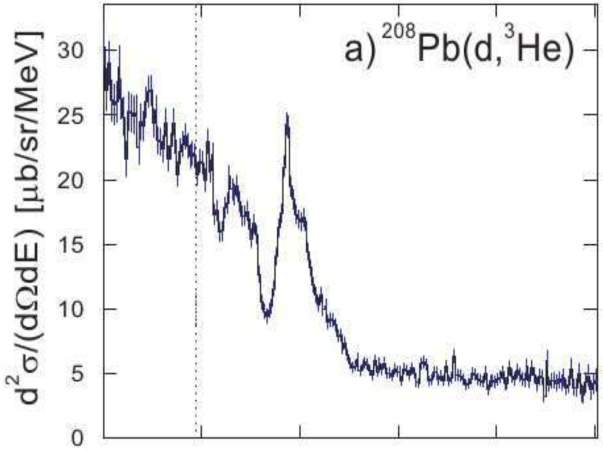

$(^{207}\text{Pb-}\pi^-)_{bound}$, 600MeV d beam
narrow peak below the ^{208}Pb(d,^{3}He) reaction threshold
B_π(2p)=5.3 MeV and Γ=0.5 MeV,
(π^-2p states with $p_{1/2}$ and $p_{3/2}$ neutron holes in ^{208}Pb)
Attractive Coulomb interaction between negatively charged pion and lead ion + strong interaction.

T. Yamazaki et al., Z. Phys. A355, 219 (1996)

Exotic systems - discovery

Kaonic bound state: kaonic cluster "K^-pp"

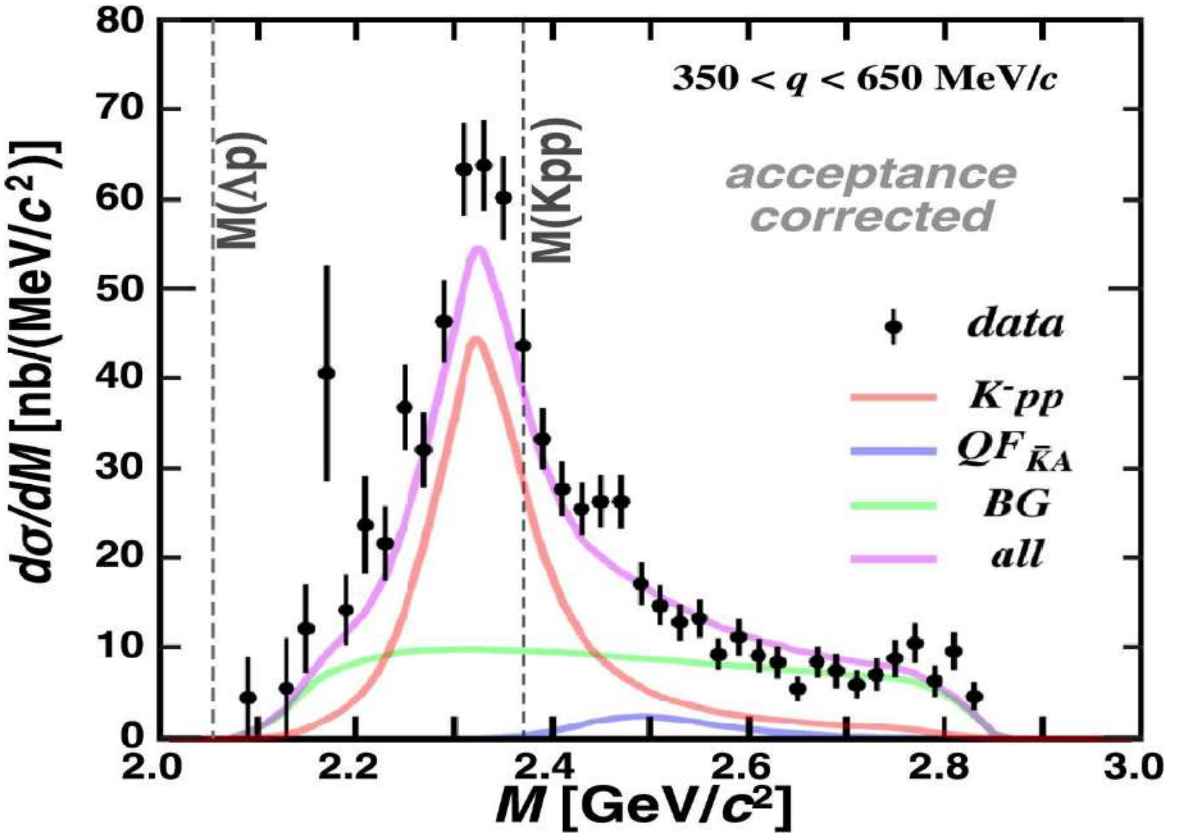

^{3}He$(K^-, \Lambda p)n$, 1GeV/c K^- beam
distinct peak in the Λp invariant mass spectrum of ^{3}He$(K^-, p)n$ below $m_{K^-} + 2m_p$
B_{K^-pp}=47±3(stat.)$^{+3}_{-6}$(syst.) MeV and Γ=0.5 MeV,

S. Ajimura et al. (J-PARC Collaboration), Phys. Lett B789, 620 (2019)

η-mesic bound state

η-mesic nucleus

^4He-η

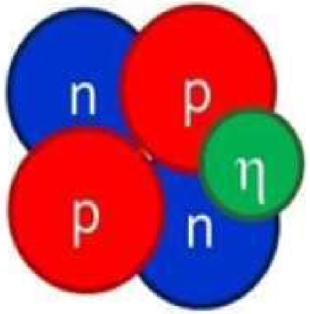

strong interaction

$$m_{bound} = m_{^4He} + m_\eta - B_s$$

meson η $u\bar{u}$, $d\bar{d}$, $s\bar{s}$

$$\eta_1 = \frac{1}{\sqrt{3}}(d\bar{d} + u\bar{u} + s\bar{s}),$$
$$\eta_8 = \frac{1}{\sqrt{6}}(d\bar{d} + u\bar{u} - 2s\bar{s})$$
$$|\eta> = \eta_8 cos\theta - \eta_1 sin\theta,\ \theta = \text{-}15.5^\circ \pm 1.3^\circ$$

m_η=547.86 MeV
Γ=1.31 keV
$\tau=10^{-18}$ s

main decay channels:

$\eta \to 2\gamma$	~39%
$\eta \to 3\pi^0$	~33%
$\eta \to \pi^0\pi^+\pi^-$	~23%

(PDG 2023)

$|Re(a_{\eta N})| > Im(a_{\eta N})$

attraction > absorption

η interaction with nucleon

For low energies η-N interaction dominated by N^*

<u>N^* resonance:</u> $m^*_N \approx$1535MeV $\Gamma \approx$150MeV $J^P = \frac{1}{2}^-$

Main decay channels:

$N^* \rightarrow \pi N$ (35-55 %)

$N^* \rightarrow \eta N$ (30-55 %)

$N^* \rightarrow \pi\pi N$ (1-10 %)

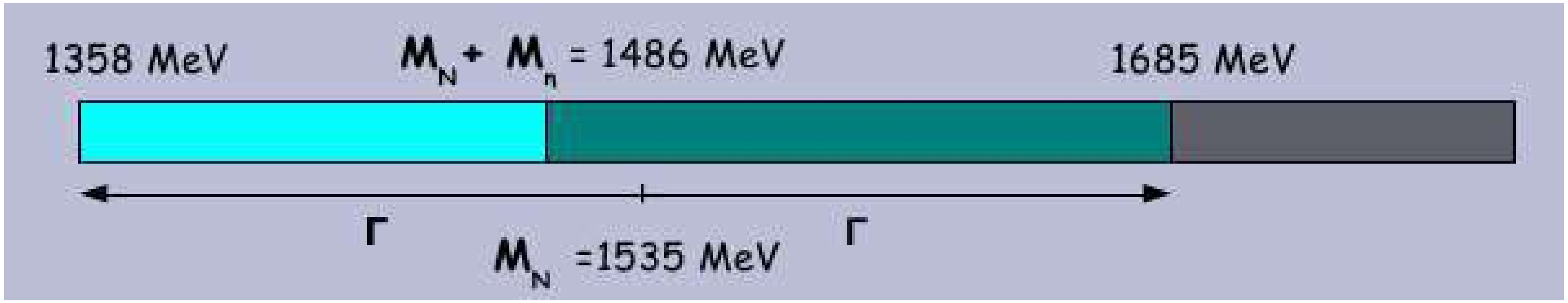

impossible to create the η beams $\Rightarrow$ η-N studies based on the investigation of ηN scattering amplitude for the processes like πN $\rightarrow$ ηN, γN $\rightarrow$ ηN $\Rightarrow$ N^* domination (coupled mainly to ηN and πN)

Coupled channel calculations $\Rightarrow$ fit to available experimental data

Attractive and strong interaction between η and nucleon

R. Bhalerao, L. C. Liu, Phys. Lett. B54, 685 (1985)

($a_{\eta N}$=0.28+i0.19 fm)

$\Downarrow$

Possible existence of η-mesic bound states postulated for atomic nuclei with A>12

Q. Haider, L. C. Liu, Phys. Lett. B172, 257 (1986)

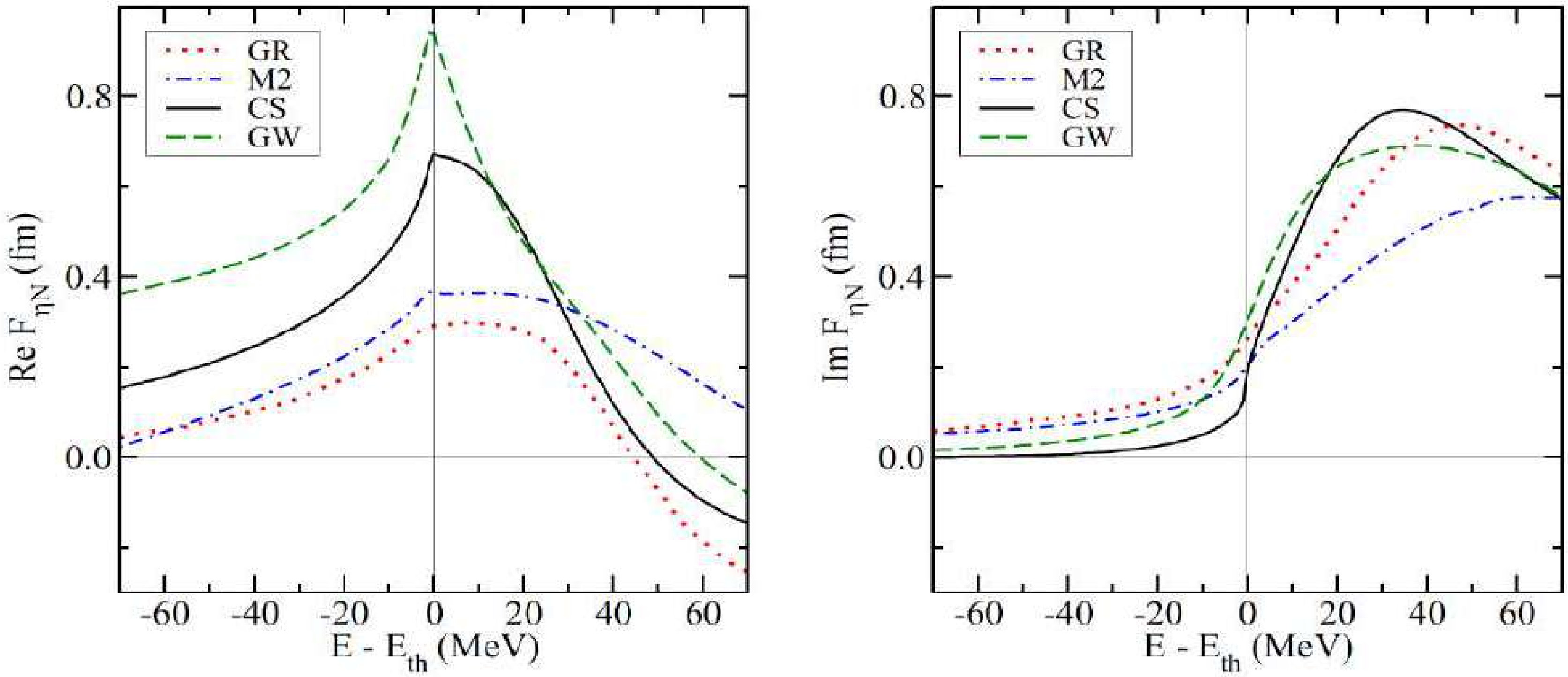

GW: A. M. Green and S. Wycech, Phys. Rev. C71, 014001 (2005).

CS: A. Cieply and S. Smejkal, Nucl. Phys. A919, 46 (2013).

M2: M. Mai, P. C. Bruns, U.-G. Meissner, Phys. Rev. C86, 015201 (2013).

GR: T. Inoue and E. Oset, Nucl. Phys. A710 (2002) 354.

Attractive and strong interaction between η and nucleon

R. Bhalerao, L. C. Liu, Phys. Lett. B54, 685 (1985) ($a_{\eta N}$=0.28+i0.19 fm)

$\Downarrow$

Possible existence of η-mesic bound states postulated for atomic nuclei with A$>$12

Q. Haider, L. C. Liu, Phys. Lett. B172, 257 (1986)

Recent theoretical studies of hadronic- and photoproduction of η meson support the existence of light η-mesic nuclei like $(^3\text{He-}\eta)_{bound}$ $(^4\text{He-}\eta)_{bound}$

$B_s \in (1, 40)$ MeV, $\Gamma \in (1, 45)$ MeV

0.18 fm<Re($a_{\eta N}$)<1.03fm

0.16 fm<Im($a_{\eta N}$)<0.49 fm

$dd \to (^4\text{He-}\eta)_{bound} \to {}^3\text{He}p\pi^-$: σ=**4.5 nb** | $pd \to (^3\text{He-}\eta)_{bound} \to Xp\pi^-$: σ=**80 nb**

J.-J. Xie et al., Eur. Phys. J. A 55 no.1, 6 (2019)
J.-J. Xie et al., Phys. Rev. C 95, 015202 (2017)
M. Skurzok et al., Nucl. Phys. A 993, 121647 (2020)
N. Ikeno et al., Eur. Phys. J A 53 no. 10, 194 (2017)
T. Ishikawa et al., Phys. Rev. C 105, 045201 (2022)
T. Sekihara, H. Fujioka, T. Ishikawa, Phys. Rev. C 97, 045202 (2017)
A. Fix and O. Kolesnikov, Phys. Rev. C 97, 044001 (2018)
V. Metag, M. Nanova, E. Paryev, Prog. Part. Nucl. Phys. 97, 199 (2017)
J. Mares et al., Acta. Phys. Polon. B 51, 129 (2020)
N. G. Kelkar, H. Kamada, M. Skurzok, Int. J. Mod. Phys. E 28, 1950066 (2019)
N. G. Kelkar, D. Bedoya Fierro, H. Kamada, M. Skurzok, Nucl. Phys. A 996, 121698 (2020)
S. D. Bass and P. Moskal, Rev.Mod. Phys. 91, 015003 (2019)
S. Wycech, W. Krzemien, Acta. Phys. Polon B 45, 745 (2014)
C. Wilkin, Acta. Phys. Polon. B 45, 603 (2014)

Exp. indications of the existence of the ^{4}He-η bound state

total cross section $\quad dd \to {}^4\text{He-}\eta \quad |f_s|^2 = \frac{p_d}{p_\eta}\frac{\sigma}{4\pi}$

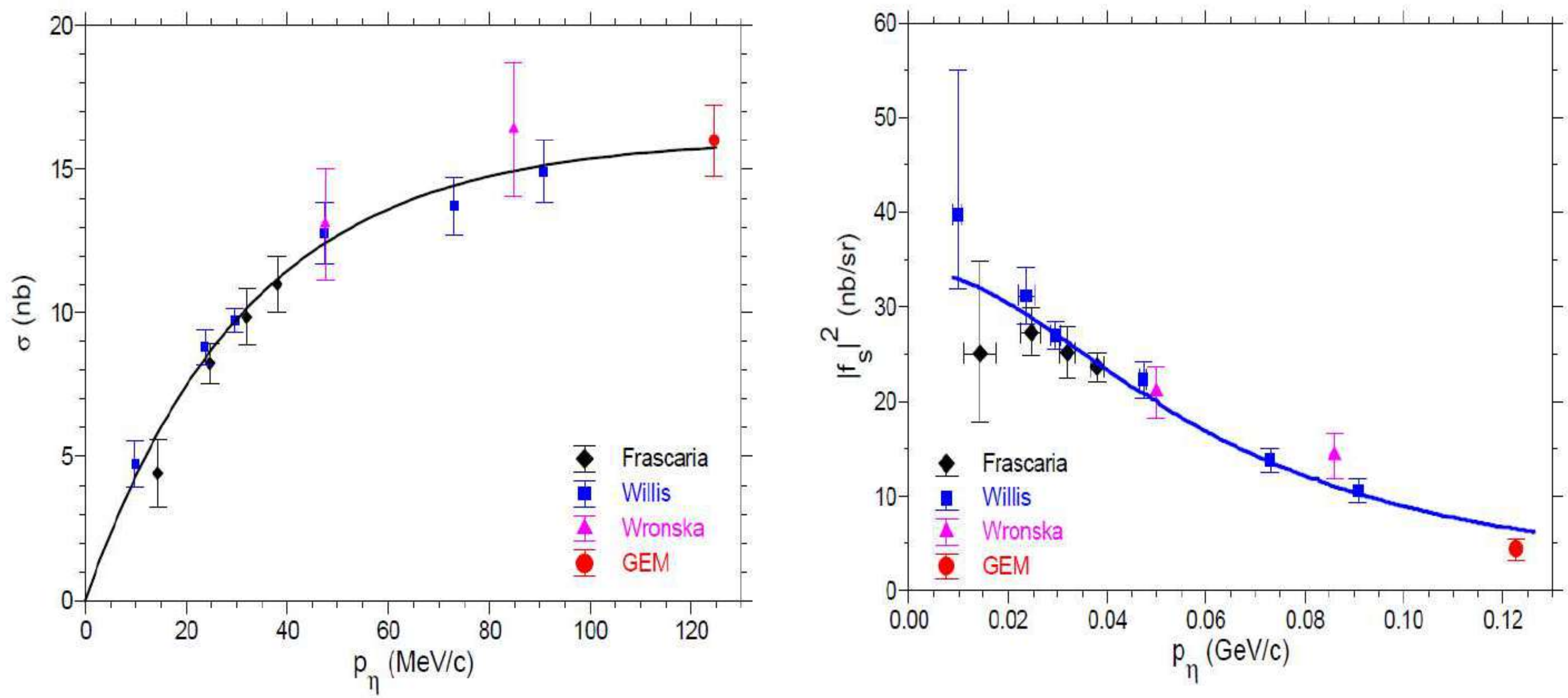

R. Frascaria et al., Phys. Rev. C50, 573 (1994)
N. Willis et al., Phys. Lett. B406, 14 (1997)
A. Wronska et al., Eur. Phys. J. A26, 421428 (2005)
A. Budzanowski et al., Nucl. Phys. A821, 193 (2009)

Exp. indications of the existence of the ^{3}He-η bound state

total cross section $pd \rightarrow {}^3$He-η γ^3He $\rightarrow {}^3$He-η

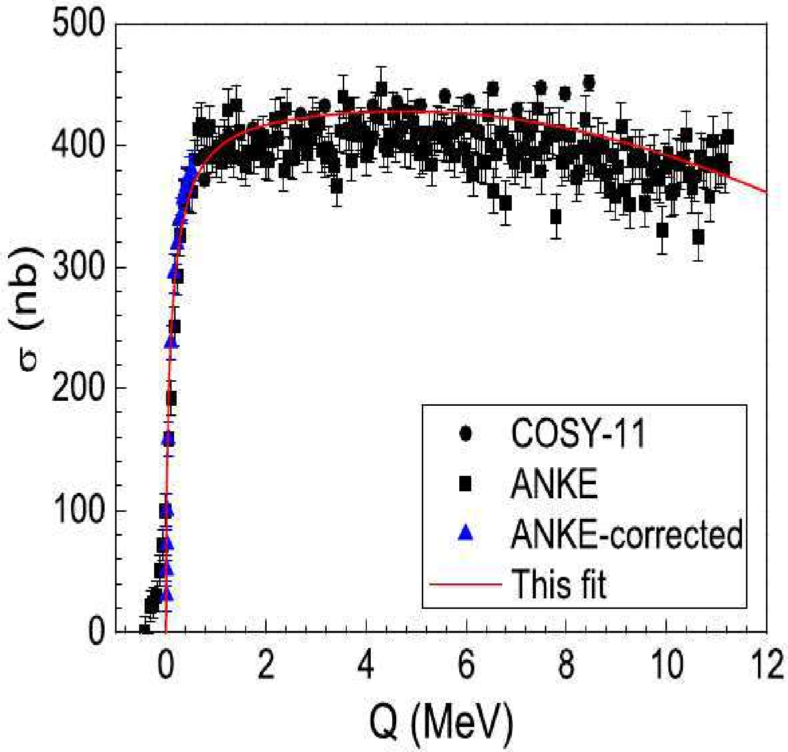

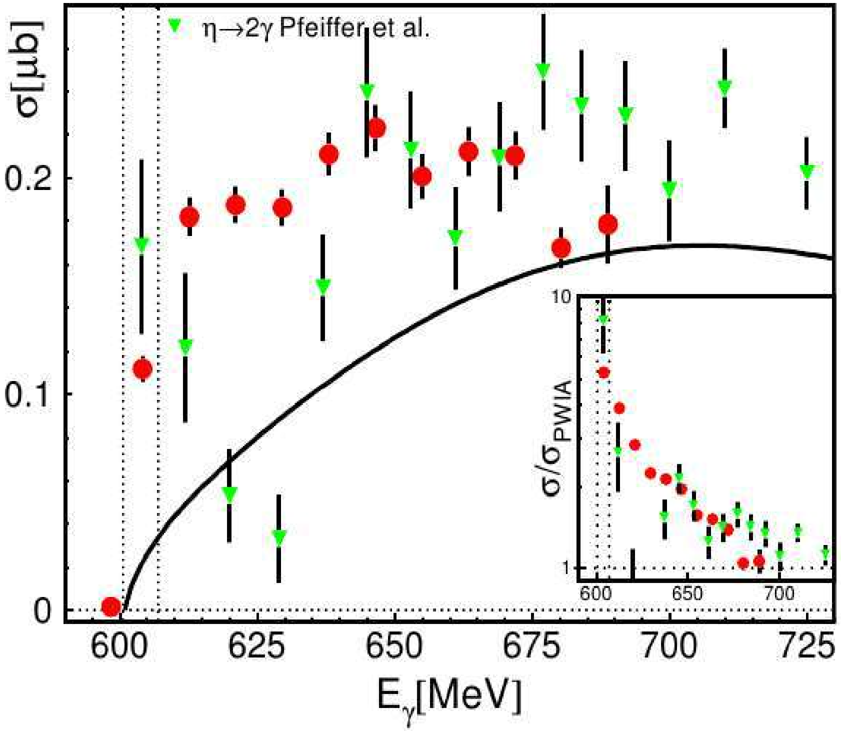

⇓

J. Smyrski, et al., Phys. Lett. 649, 258 (2007)
T. Mersmann, et al., Phys. Rev. Lett. 98, 242301 (2007)
J.-J. Xie, et al., Phys. Rev. C 95, 015202 (2017)
B. Krusche, C. Wilkin, Prog. Part. Nucl. Phys. 80, 43 (2014)

Why to search for the η-mesic bound states?

- Search for new kind of nuclear matter
- Investigation of η interaction with nucleons inside a nuclear matter
- Information about η meson structure:
  the η meson binding inside nuclear matter is very sensitive to the singlet component (η-η' mixing) in the wave function of the η meson
  η-η' mixing $\Rightarrow$ binding increase
  S. D. Bass and P. Moskal, Rev. Mod. Phys. 91, 015003 (2019)
  S. D. Bass, A. W. Thomas, Phys. Lett. B634, 368 (2006)
  S. Hirenzaki, H. Nagahiro, Acta Phys. Polon. B45, 619 (2014)
- Study of N*(1535) properties in medium (probe of testing different N*(1535) models)
  S. Hirenzaki et al., Acta Phys. Polon. B41, 2211 (2010)
  D. Jido, H. Nagahiro, S. Hirenzaki, Phys. Rev. C66, 045202 (2002)
  Z.-W. Liu et al., Phys. Rev. Lett. 116, 082004 (2016)

Forschungszentrum Jülich, Germany

COoler SYnchrotron COSY

COoler SYnchrotron COSY

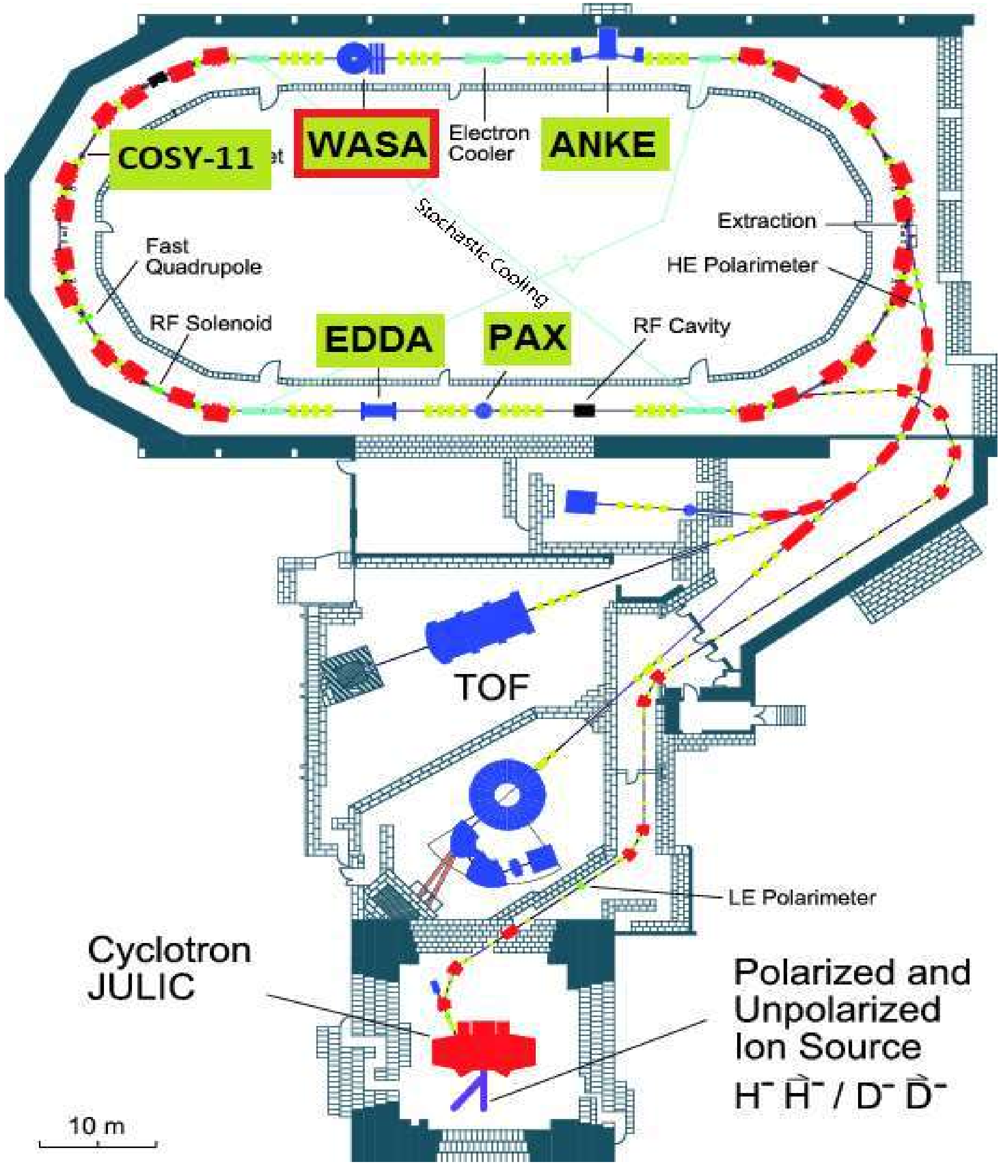

- 184 m circumference cooler synchrotron
- Polarized and unpolarized proton and deuteron beam
- Momentum range 0.3 - 3.7 GeV/c
- Stochastic and electron cooling
- 10^{11} particles in ring - luminosities 10^{31} - 10^{32} $cm^{-2}s^{-1}$
- Ramped beam (search for η-mesic nuclei)

WASA-at-COSY experiment

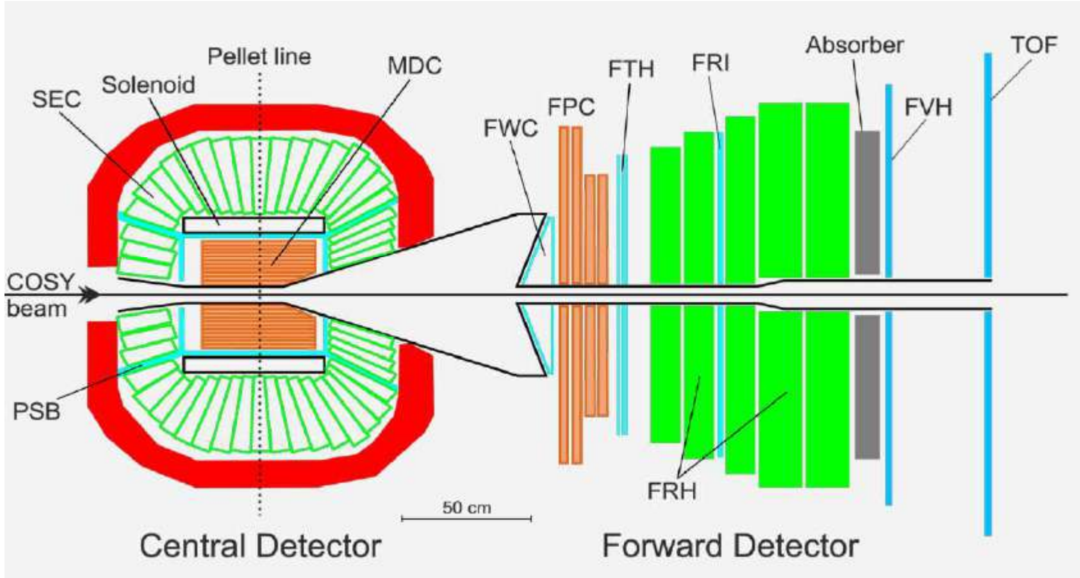

- **Pellet Target**
  - frozen pellets of hydrogen or deuterium

- **Forward Detector**
  - identification of heavier projectiles and target-recoil particles such as p, d and He in forward direction
  - angular information about the particles provided by FPC
  - PID based on measurement of energy loss in scintillators

- **Central Detector**
  - charged particles momenta reconstructed in magnetic field (MDC)
  - PID based on measurement of energy loss in scintillators
  - photons identified in calorimeter

WASA-at-COSY Collaboration

Collaboration:

32 member institutions from 8 countries (Germany. Sweeden, **Poland**, Russia, India, Japan, China, Bulgaria)

In Poland:

- Institute of Physics, Jagiellonian University, Cracow
- National Centre for Nuclear Research (NCBJ), Warsaw
- Institute of Nuclear Physics, Polish Acedemy of Science, Cracow
- Institute of Physics, University of Silesia, Katowice
- Institute of Experimental Physics, Faculty of Physics, Warsaw University

Status of the search for η-mesic Helium at WASA

$(^4\text{He-}\eta)_{bound}$

- **2008**: $dd \rightarrow {}^3\text{He}p\pi^-$ reaction

  P. Adlarson et al., Phys. Rev. C87, 035204 (2013)

- **2010**: $dd \rightarrow {}^3\text{He}n\pi^0$ and $dd \rightarrow {}^3\text{He}p\pi^-$ reactions

  P. Adlarson et al., Nucl. Phys. A 959, 102-115 (2017)

  M. Skurzok, P. Moskal, et al., Phys. Lett. B782, 6-12 (2018)

$\Uparrow$

η meson absorption and excitation of one of the nucleons to an N^* resonance, which subsequently decays into an N - π pair

$(^3\text{He-}\eta)_{bound}$

- **2014**:

  - $pd \rightarrow {}^3\text{He}2\gamma({}^3\text{He}6\gamma)$ reactions

  P. Adlarson et al., Phys. Lett. B 802, 135205 (2020)

  decay of the η - meson while it is still "orbiting" around a nucleus

  - $pd \rightarrow ppp\pi^-(ppn\pi^0, dp\pi^0)$ reactions

  P. Adlarson et al., Phys. Rev. C 102, 044322 (2020)

η meson absorption and excitation of one of the nucleons to an N^* resonance, which subsequently decays into an N - π pair

Papers available at http://koza.if.uj.edu.pl/publications/wasa-at-cosy

Experimental method

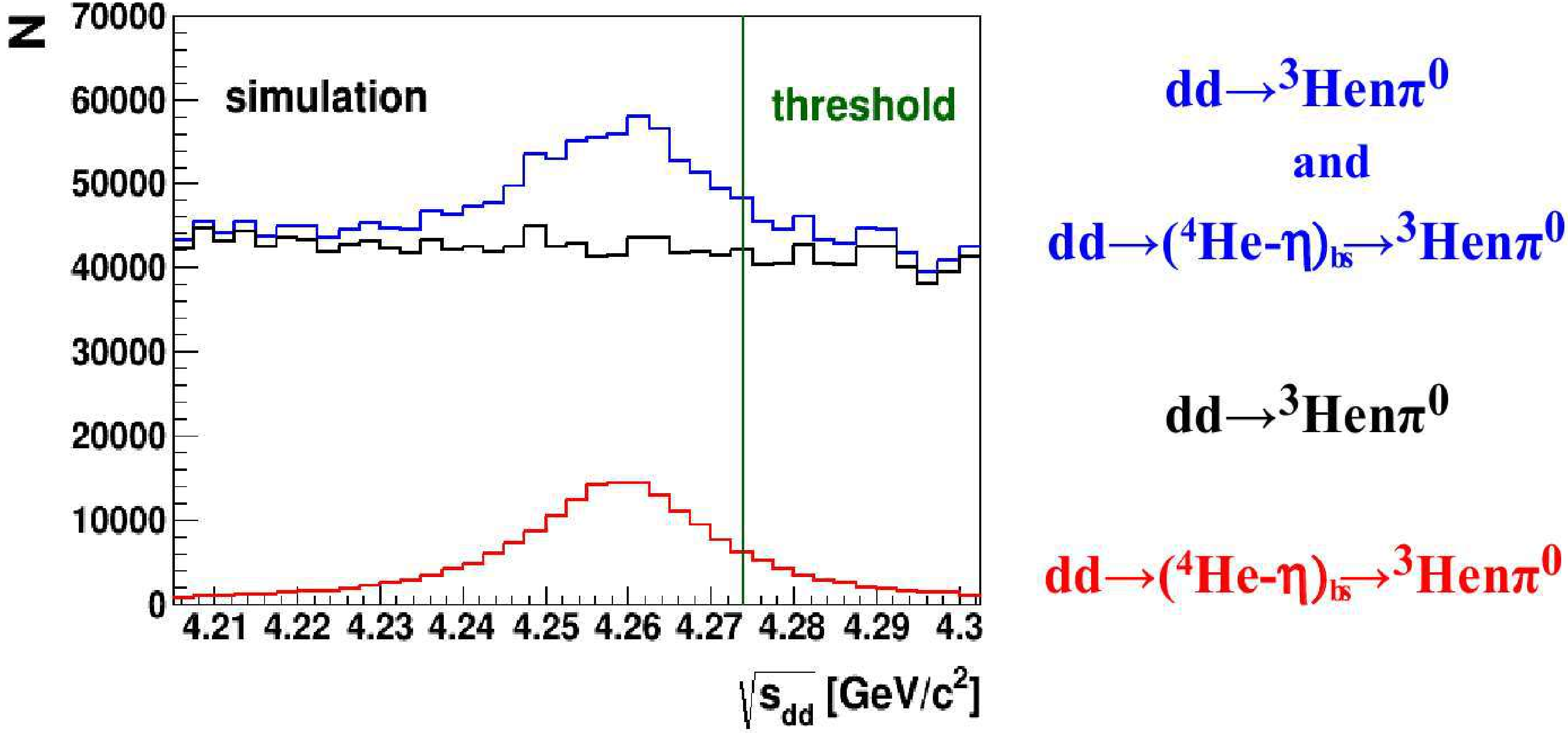

Excitation function

(^{4}He-η)$_{bound}$ existence manifested by resonant-like structure below η production threshold

Exp. 186.1 & 186.2, FZ Jülich, Germany, 2008 and 2010

P. Moskal, W. Krzemien, J. Smyrski, *COSY proposal No. 186.1 & 186.2*

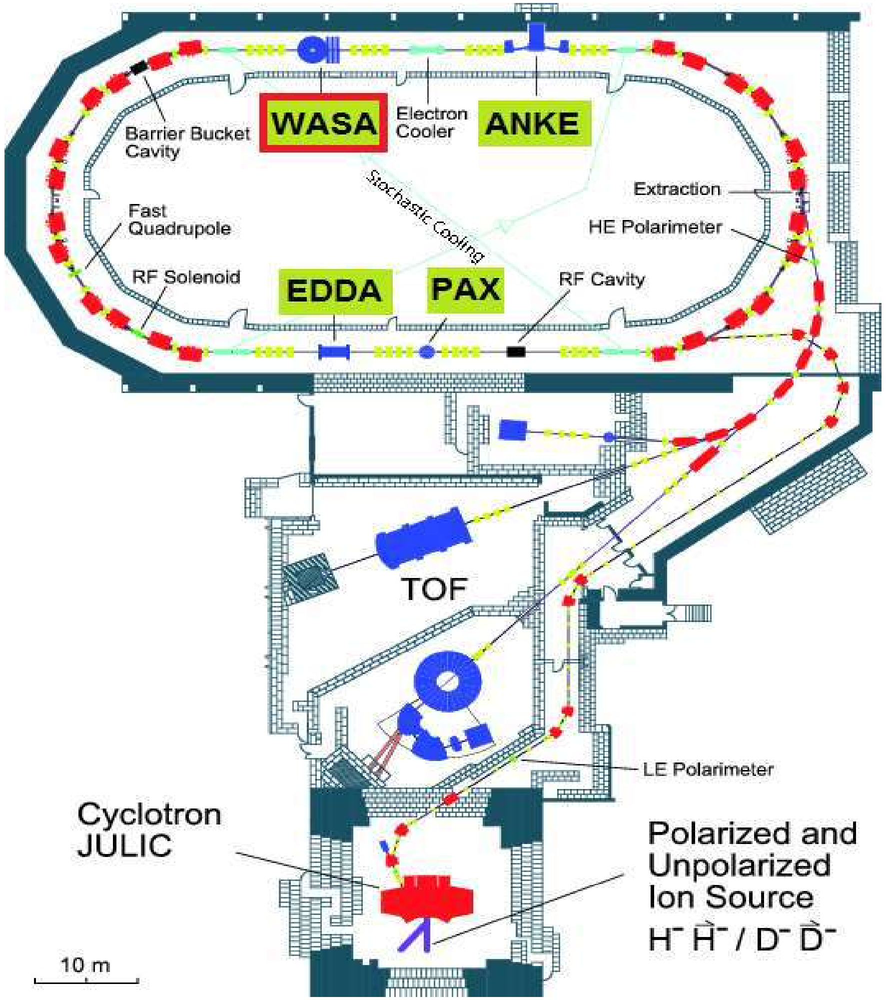

$dd \rightarrow {}^3\mathbf{He}n\pi^0$ | $dd \rightarrow {}^3\mathbf{He}p\pi^-$

- **Measurement** with the **deuteron** beam momentum ramped and with the **deuteron** pellet target

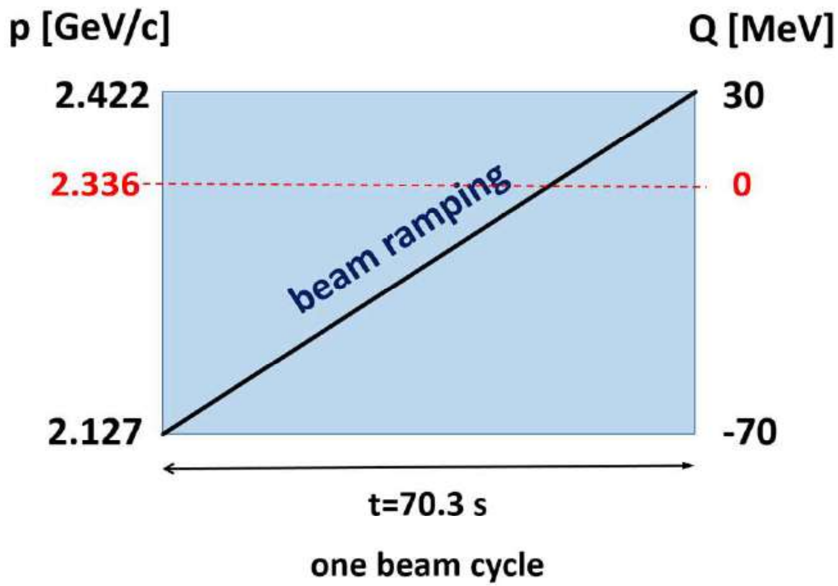

- **Data** were effectively taken with high acceptance (58%)

Exp. 186.3, FZ Jülich, Germany 2014

P. Moskal, W. Krzemien, M. Skurzok, *COSY proposal No. 186.3*

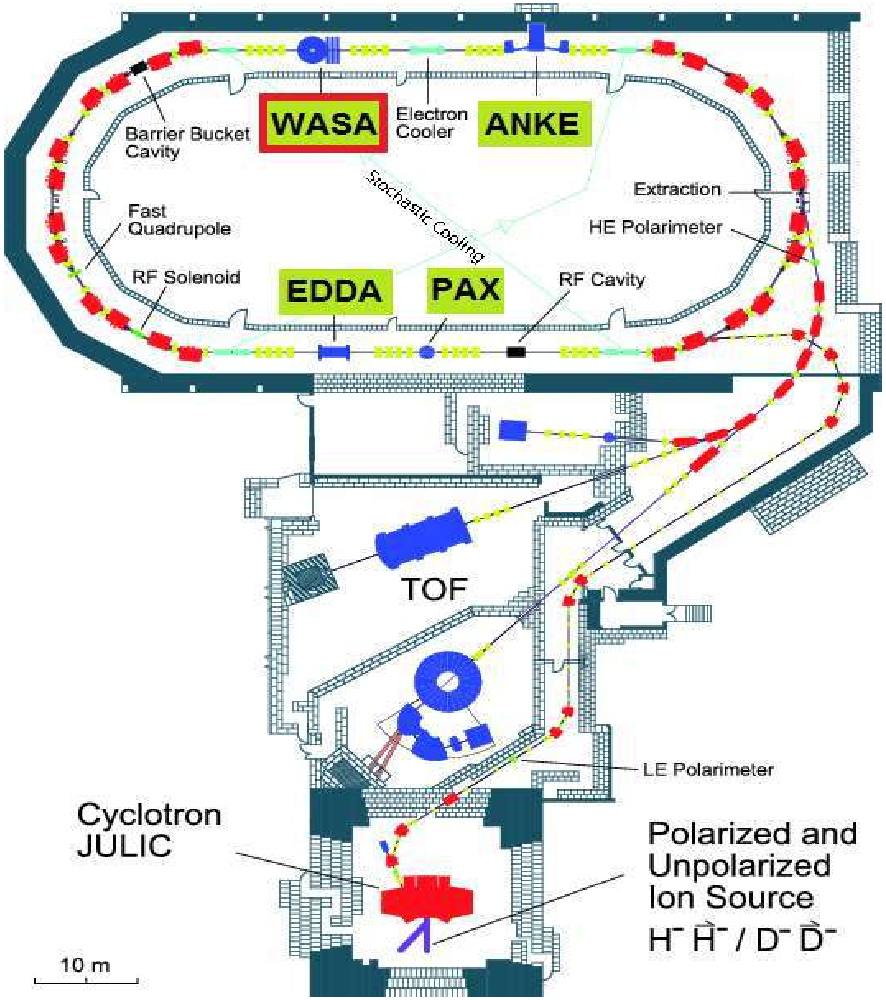

$pd \rightarrow ppp\pi^-(ppn\pi^0, dp\pi^0)$

$pd \rightarrow {}^3\mathbf{He}2\gamma\ ({}^3\mathbf{He}6\gamma)$

- **Measurement** with the **proton** beam momentum ramped and with the **deuteron** pellet target

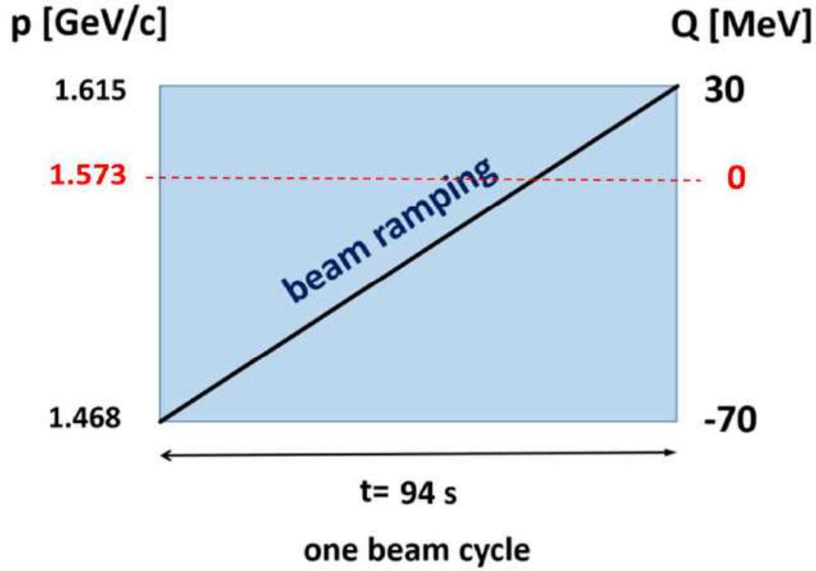

- **Data** were effectively taken with high acceptance

Kinematical mechanism of the reaction (via N^*)

$$dd \rightarrow (^4\text{He-}\eta)_{bs} \rightarrow {}^3\text{He}p\pi^-$$

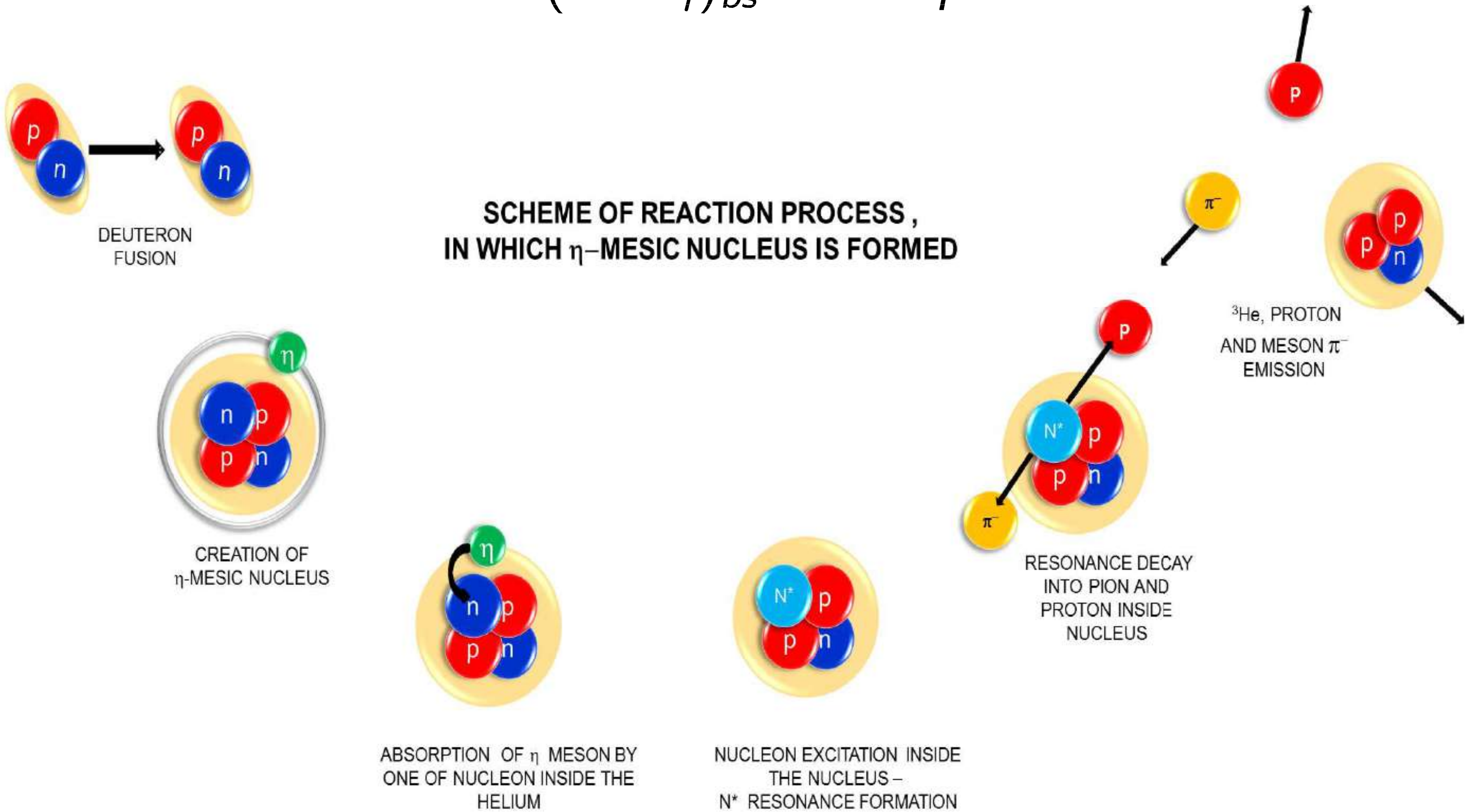

Kinematical mechanism of the reaction (via N^*)

$$dd \to (^4\text{He-}\eta)_{bs} \to {}^3\text{He}n\pi^0$$

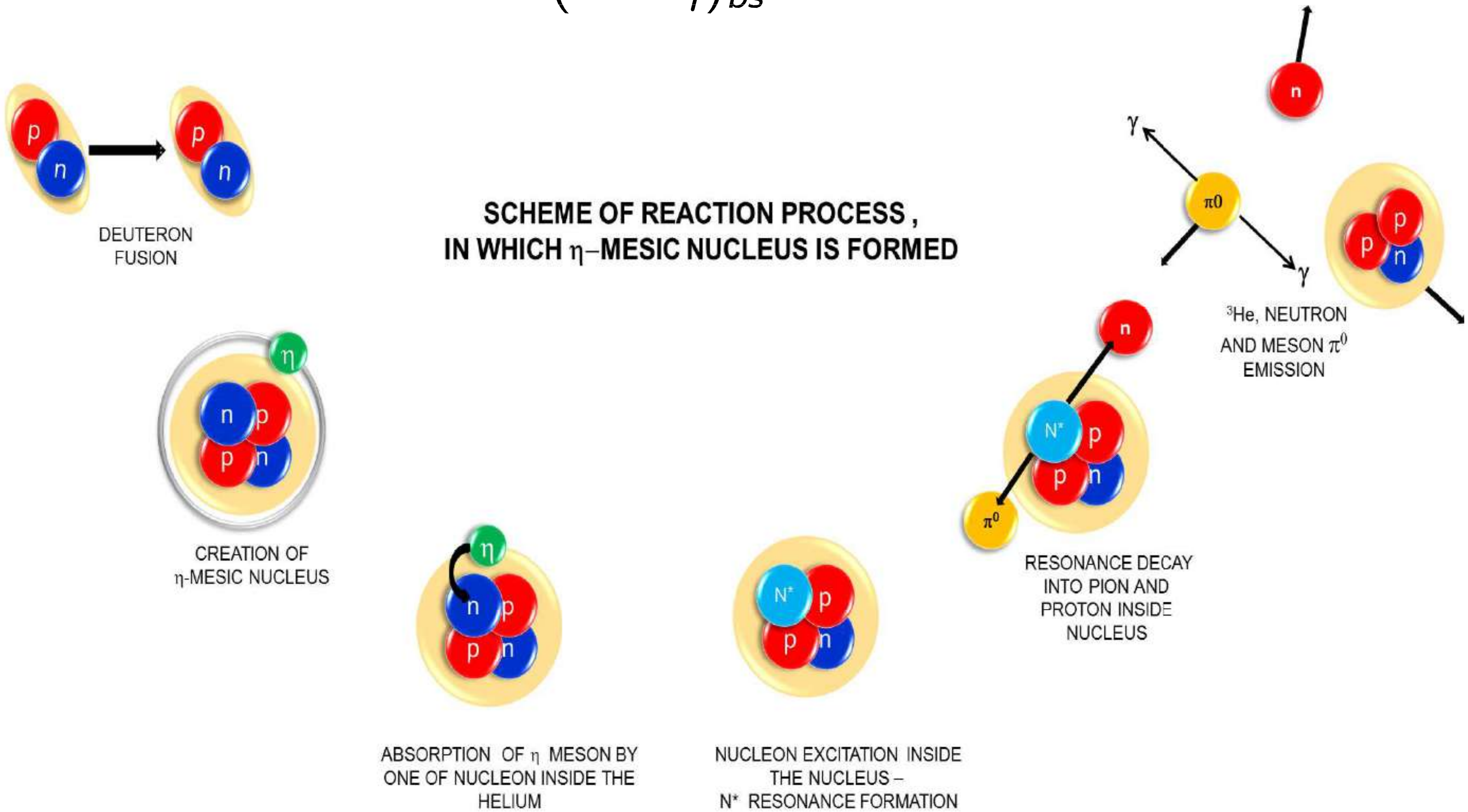

Simulation of $(^4\text{He-}\eta)_{bound}$ production and decay

Breit-Wigner distribution

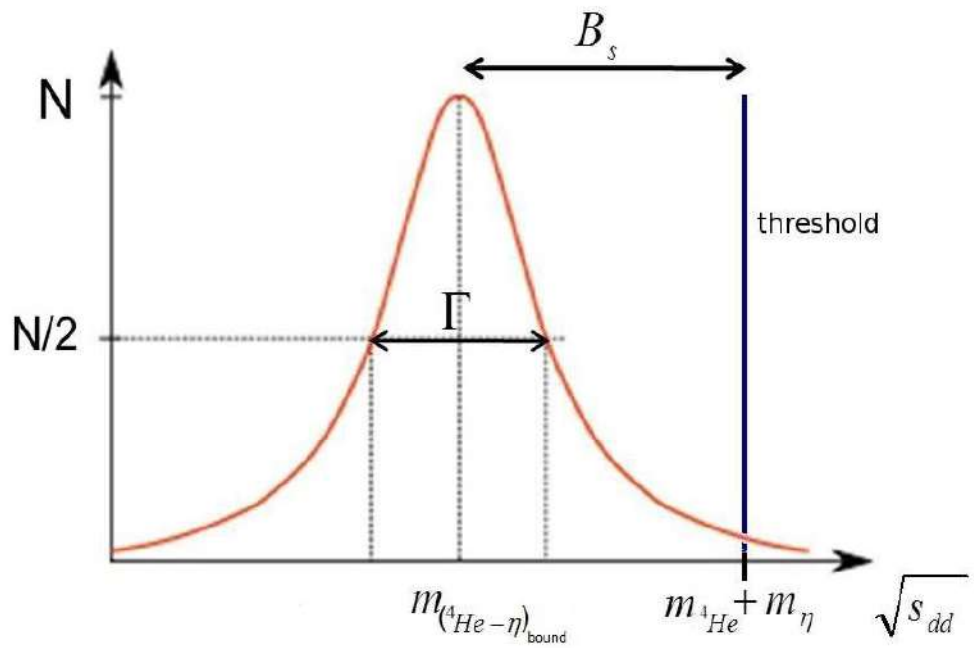

Spectator Model

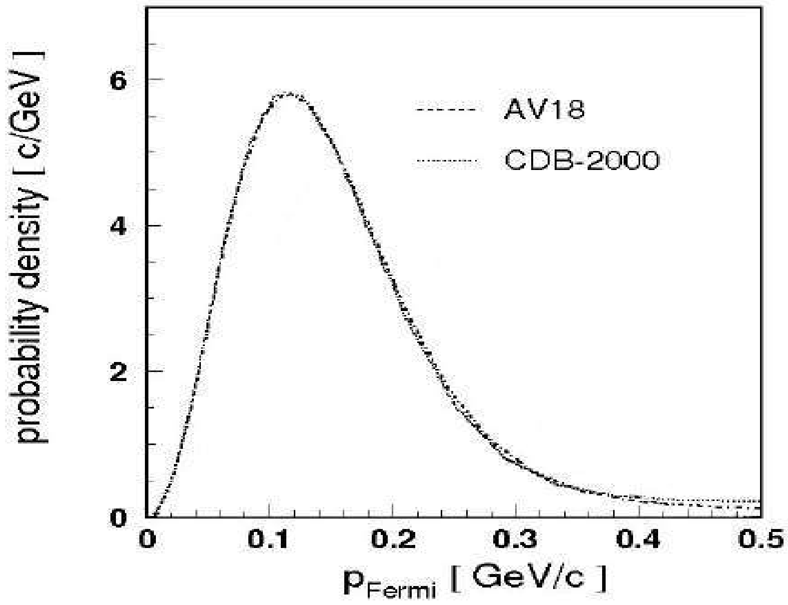

$$N\left(\sqrt{s_{dd}}\right) = \frac{1}{2\pi}\frac{\Gamma^2/4}{\left(\sqrt{s_{dd}}-m_{(^4He-\eta)_{bound}}\right)^2+\Gamma^2/4}$$

$$|\mathbb{P}_{^3He}|^2 = m^2_{^3He}$$

$$m_{(^4He-\eta)_{bound}} = m_{^4He} + m_\eta - B_s$$

Simulation of $(^4\text{He-}\eta)_{bound}$ production and decay

$$\eta + N \Rightarrow N^*(1535) \Rightarrow N + \pi = \begin{cases} p + \pi^- \\ n + \pi^0 \end{cases}$$

- relative N-π angle in the CM: $\theta_{cm}^{N,\pi} \sim 180^\circ$
- low ^{3}He momentum in the CM

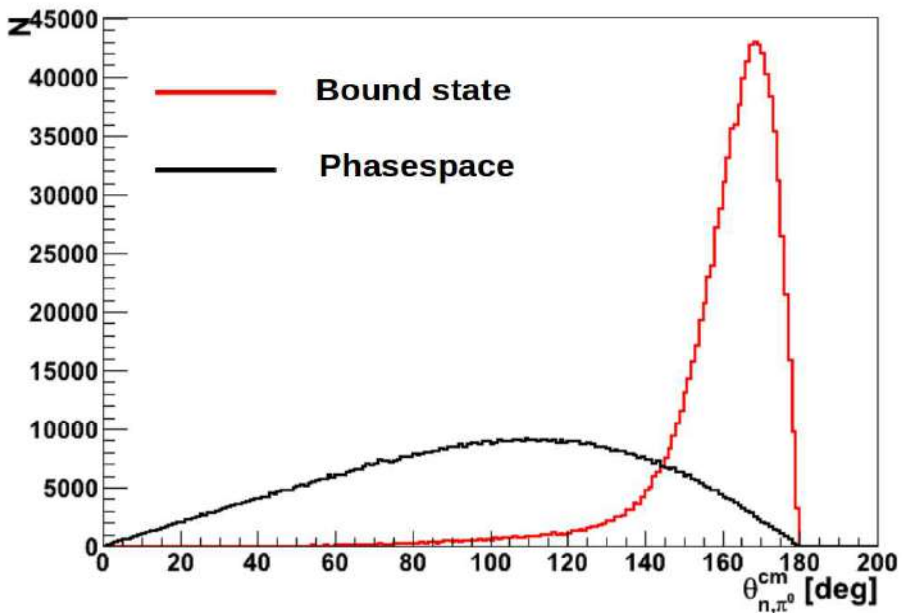

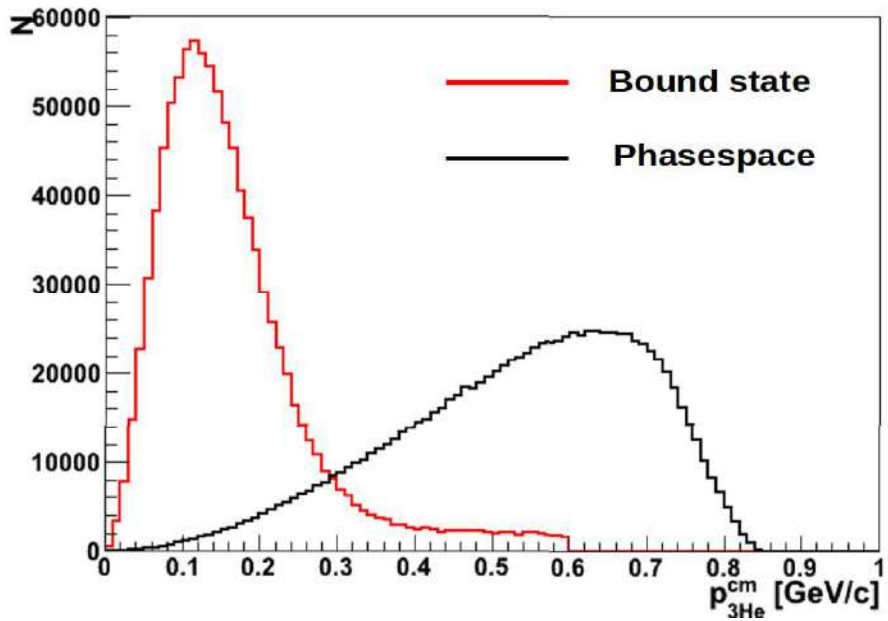

Experiment-May 2008

- **Channel:** $dd \rightarrow (^4\text{He-}\eta)_{bound} \rightarrow {}^3\text{He}p\pi^-$ (norm: $dd \rightarrow {}^3\text{He}n$)
- **Measurement:** beam momentum ramped from **2.185GeV/c to 2.400GeV/c** $\Rightarrow$ the range of excess energy **Q∈(-51,22)MeV**
- **Luminosity:** $\text{L}=118\frac{1}{nb}$
- **Acceptance:** A=53%

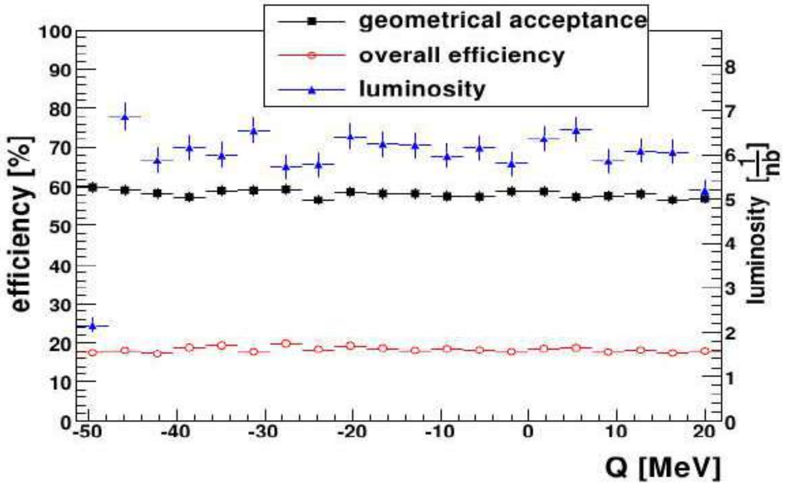

Excitation function

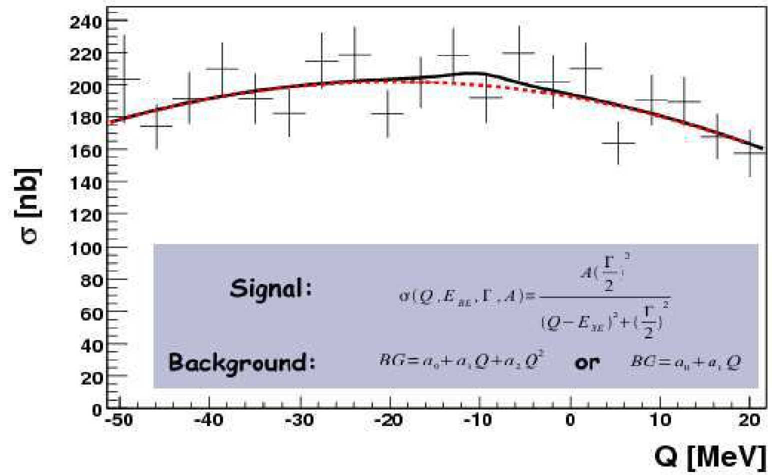

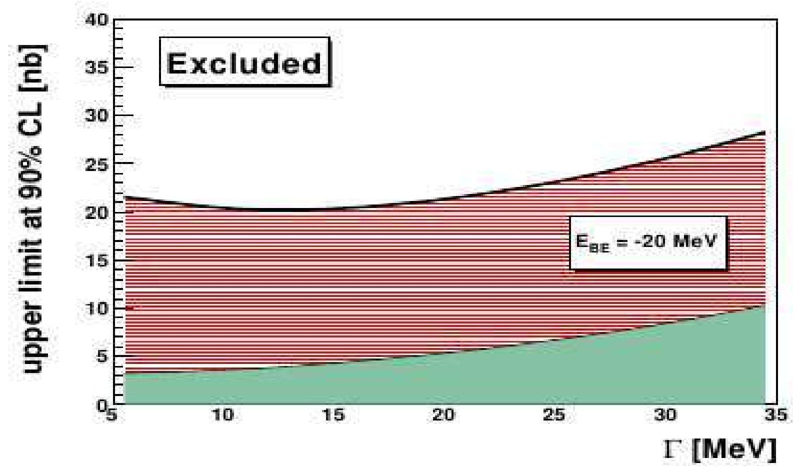

P. Adlarson et al., Phys. Rev. C87 (2013), 035204
W. Krzemien, Ph. D Thesis, Jagiellonian University (2012)

RESULT: $\sigma_{dd\rightarrow(^4He-\eta)_{bound}\rightarrow{}^3Hep\pi^-} < 27\ nb$

Experiment-Nov/Dec 2010

- **Channels:** $dd \rightarrow (^4\text{He-}\eta)_{bound} \rightarrow {}^3\text{He}p\pi^-$
  $dd \rightarrow (^4\text{He-}\eta)_{bound} \rightarrow {}^3\text{He}n\pi^0$
  (norm: $dd \rightarrow {}^3\text{He}n$ and $dd \rightarrow ppn_{sp}n_{sp}$)
- **Measurement:** beam momentum ramped from **2.127GeV/c to 2.422GeV/c** $\Rightarrow$ the range of excess energy **Q$\in$(-70,30)MeV**
- **Luminosity:** $L=1200\frac{1}{nb}$
- **Acceptance:** A=53%

$\Downarrow$

about 10 times higher statistics than in 2008

ANALYSIS:

- Particles identification
- Selection bound state region
- Determination of excitation functions
- Determination the upper limit of the total cross section

Search for $(^{4}\text{He-}\eta)_{bound}$ in $dd \to {}^{3}\text{He}N\pi$ reaction | PID

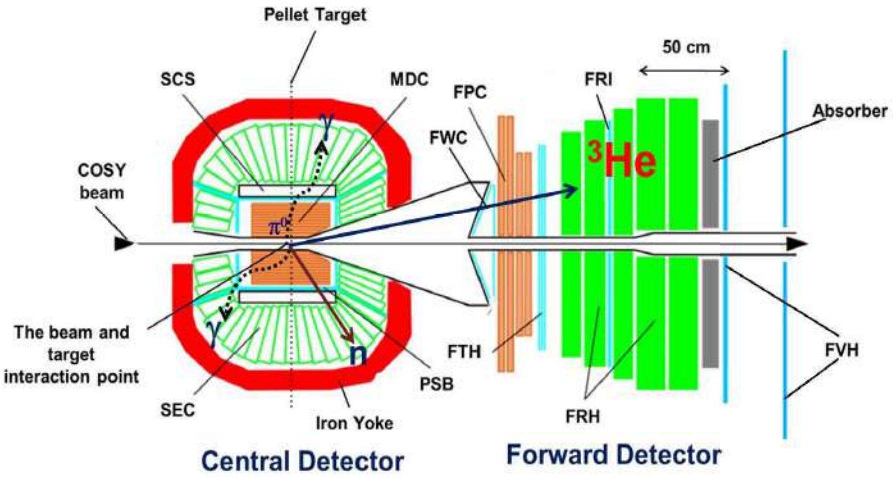

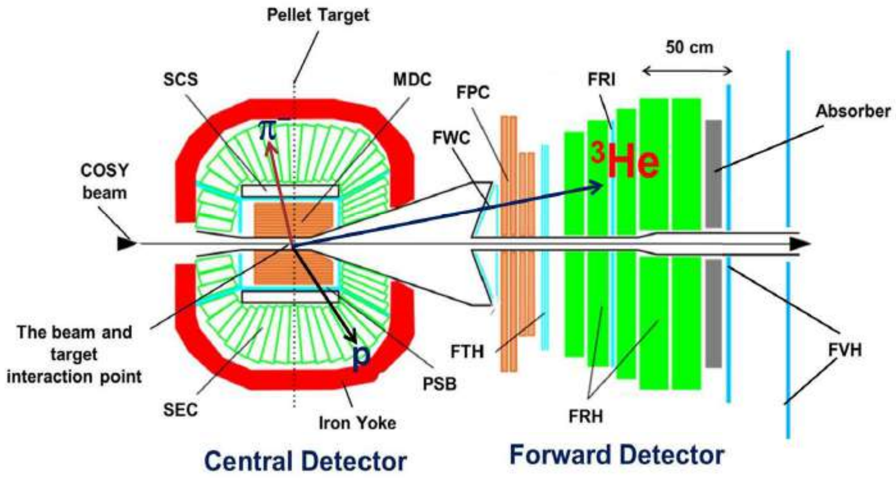

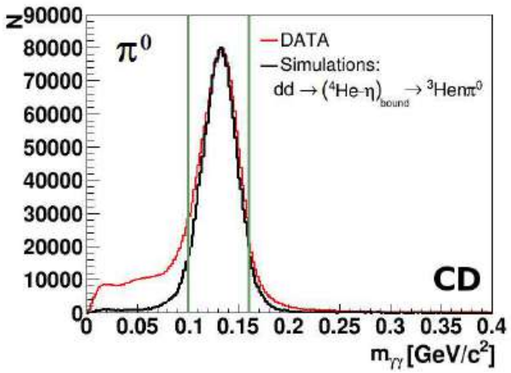

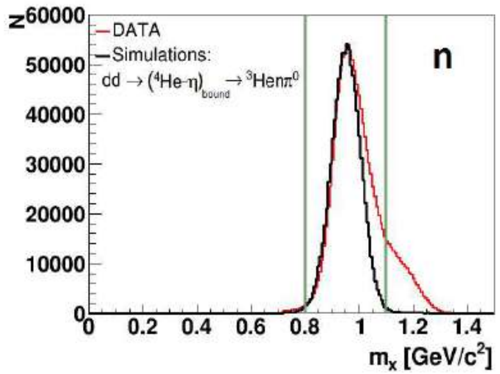

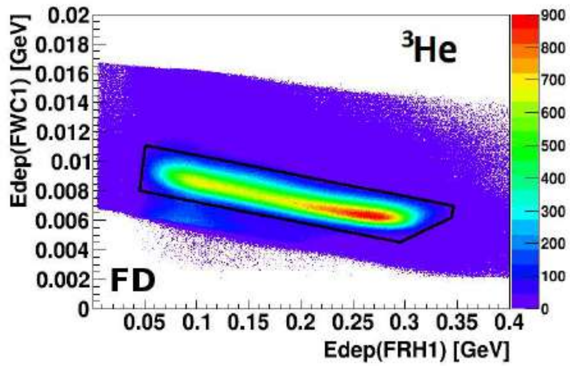

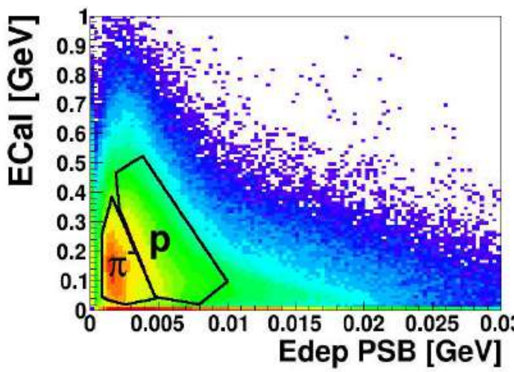

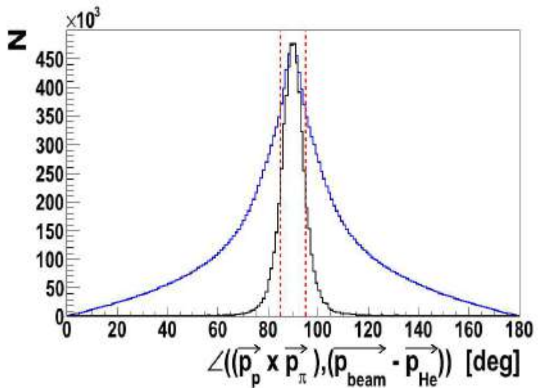

Determination of the excitation function

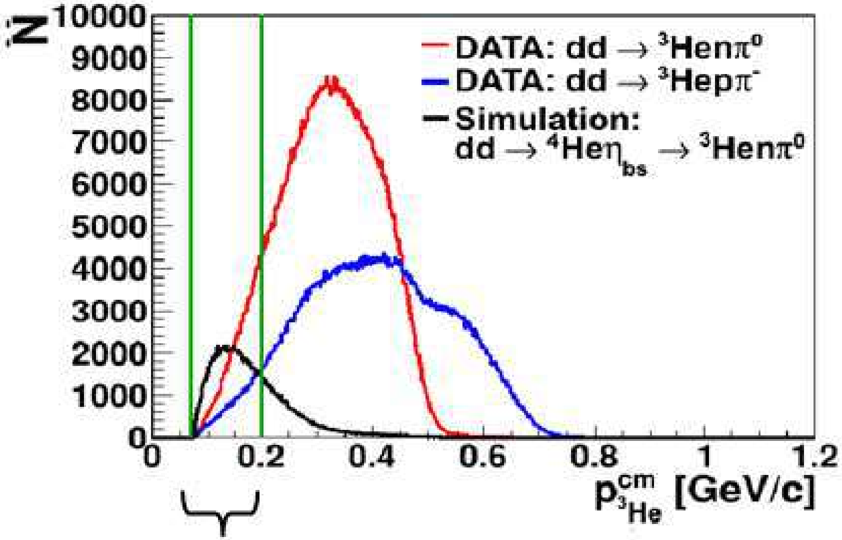

region rich in signal

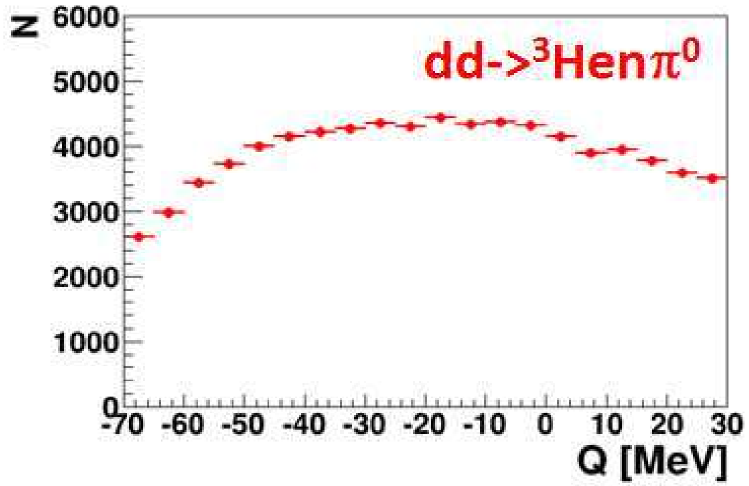

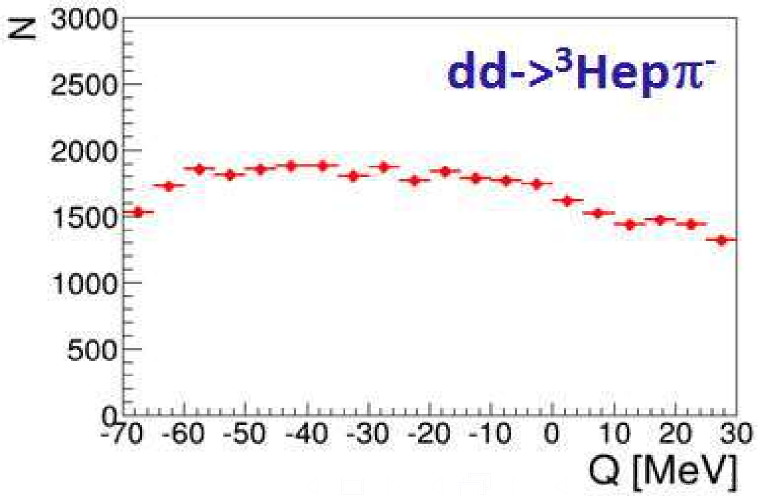

Determination of the total cross section for $dd \rightarrow {}^3\mathrm{He}n\pi^0$ reaction

Cross section

$$\sigma(Q) = \frac{N(Q)}{L(Q)\epsilon(Q)}$$

N - number of experimental events

L - integrated luminosity

ϵ - full detection efficiency

Excitation function

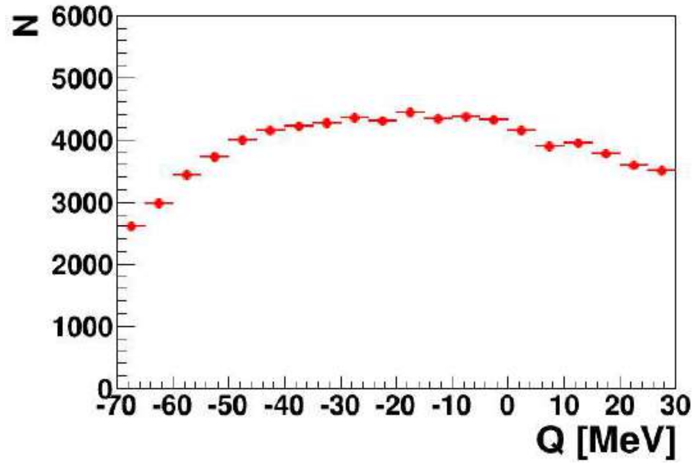

Efficiency

$dd \rightarrow ({}^4\mathrm{He}\text{-}\eta)_{bound} \rightarrow {}^3\mathrm{He}n\pi^0$

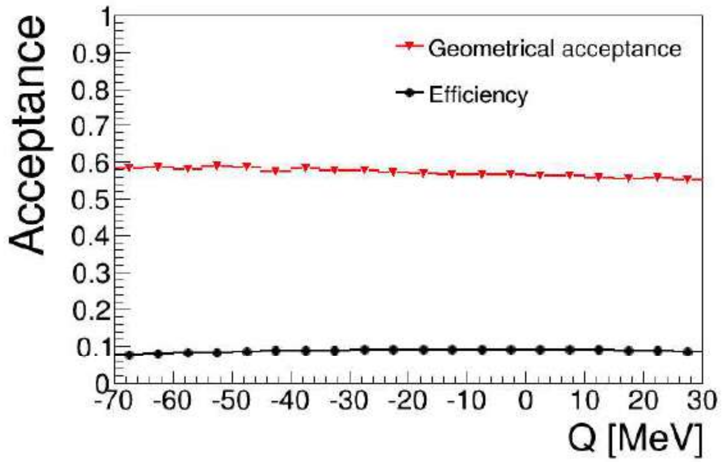

from simulations: $\epsilon = \frac{N_{acc}}{N_{gen}}$

Integrated luminosity

$dd \rightarrow ppn_{sp}n_{sp}$

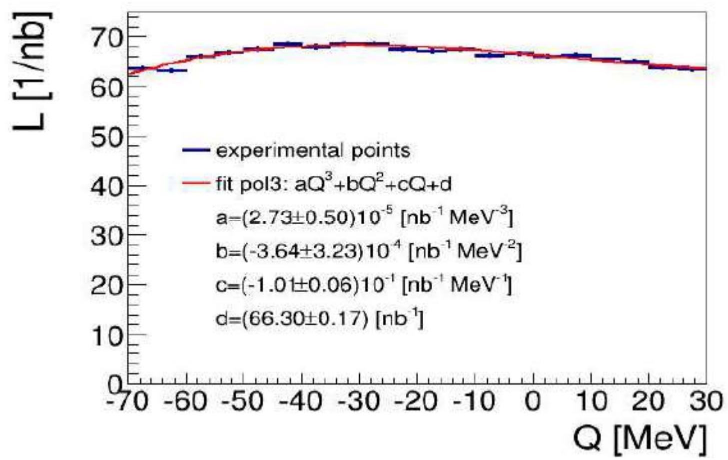

$dd \rightarrow ppn_{sp}n_{sp}$: L=$(1329 \pm 2_{stat} \pm 108_{syst} \pm 64_{norm})nb^{-1}$

$dd \rightarrow {}^3\mathrm{He}n$: L=$(1102 \pm 2_{stat} \pm 28_{syst} \pm 107_{norm})nb^{-1}$

Cross section

$$\sigma(Q) = \frac{N(Q)}{L(Q)\epsilon(Q)}$$

N - number of experimental events

L - integrated luminosity

ϵ - full detection efficiency

Excitation function

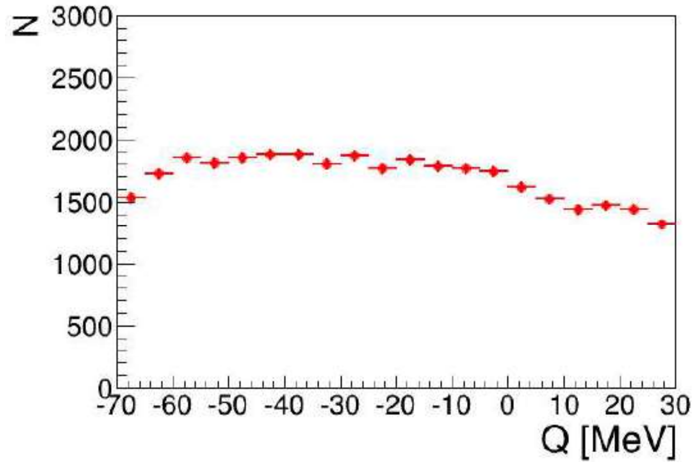

Efficiency

$dd \to ({}^4\mathrm{He}\text{-}\eta)_{bound} \to {}^3\mathrm{He}n\pi^0$

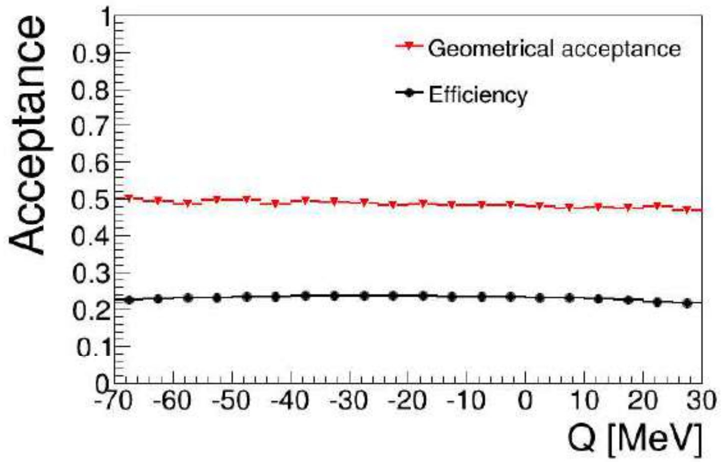

from simulations: $\epsilon = \frac{N_{acc}}{N_{gen}}$

Integrated luminosity

$dd \to ppn_{sp}n_{sp}$

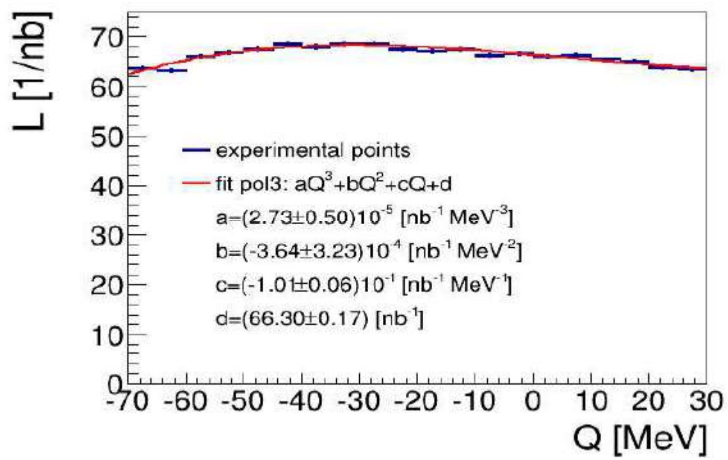

$dd \to ppn_{sp}n_{sp}$: L=$(1329 \pm 2_{stat} \pm 108_{syst} \pm 64_{norm})nb^{-1}$

$dd \to {}^3\mathrm{He}n$: L=$(1102 \pm 2_{stat} \pm 28_{syst} \pm 107_{norm})nb^{-1}$

Determination of the upper limit of the total cross section for $dd \to (^4\text{He-}\eta)_{bound} \to {}^3\text{He}N\pi$ processes at CL=90%

$dd \to (^4\text{He-}\eta)_{bound} \to {}^3\text{He}n\pi^0$

$\Downarrow$

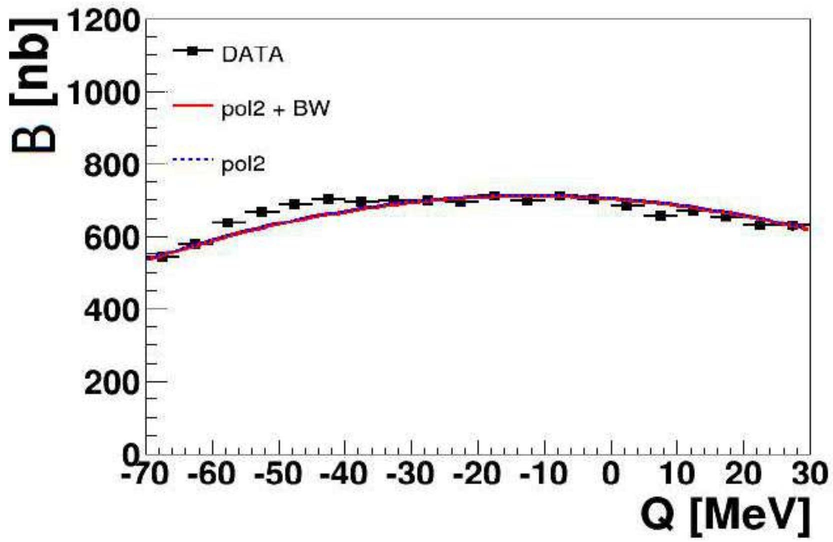

$dd \to (^4\text{He-}\eta)_{bound} \to {}^3\text{He}p\pi^-$

$\Downarrow$

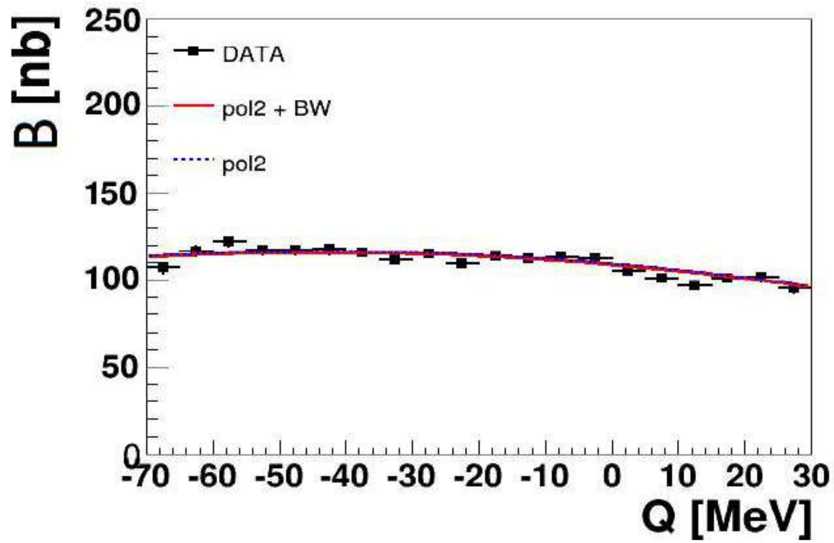

simultaneous fit with $\frac{A\cdot\Gamma^2/4}{(Q-B_s)^2+\Gamma^2/4} + BQ^2 + CQ + D$

Breit-Wigner (signal) + pol2 (background)

taking into account the **isospin relation** between the both of the considered channels:

$$P(N^* \to p\pi^-)=2P(N^* \to n\pi^0)$$

B_s,Γ - fixed parameters | A, B, C, D - free parameters || $\sigma^{upp}_{CL=90\%} = k \cdot \sigma_A$, k=1.64 (for CL=90%)

Determination of the upper limit of the total cross section for $dd \to (^4\text{He-}\eta)_{bound} \to {}^3\text{He}p\pi^-$ process at CL=90%

$\sigma^{upp}_{CL=90\%}$ for

$dd \to (^4\text{He-}\eta)_{bound} \to {}^3\text{He}n\pi^0$

$\Downarrow$

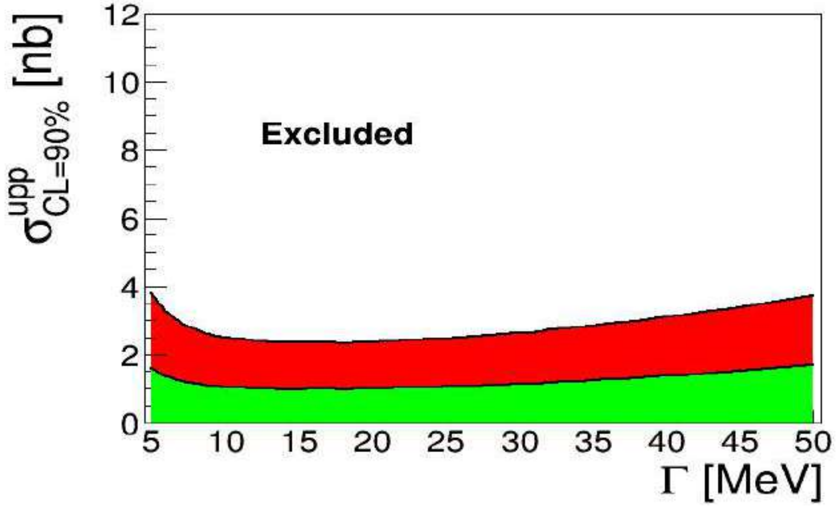

$\sigma^{upp}_{CL=90\%}$ for

$dd \to (^4\text{He-}\eta)_{bound} \to {}^3\text{He}p\pi^-$

$\Downarrow$

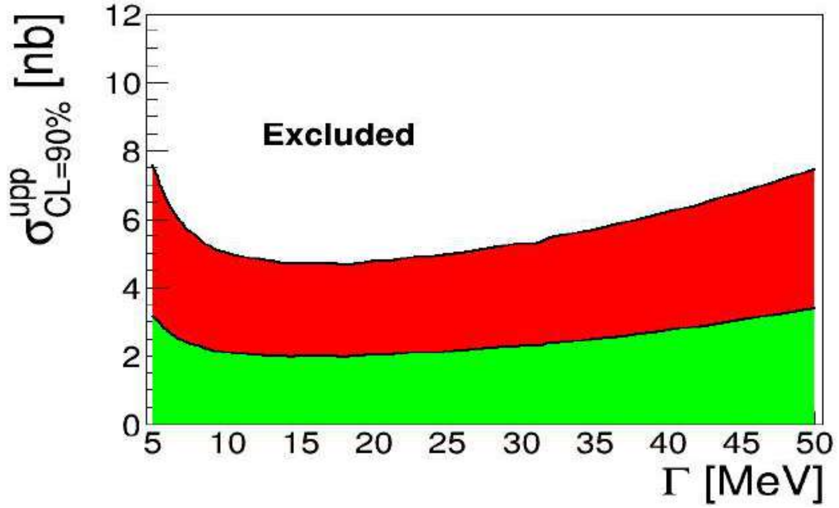

RESULT:

$\sigma_{dd\to(^4He-\eta)_{bound}\to{}^3Hen\pi^0} < 3.5\ nb$

RESULT:

$\sigma_{dd\to(^4He-\eta)_{bound}\to{}^3Hep\pi^-} < 7\ nb$

2008: $\sigma < 27\ nb$

P. Adlarson et al., Nucl. Phys. A 959, 102-115 (2017)

Main contribution: momentum distribution for N^* inside He

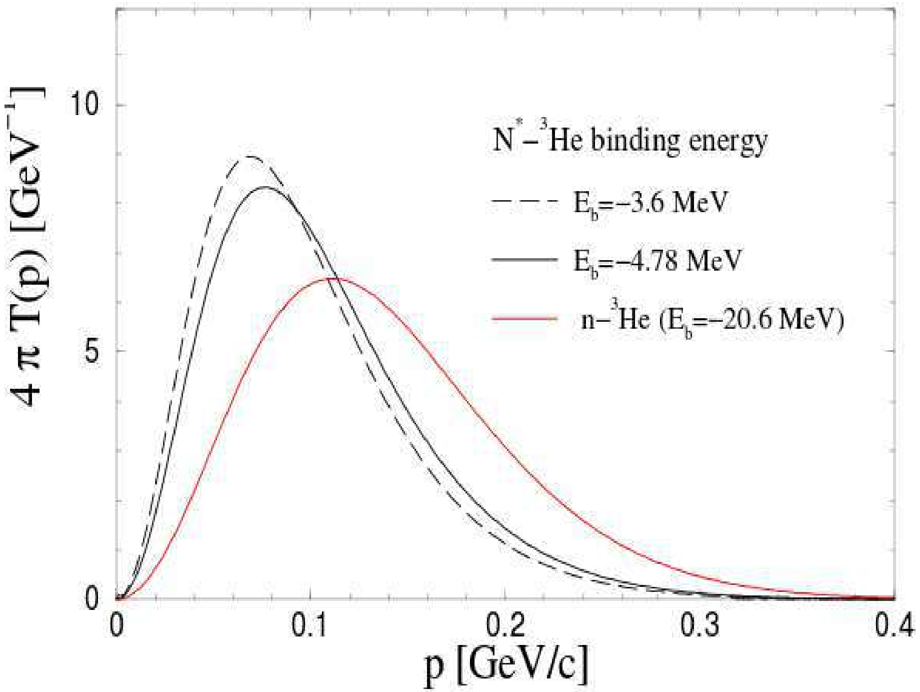

assumption that N^* resonance has a momentum distribution identical to the distribution of nucleons inside He

N^*-^3He momentum distribution determined: the elementary $NN^* \to NN^*$ interaction constructed within π and η meson exchange model $\Rightarrow$ N^*-He potential evaluated by folding NN^* interaction with a nuclear density

$\Downarrow$

Details:

N. G. Kelkar, Eur. Phys. J. A 52, 309 (2016)
N. G. Kelkar, D. Bedoya Ferro, P. Moskal, Acta Phys. Pol. B 47, 299 (2016)

Comparison with N. Ikeno et al. model prediction

N. Ikeno, H. Nagahiro, D. Jido, S. Hirenzaki, Eur. Phys. J. A 53, 194 (2017)

- total cross sections for the $dd \rightarrow (^4\text{He-}\eta)_{bound} \rightarrow {}^3\text{He}N\pi$ reaction determined based on phenomenological calculations
- the model reproduced the data on the $dd \rightarrow {}^4\text{He}\,\eta$ reaction quite well
- $\sigma = \sigma_{conv} + \sigma_{esc}$
- σ_{conv} - determined for different parameters V_0 and W_0 of a spherical η-^{4}He optical potential $V(r) = (V_0 + iW_0)\frac{\rho_\alpha(r)}{\rho_\alpha(0)}$ (the total cross section in the subthreshold excess energy region where the η meson is absorbed by the nucleus)
- normalization in the sense that the escape part reproduces the measured cross sections for the $dd \rightarrow {}^4\text{He}\eta$ process

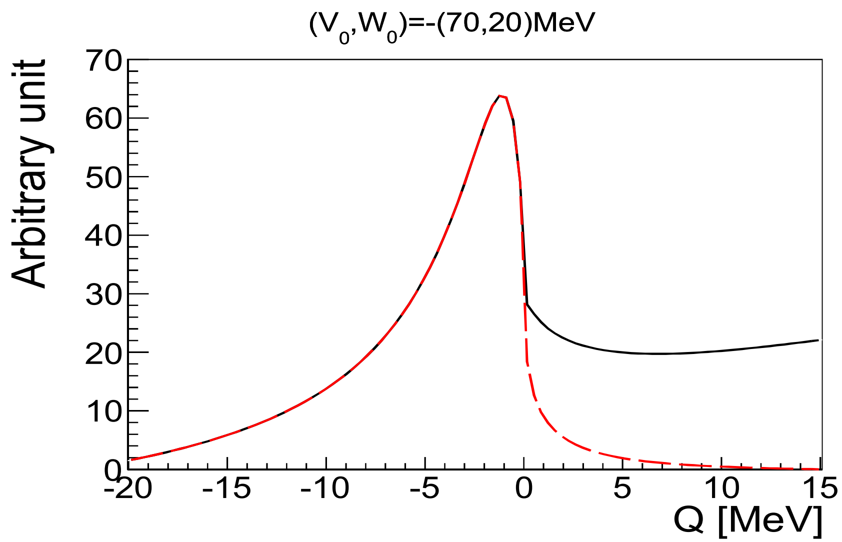

σ —

σ_{conv} - -

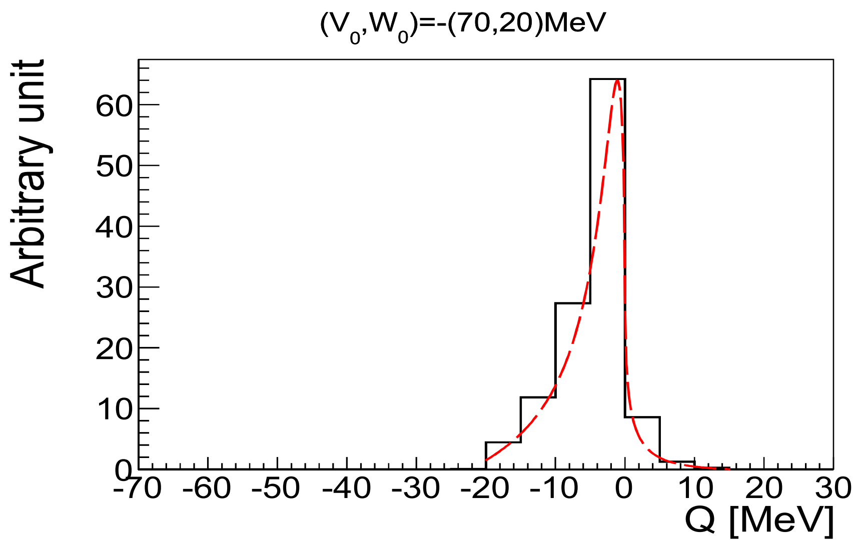

σ_{conv} spectrum convoluted with the experimental resolution functions

Comparison with N. Ikeno et al. model prediction

$dd \to ({}^4\text{He-}\eta)_{bound} \to {}^3\text{He}n\pi^0$

$\Downarrow$

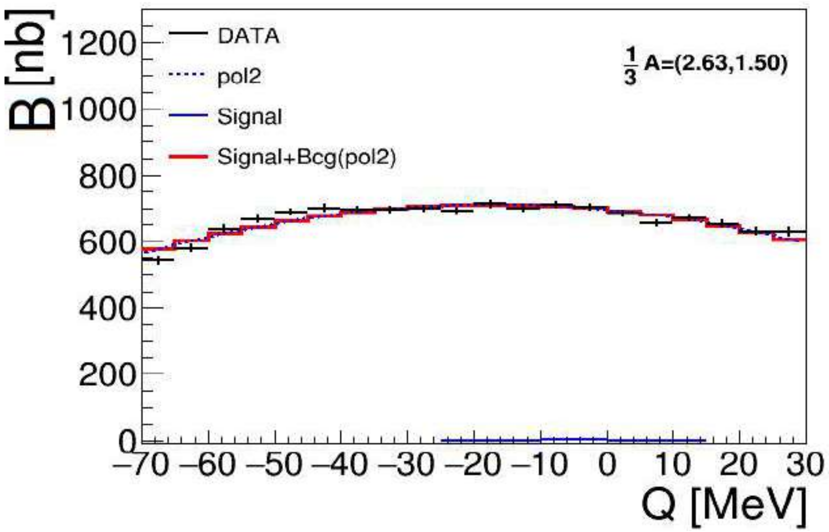

$dd \to ({}^4\text{He-}\eta)_{bound} \to {}^3\text{He}p\pi^-$

$\Downarrow$

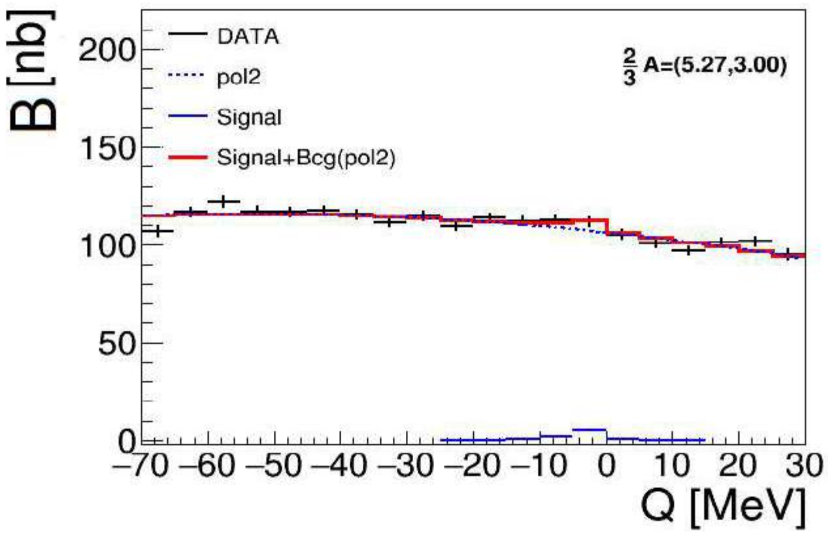

$$\sigma_{n\pi^0}(Q) = \tfrac{1}{3}A \cdot Theory(Q) + B_1 Q^2 + C_1 Q + D_1$$

$$\sigma_{p\pi^-}(Q) = \tfrac{2}{3}A \cdot Theory(Q) + B_2 Q^2 + C_2 Q + D_2$$

isospin relation between the both of the considered channels

$Theory(Q)$ - theoretical function after binning with the amplitude normalized to unity
$B_{1,2}Q^2 + C_{1,2}Q + D_{1,2}$ - polynomial of the second order

Fit performed for theoretical spectra obtained for different optical potential parameters (V_0, W_0)

Comparison with N. Ikeno et al. model prediction

results obtained for different optical potential parameters (V_0, W_0)

V_0	W_0	A (fit) [nb]	$\sigma_{upp}^{CL=90\%}$ [nb]
-30	-5	-5.0±3.9	6.5
-30	-20	-2.2±3.5	5.8
-30	-40	0.2±3.8	6.3
-50	-5	0.1±3.8	6.3
-50	-20	3.3±4.1	6.8
-50	-40	6.0±4.2	6.9
-70	-5	6.4±4.5	7.4
-70	-20	7.9±4.5	7.4
-70	-40	7.5±3.7	6.1
-100	-5	6.3±4.5	7.4
-100	-20	6.9±3.9	6.4
-100	-40	5.3±3.1	5.2

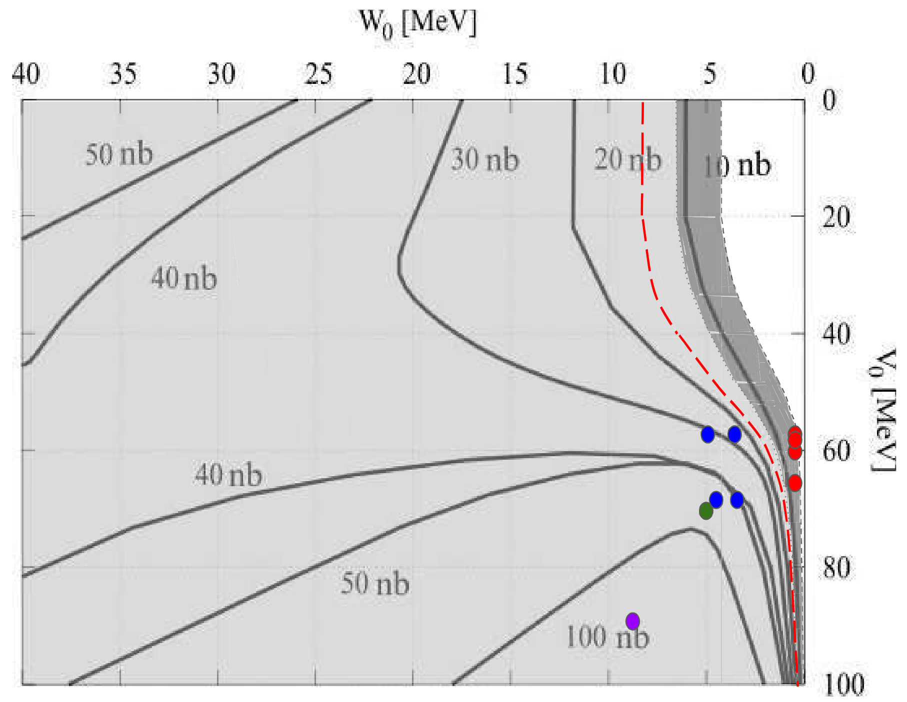

Contour plot of the theoretically determined conversion cross section in $V_0 - W_0$ plane.

The allowed parameter space ($|V_0| <\sim 60$ MeV and $|W_0| <\sim 7$ MeV) excludes most optical model predictions of $\eta-^4$He nuclei except for some loosely bound narrow states.

M. Skurzok, P. Moskal, et al., Phys. Lett. B 708, 6 (2018)

Search for $(^3\text{He-}\eta)_{bound}$ with WASA-at-COSY

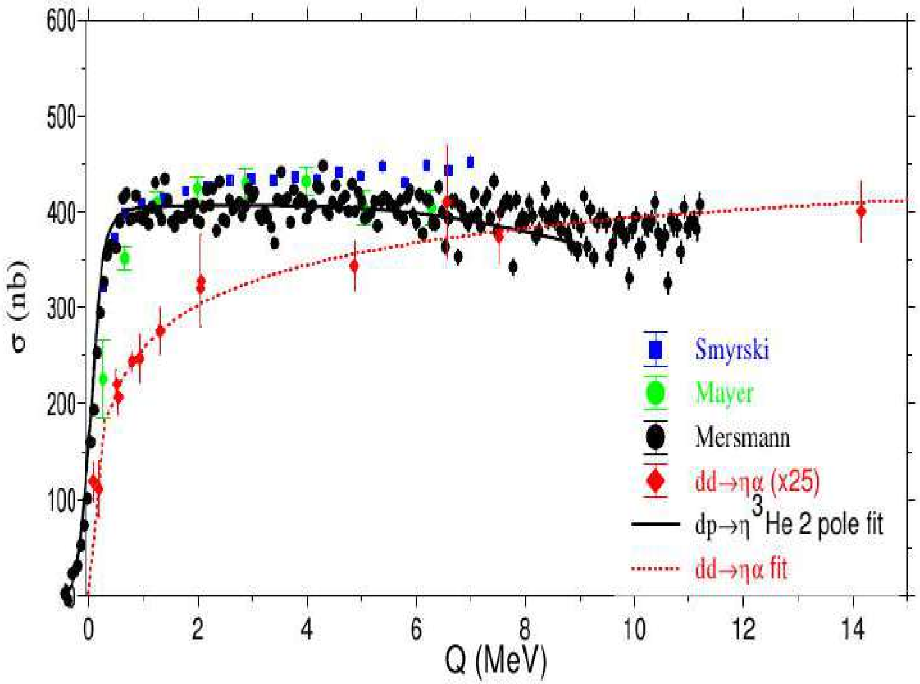

$$\sigma_{pd\to^3He-\eta} \approx 25\sigma_{dd\to^4He-\eta}$$

About 2 weeks of measurement allowed us to reach sensitivity of **few nb** ($L \approx 4500\frac{1}{nb}$)

Measurement: p_{beam} : 1.468-1.615GeV/c, **Q∈(-70,30)MeV**

Channels:

- **Via the resonance decay N^*:**
  1) $pd \to (^3\text{He-}\eta)_{bound} \to ppp\pi^-$
  2) $pd \to (^3\text{He-}\eta)_{bound} \to ppn\pi^0$
  3) $pd \to (^3\text{He-}\eta)_{bound} \to dp\pi^0$

  Aleksander Khreptak PhD

- **Absorption of orbiting η**
  4) $pd \to (^3\text{He-}\eta)_{bound} \to {}^3\text{He}\ 2\gamma$
  5) $pd \to (^3\text{He-}\eta)_{bound} \to {}^3\text{He}\ 6\gamma$

  Oleksandr Rundel PhD

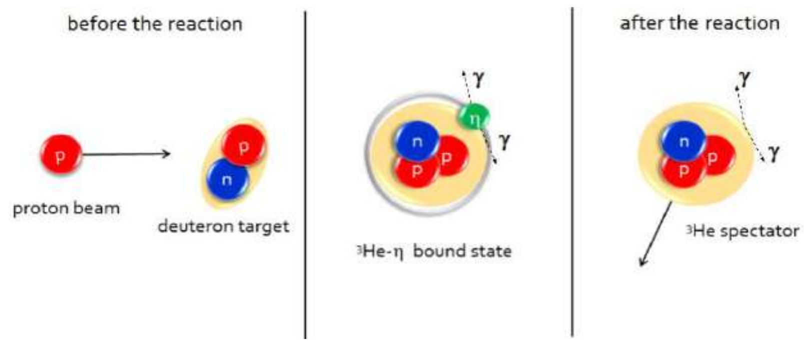

$pd \to (^3\mathrm{He}\text{-}\eta)_{bound} \to dp\pi^0$ analysis

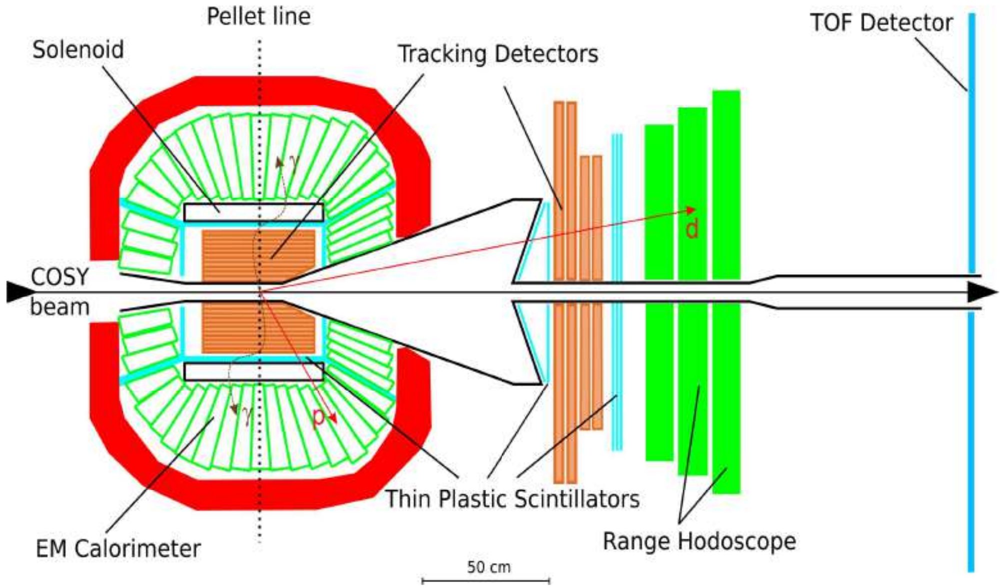

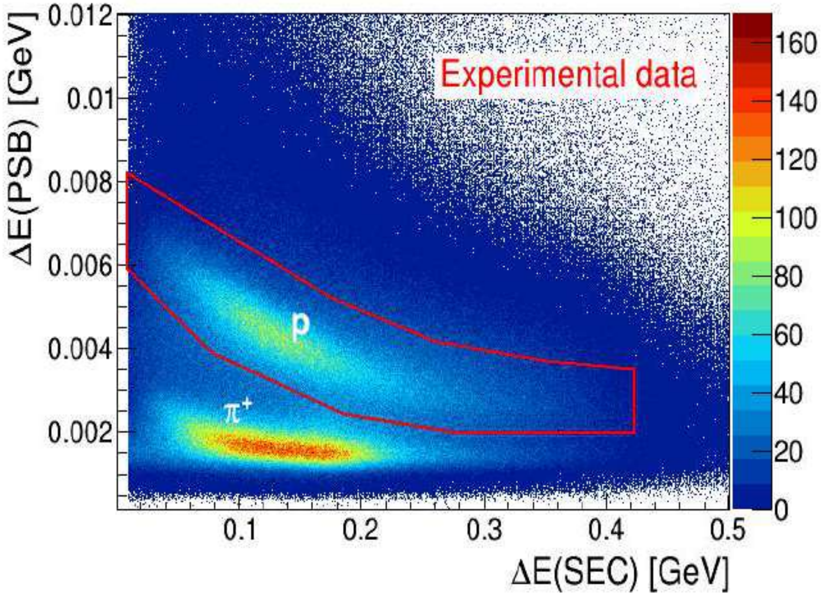

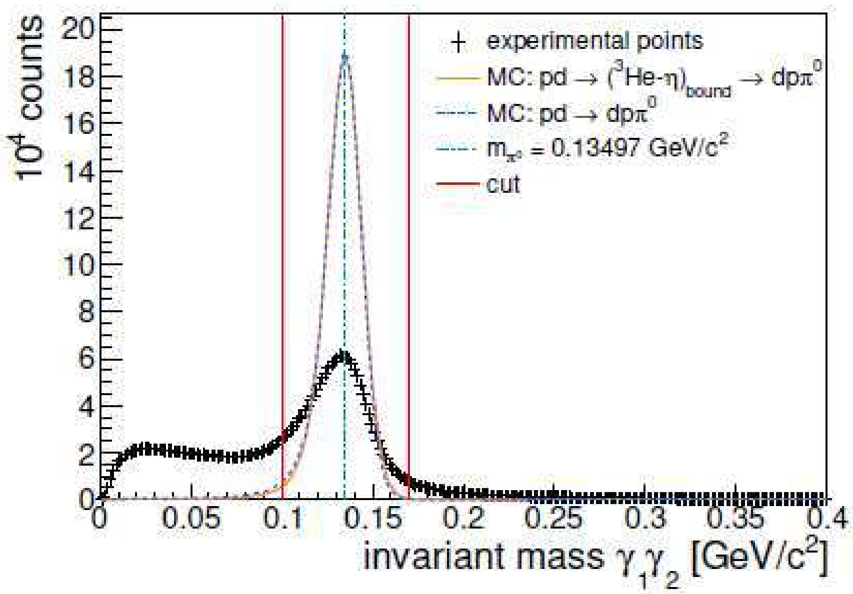

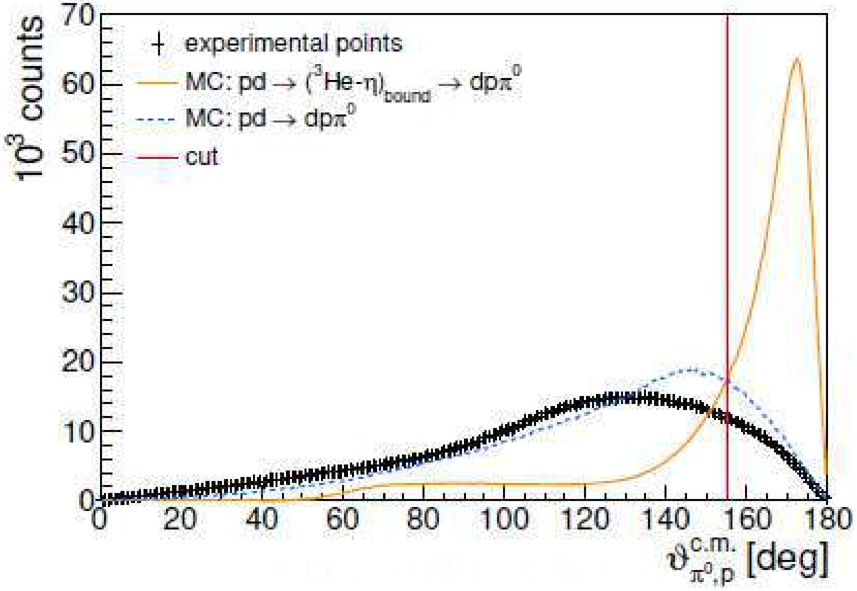

$pd \rightarrow (^3\text{He-}\eta)_{bound} \rightarrow dp\pi^0$ analysis

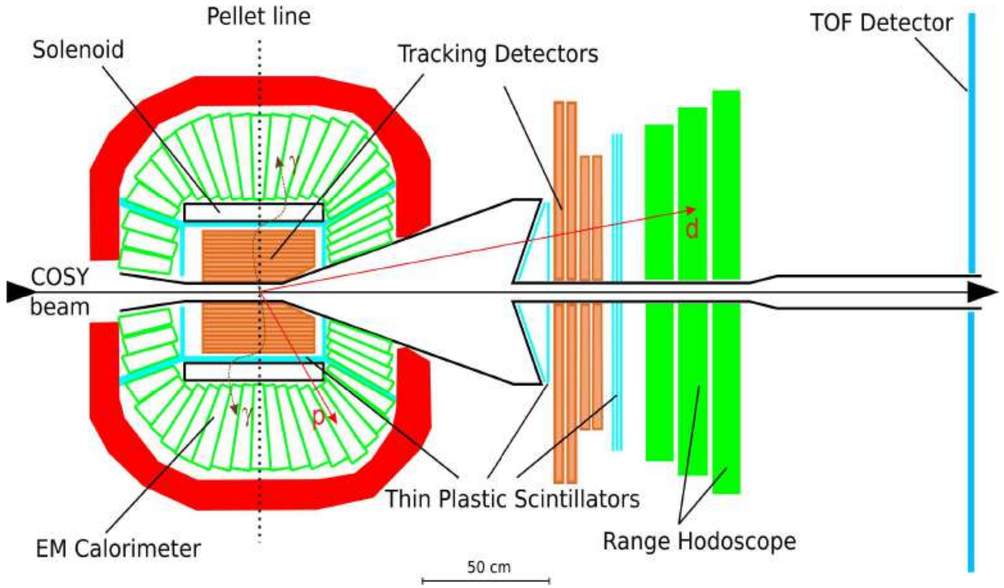

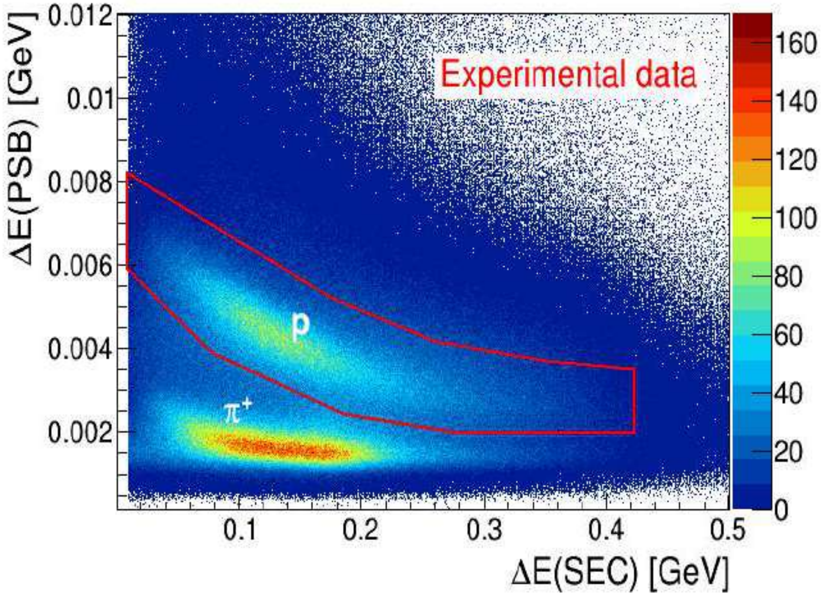

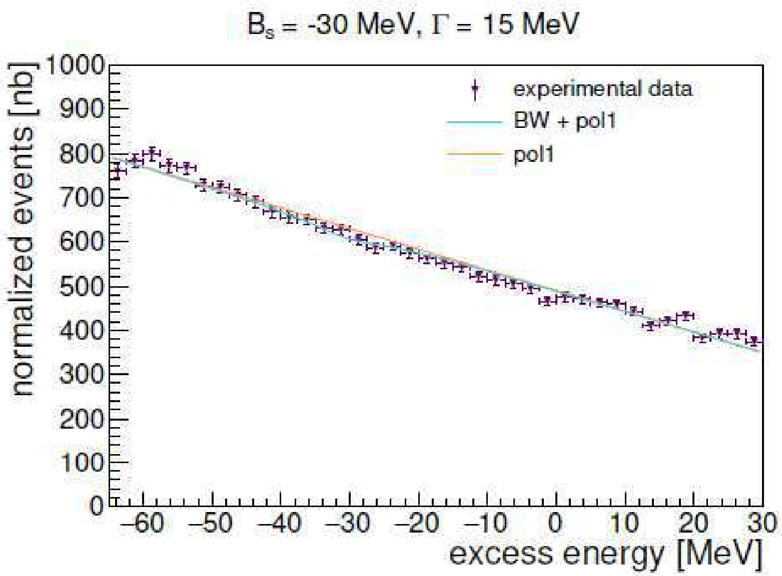

$$\frac{A \cdot \frac{\Gamma^2}{4}}{(Q - B_s)^2 + \frac{\Gamma^2}{4}} + BQ + C$$

Breit-Wigner (signal) + pol1 (background)

B_s and Γ fixed parameters

A, B, C free parameters

$$\sigma^{upp}_{CL=90\%} = k \cdot \sigma_A, \ k = 1.64 \ (CL = 90\%)$$

Upper limit of the total cross section

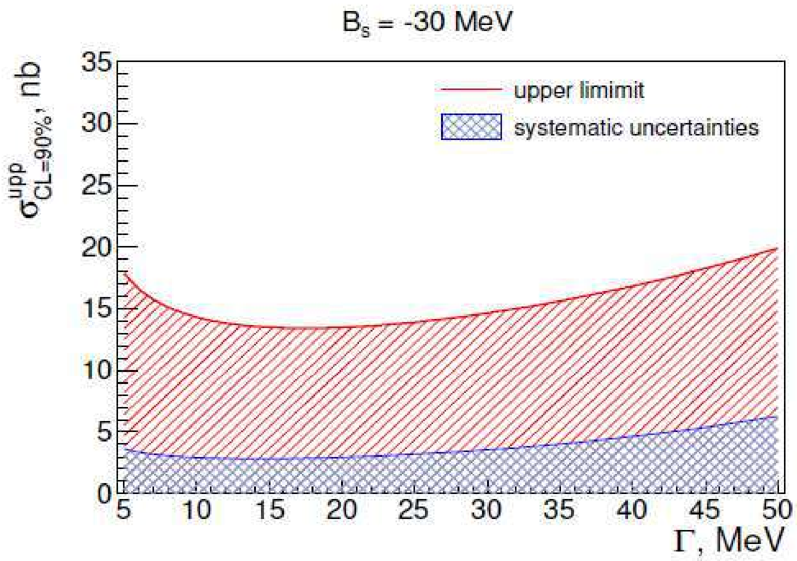

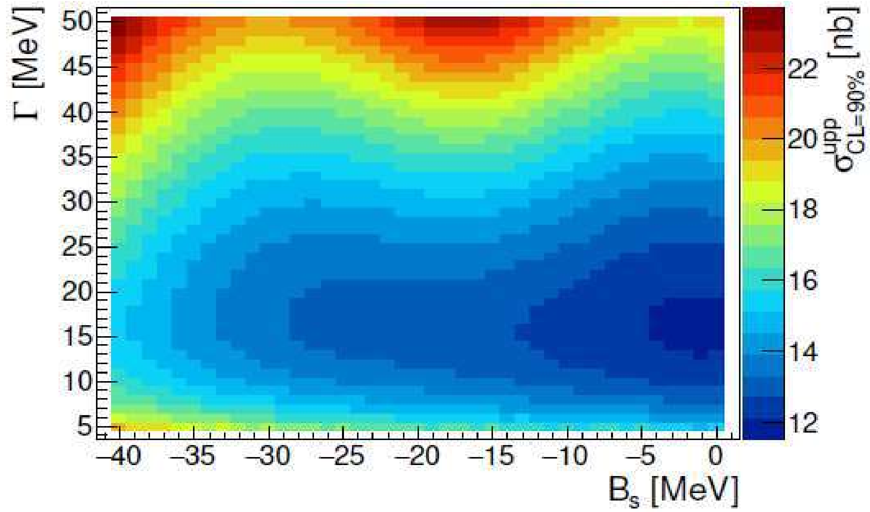

Result

$$13\ nb \leq \sigma^{upp}_{pd\to(^3\text{He-}\eta)_{bound}\to dp\pi^0} \leq 24\ nb$$

P. Adlarson et al., Phys. Rev. C 102, 044322 (2020)

Previous result:

COSY-11 $\sigma_{pd\to(^3He-\eta)_{bound}\to {}^3He\pi^0} < 70\ nb$

J. Smyrski et al., Nucl. Phys. A 790 (2007) 438

Simulation of $pd \to (^3\text{He-}\eta)_{bound} \to {}^3\text{He}\ 2\gamma(6\gamma)$

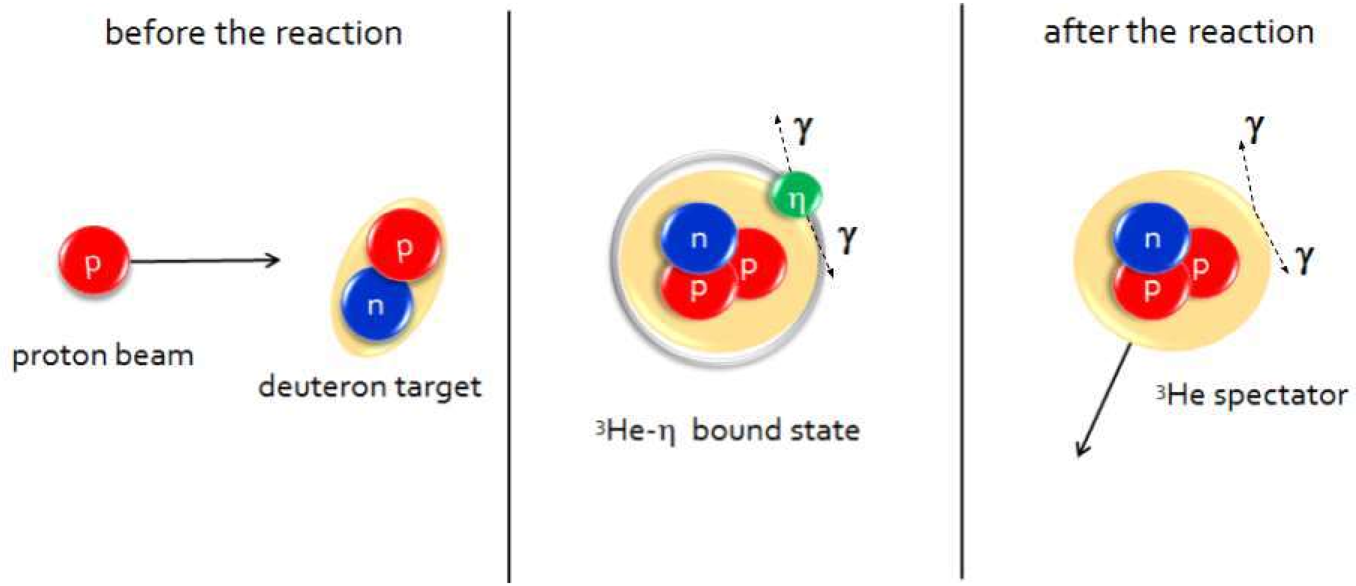

- ^{3}He is spectator $|\mathbb{P}_{^3He}|^2 = m^2_{^3He}$
- **Fermi momentum distribution of the η meson in ^{3}He-η bound system**

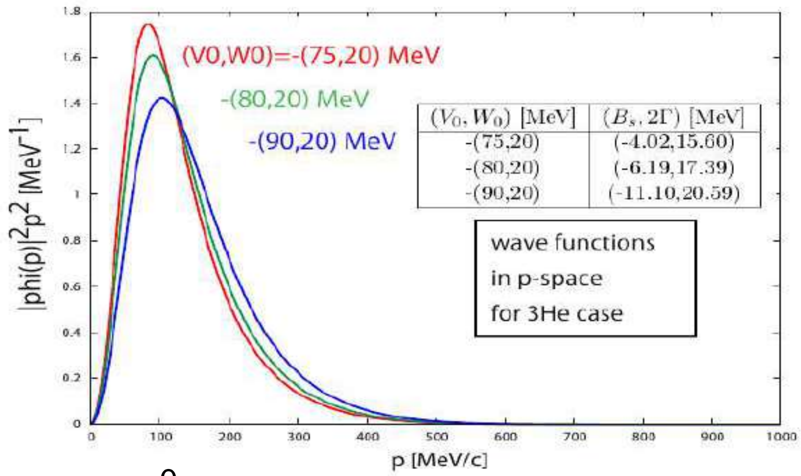

- **bound η decays to 2γ or $3\pi^0$**

Simulation of $pd \to (^3\text{He-}\eta)_{bound} \to {}^3\text{He}\ 2\gamma(6\gamma)$

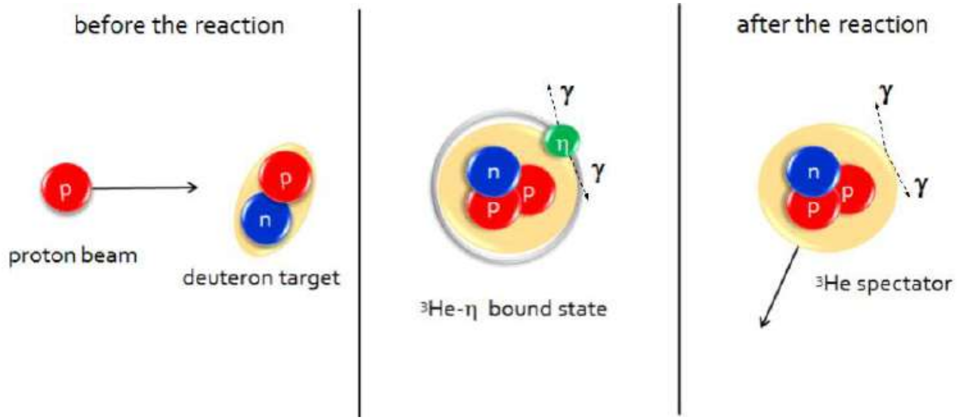

- **^{3}He is spectator** $|\mathbb{P}_{^3He}|^2 = m^2_{^3He}$
- **Fermi momentum distribution of the η meson in ^{3}He-η bound system**

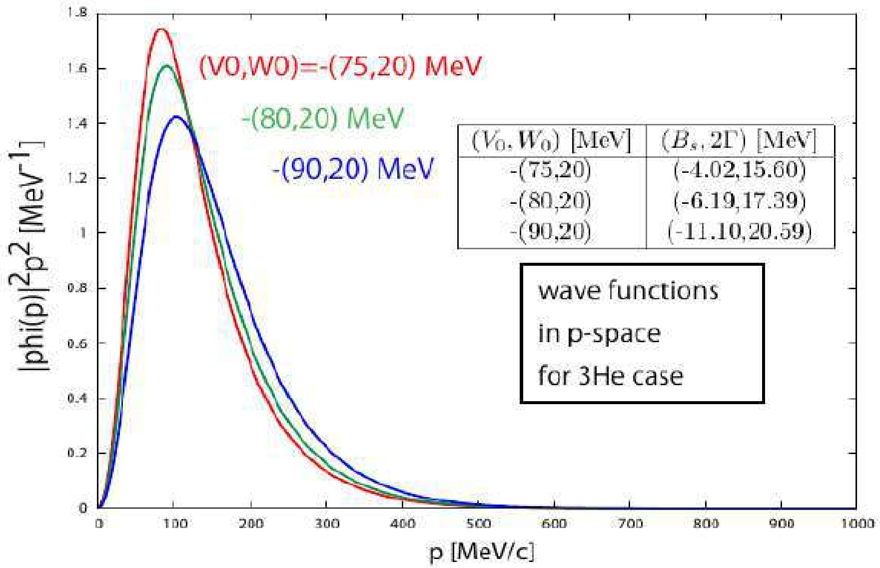

- **bound η decays to 2γ or $3\pi^0$**

M. Skurzok et al., Nucl. Phys. A 993, 121647 (2020)

Structure of hypothetical ^{3}He-η bound state can be described as a solution of Klein-Gordon equation:

$$\left[-\vec{\nabla}^2 + \mu^2 + 2\mu U_{opt}(r)\right]\psi(\vec{r}) = E^2_{KG}\psi(\vec{r})$$

where: E_{KG} - Klein -Gordon energy, μ - ^{3}He-η reduced mass

optical potential:

$$U_{opt}(r) = (V_0 + iW0)\frac{\rho(r)}{\rho_0}$$

where: $\rho(r)$ - density distr. for ^{3}He, ρ_0 - normal nuclear density

KG equation solved for several sets of (V_0, W_0)

$$\Downarrow$$

$$E_{KG},\ \psi(\vec{r})$$

Search for $(^3\text{He-}\eta)_{bound}$ | Selection criteria

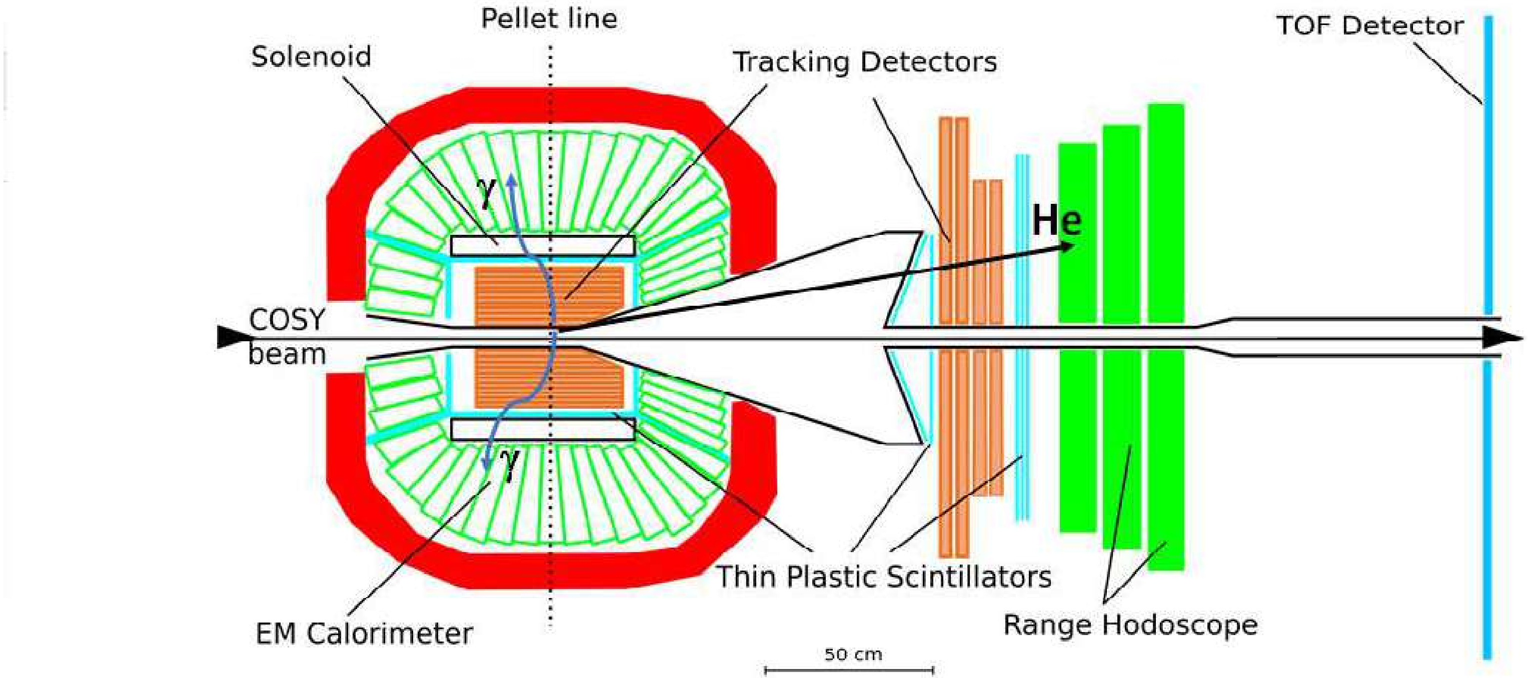

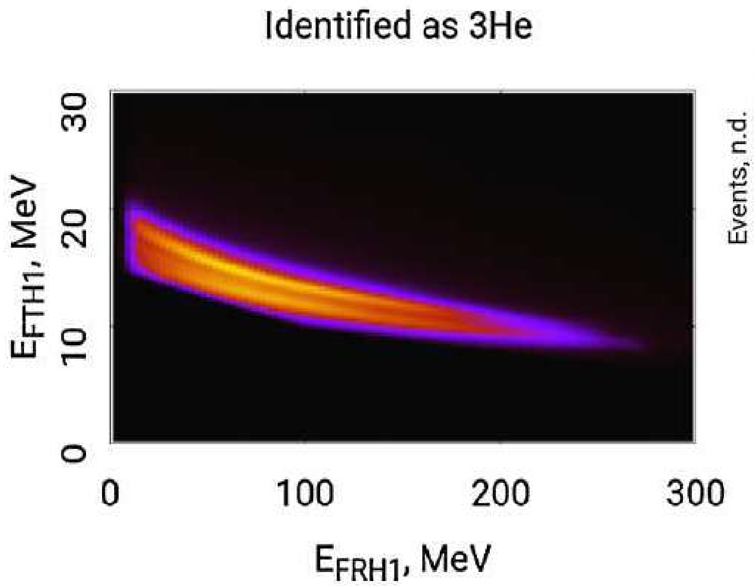

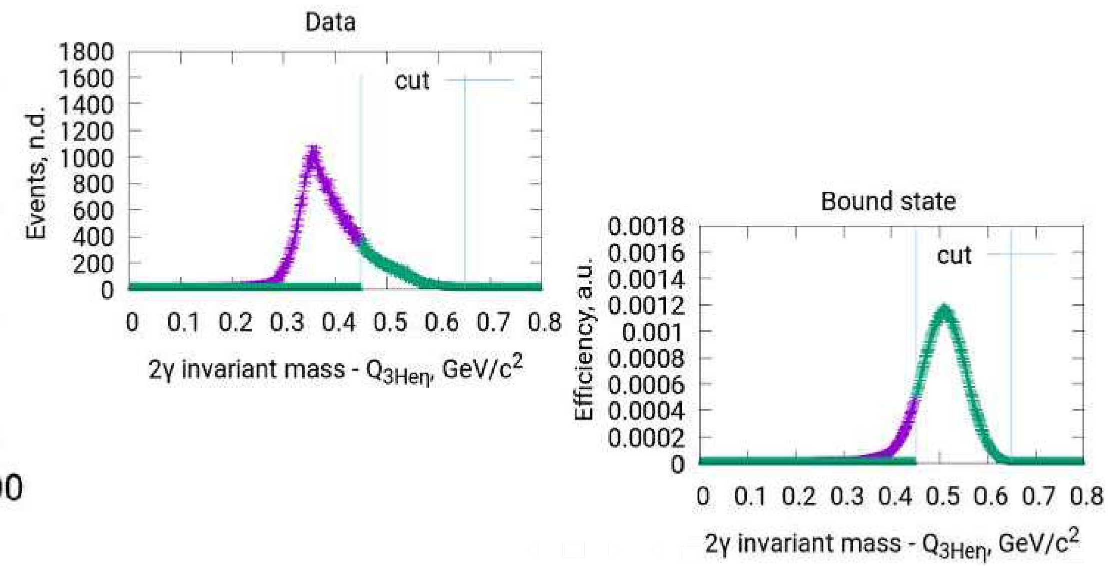

Excitation function $pd \rightarrow (^3\text{He-}\eta)_{bound} \rightarrow {}^3\text{He}\ 2\gamma$

Cross section

$$\sigma(Q) = \frac{N(Q)}{L(Q)\epsilon(Q)}$$

N - number of experimental events

L - integrated luminosity

ϵ - full detection efficiency

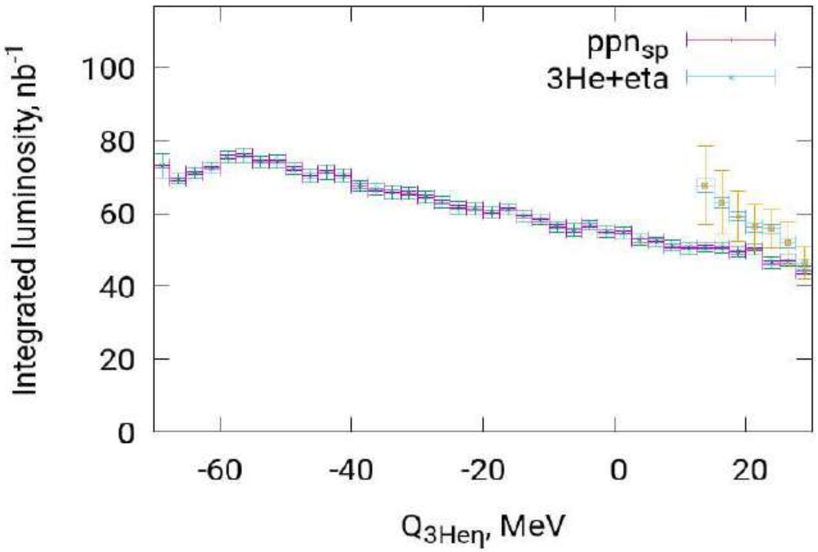

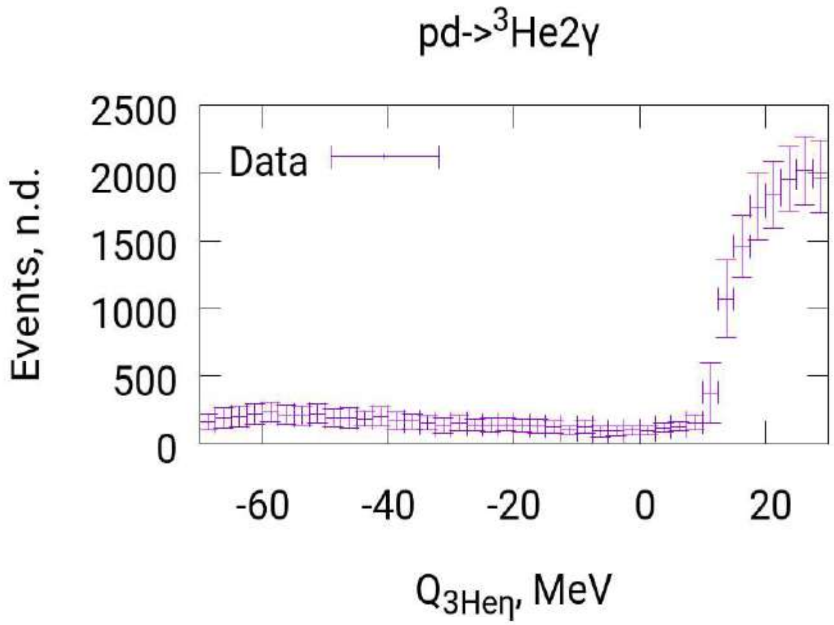

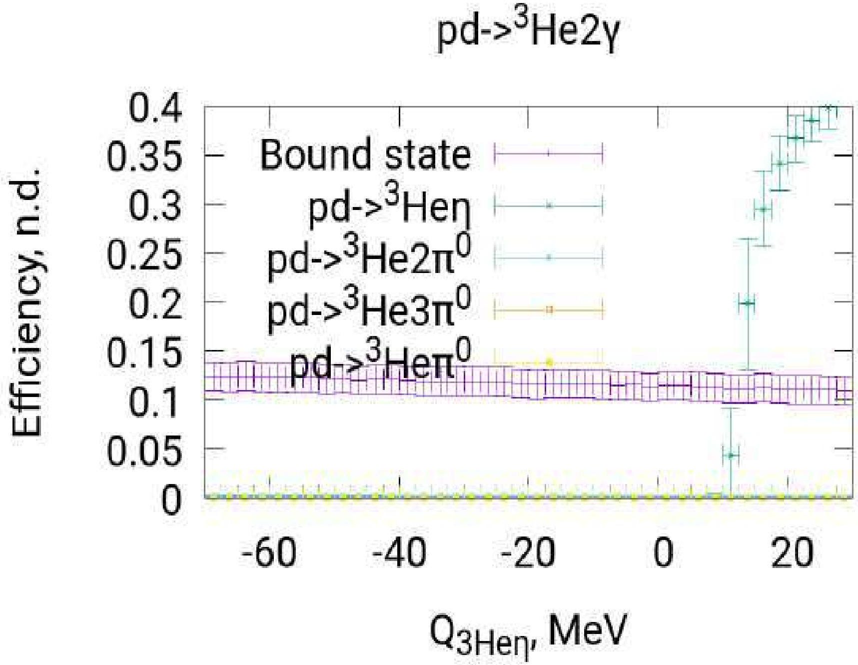

Determination of the upper limit of the total cross section for $pd \to ({}^3\text{He-}\eta)_{bound} \to {}^3\text{He}2\gamma(6\gamma)$ processes at CL=90%

$pd \to ({}^3\text{He-}\eta)_{bound} \to {}^3\text{He}2\gamma$ $\Downarrow$

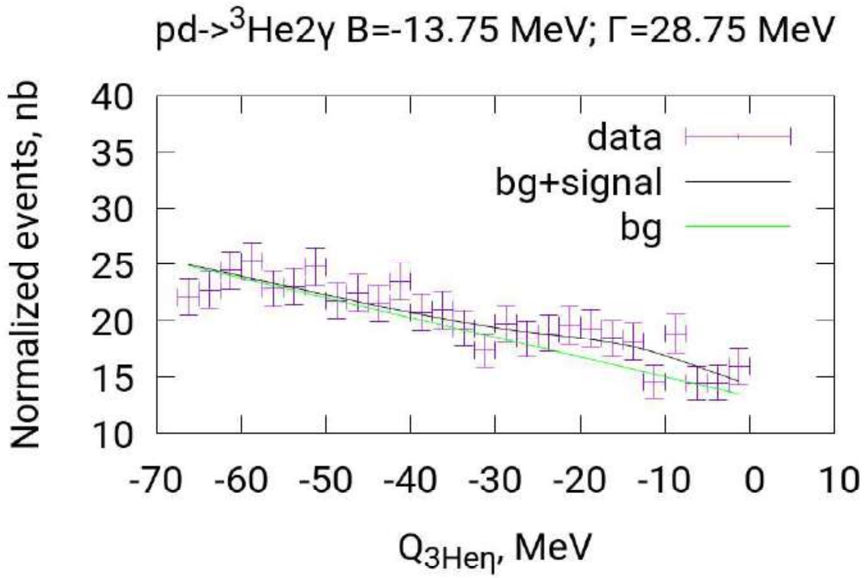

$pd \to ({}^3\text{He-}\eta)_{bound} \to {}^3\text{He}6\gamma$ $\Downarrow$

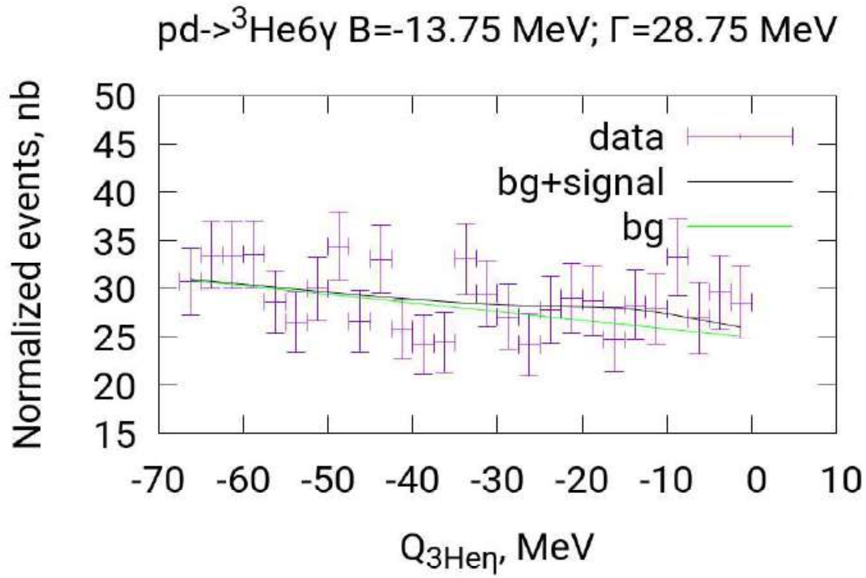

simultaneous fit with $P_{\eta decay} \frac{A \cdot \Gamma^2/4}{(Q - B_s)^2 + \Gamma^2/4} + BQ + C$

Breit-Wigner (signal) + pol2 (background)

where $P_{\eta decay}$ are branching ratios for η decays:
$P_{\eta \to 2\gamma} = 0.3941$, $P_{\eta \to 3\pi^0} = 0.3268$

B_s, Γ - fixed parameters | A, B, C - free parameters || $\sigma^{upp}_{CL=90\%} = A + k \cdot \sigma_A$, k=1.64 (for CL=90%)

Determination of the upper limit of the total cross section for $pd \to (^3\text{He-}\eta)_{bound} \to {}^3\text{He}2\gamma(6\gamma)$ process at CL=90%

$\sigma^{upp}_{CL=90\%}$ for

$pd \to (^3\text{He-}\eta)_{bound} \to {}^3\text{He}2\gamma(6\gamma)$

$\Downarrow$

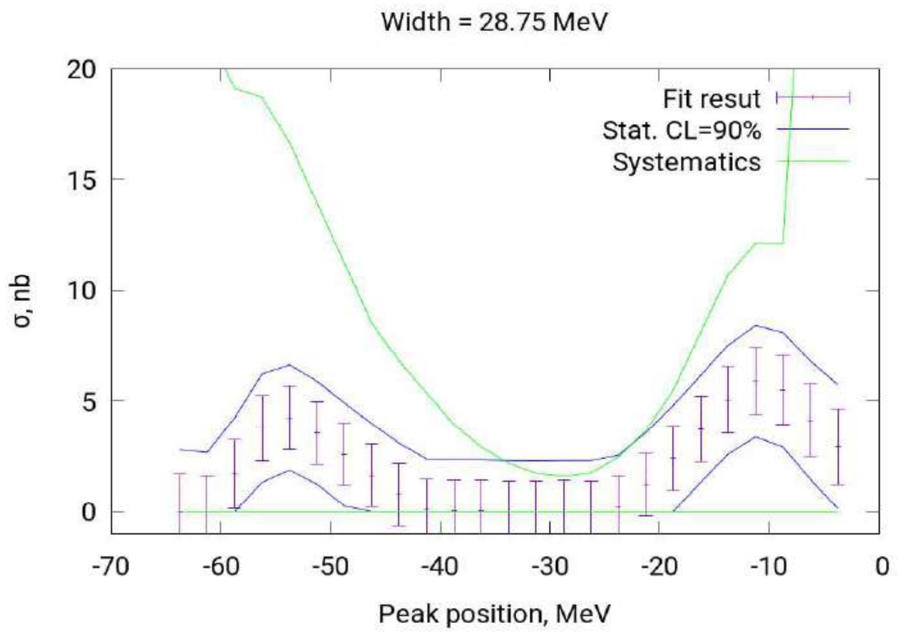

RESULT:

$\sigma_{pd\to(^3He-\eta)_{bound}\to^3He2\gamma(6\gamma)} < 15\ nb$

INDICATION:-)

slight indication of the signal from the bound state for $\Gamma > 20$ MeV and $B_s \in (0, 15)$ MeV

$\Downarrow$

However, the observed indication is within the range of the systematic error

$\Downarrow$

we cannot make a definite conclusion here on possible bound state formation

Previous result:
COSY-11

$\sigma_{pd\to(^3He-\eta)_{bound}\to^3He\pi^0} < 70\ nb$

J. Smyrski et al., Nucl. Phys. A 790 (2007) 438

P. Adlarson et al., Phys. Lett. B 802, 135205 (2020)

Summary of the search for η-mesic Helium at WASA

$({}^4\text{He-}\eta)_{bound}$

- **2008**: $dd \to {}^3\text{He}p\pi^-$ reaction

$$\sigma_{dd\to({}^4He-\eta)_{bound}\to{}^3Hep\pi^-} < 27\ nb$$

- **2010**: $dd \to {}^3\text{He}n\pi^0$ and $dd \to {}^3\text{He}p\pi^-$ reactions

$$\sigma_{dd\to({}^4He-\eta)_{bound}\to{}^3Hep\pi^-} < 7\ nb$$

$$\sigma_{dd\to({}^4He-\eta)_{bound}\to{}^3Hen\pi^0} < 3.5\ nb$$

$({}^3\text{He-}\eta)_{bound}$

- **2014**: $pd \to {}^3\text{He}2\gamma$ and $pd \to {}^3\text{He}6\gamma$ reactions

$$\sigma_{pd\to({}^3He-\eta)_{bound}\to{}^3He2\gamma(6\gamma)} < 15\ nb$$

- **2014**: $pd \to dp\pi^0$ reaction

$$\sigma_{pd\to({}^3He-\eta)_{bound}\to dp\pi^0} < 24\ nb$$

Kaonic atoms

atom

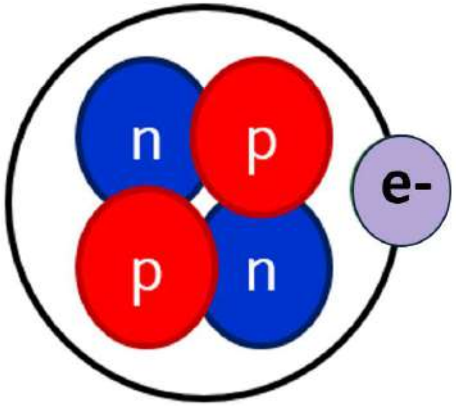

electromagnetic interaction

kaonic atom

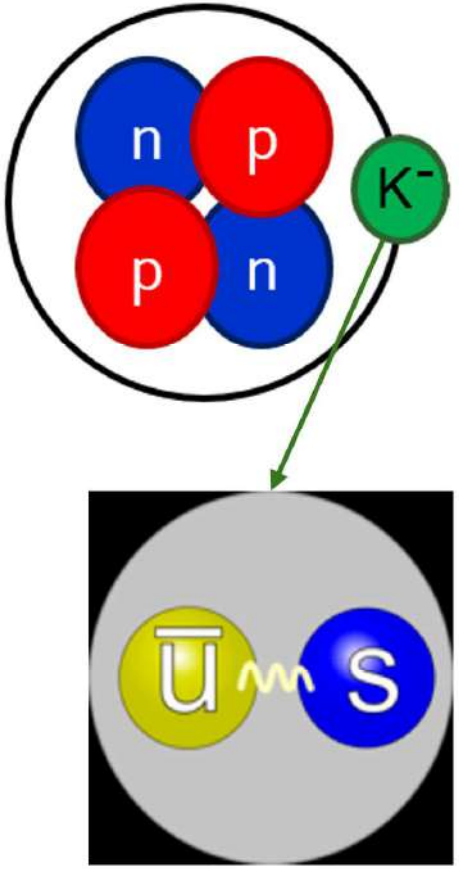

quarks!

electromagnetic interaction
+ strong!

K^- interaction with nucleon

The χPT is not applicable to the K̄N channel due to the emerging of the Λ(1405) and the Σ(1385) resonances just below the K̄N mass threshold

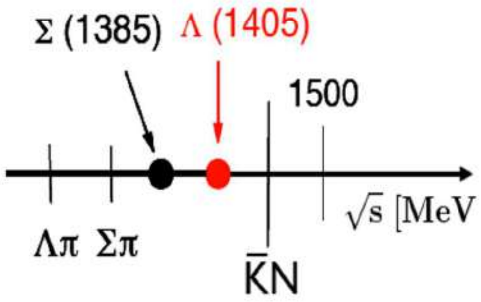

Λ(1405) I=0 $J^P = ½^-$

$M = (1405.1^{+1.3}_{-1.0})$ MeV $\Gamma = (50.5 \pm 2.0)$ MeV

decay modes: Σπ (I=0) 100%

Σ(1385) I=1 $J^P = 3/2^+$

decay modes: Λ π (I=1) (87.0 ± 1.5) %

Σ π (I=1) (11.7 ± 1.5) %

Possible solutions:

- Non-perturbative Coupled Channels approach: Chiral Unitary SU(3) Dynamics
- Phenomenological K̄N and NN potentials

The parameters of the models are constrained by the existing scattering data

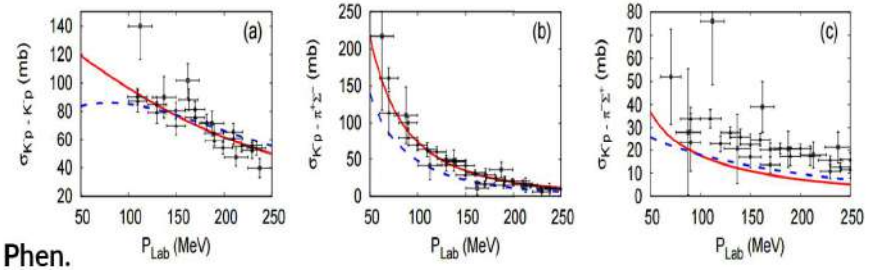

Phen.

Y. Ikeda and T. Sato, Phys. Rev. C76, 035203 (2007)

Chiral

S. Ohnishi, Y. Ikeda, T. Hyodo, W. Weise, Phys.Rev. C93 (2016) no.2, 025207

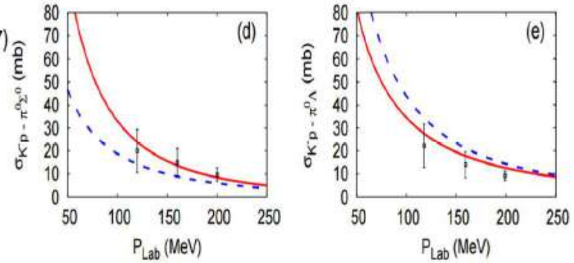

...but... large differences in the subthreshold extrapolations!
Significantly weaker attraction in chiral SU(3) models than in phenomenological potential models.

Re Im

Phen. [Y. Akaishi, T. Yamazaki, Phys. Rev. C65, 044005 (2002)]

Chiral [Y. Ikeda, T. Hyodo, W. Weise, Phys. Lett. B706, 63 (2011)]

Phenomenologic potential model

Chiral SU(3) dynamics

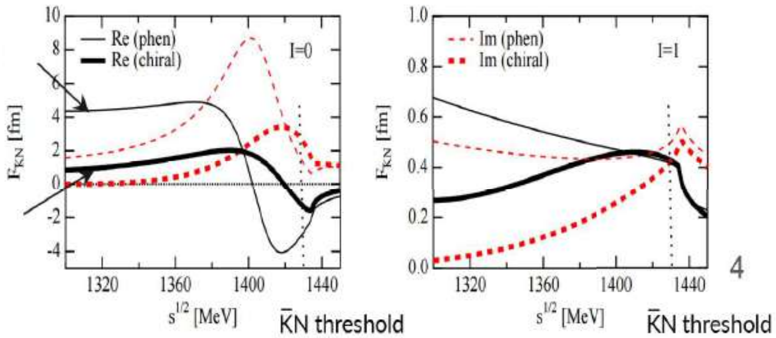

K^- interaction with nucleon

The χPT is not applicable to the $\bar{K}N$ channel due to the emerging of the Λ(1405) and the Σ(1385) resonances just below the $\bar{K}N$ mass threshold

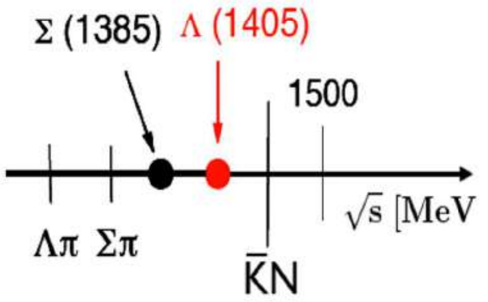

Λ(1405) I=0 $J^P = ½^-$
M = $(1405.1^{+1.3}_{-1.0})$ MeV Γ = (50.5 ± 2.0) MeV
decay modes: Σπ (I=0) 100%

Σ(1385) I=1 $J^P = 3/2^+$
decay modes: Λ π (I=1) (87.0 ± 1.5) %
Σ π (I=1) (11.7 ± 1.5) %

Possible solutions:

- Non-perturbative Coupled Channels approach: Chiral Unitary SU(3) Dynamics
- Phenomenological $\bar{K}N$ and NN potentials

Λ(1405) state is given by the superpositions of **two poles of the KN scattering amplitude**

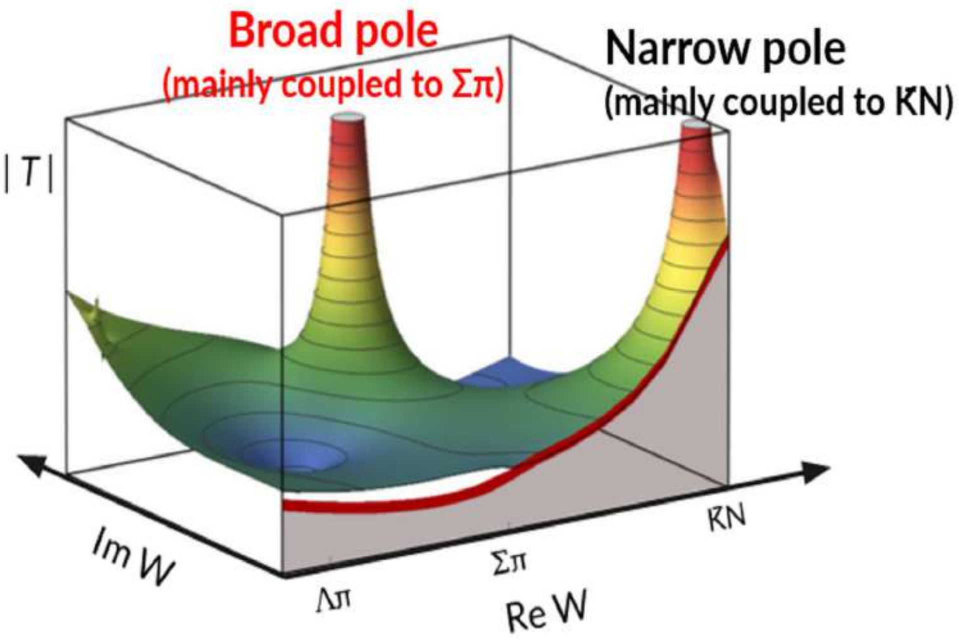

[from M. Mai talk at NSTAR19 conference]

the **Λ(1405) is a pure KN bound state** with mass M=1405 MeV, binding energy BE = 27 MeV and width Γ=50 MeV

K^- interaction with nucleon

K-p: agreement → Kaonic Hydrogen ⇨ SIDDHARTA - constraint at threshold

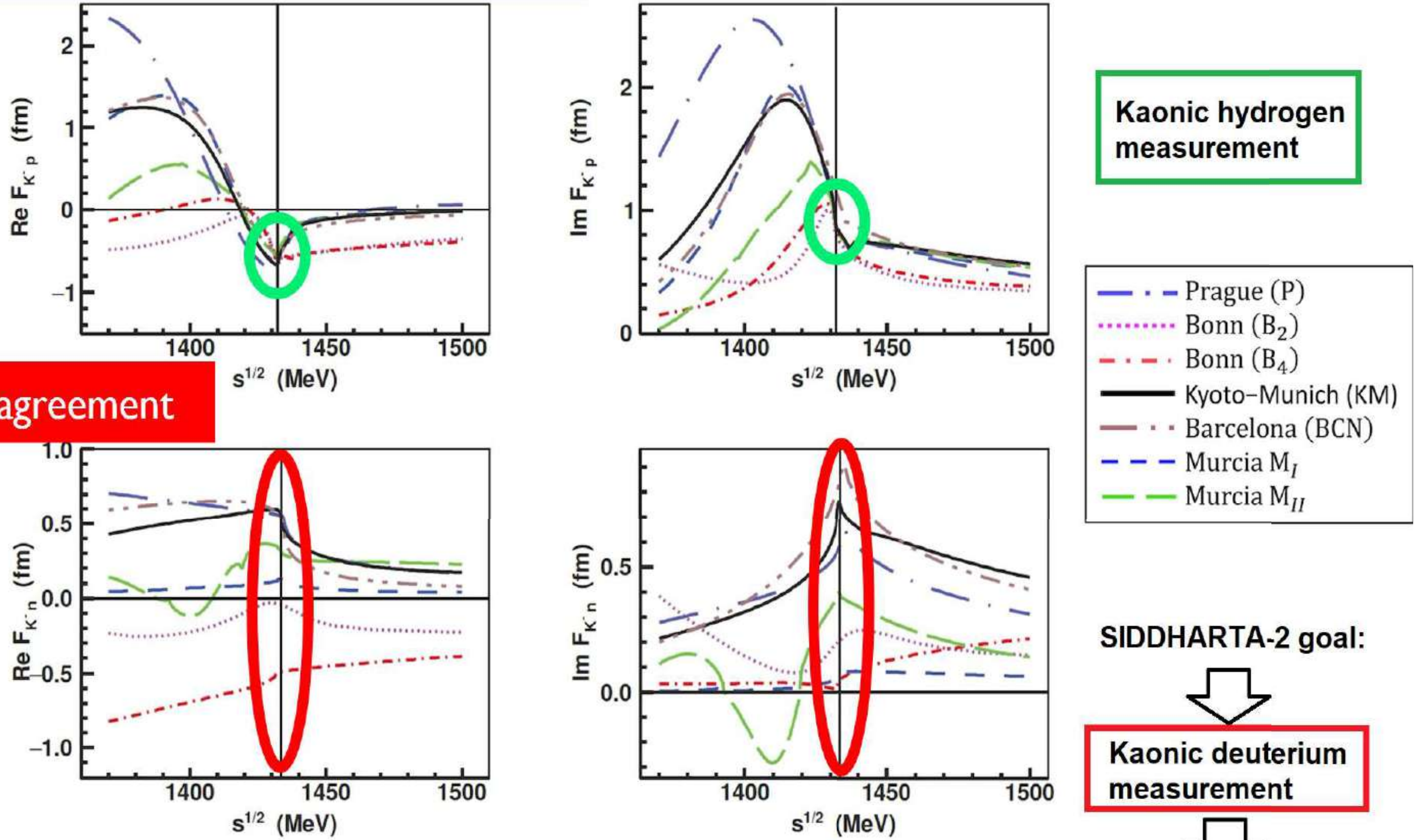

Kaonic hydrogen measurement

K-n: disagreement

SIDDHARTA-2 goal:

⇩

Kaonic deuterium measurement

⇩

constraint at threshold

Cieply, A. et al. From KN interactions to K-nuclear quasi-bound states. AIP Conf. Proc. 2249, 030014 (2020)

SIDDHARTA-2 Scientific goal

Precision measurements of kaonic atoms X-ray transitions -> **unique** info about the QCD in non-perturbative regime in the strangeness sector **not obtainable otherwise**

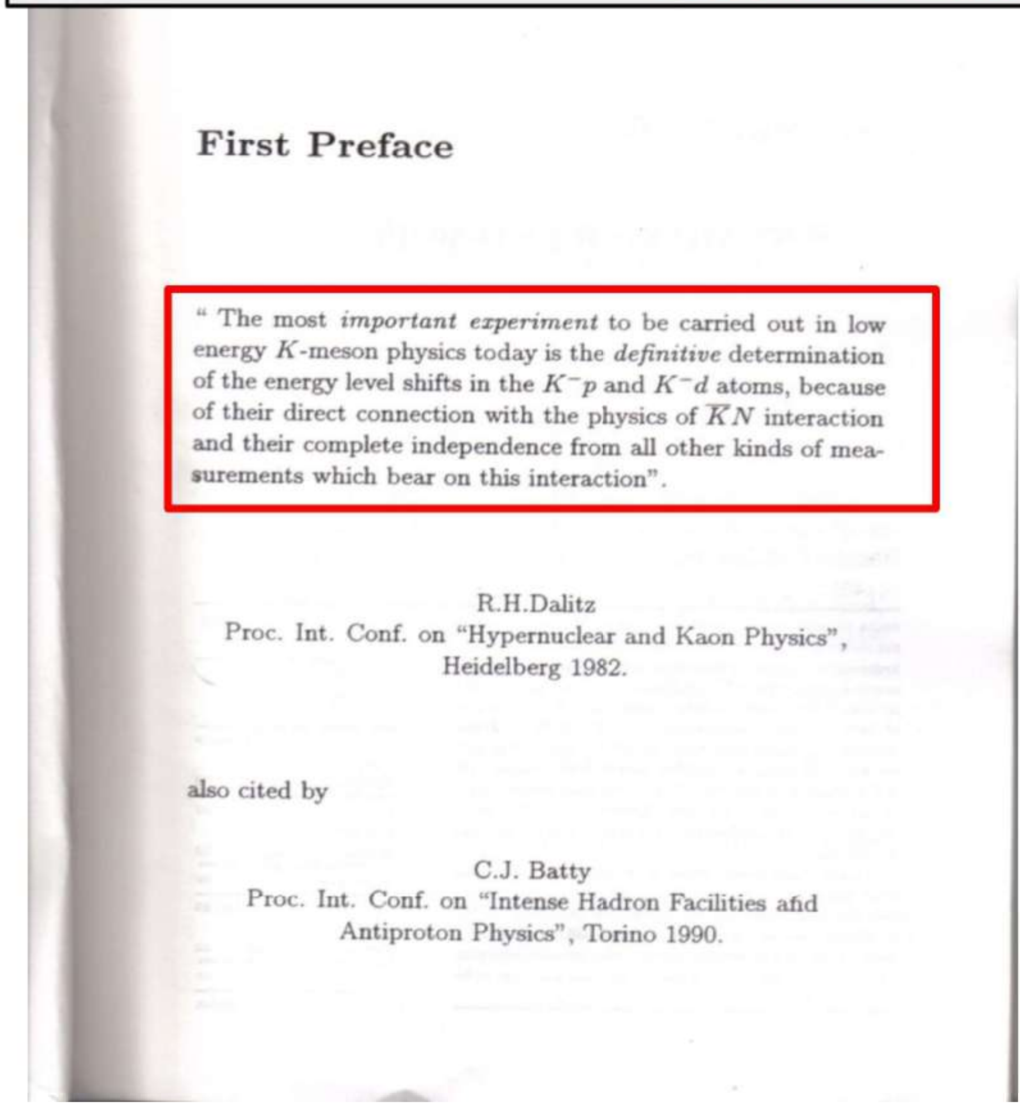

First Preface

" The most *important experiment* to be carried out in low energy K-meson physics today is the *definitive* determination of the energy level shifts in the K^-p and K^-d atoms, because of their direct connection with the physics of $\overline{K}N$ interaction and their complete independence from all other kinds of measurements which bear on this interaction".

R.H.Dalitz
Proc. Int. Conf. on "Hypernuclear and Kaon Physics", Heidelberg 1982.

also cited by

C.J. Batty
Proc. Int. Conf. on "Intense Hadron Facilities and Antiproton Physics", Torino 1990.

Precision *measurement of the shift* and *of the width*

→ of the 1s level of kaonic hydrogen (SIDDHARTA)
C. Curceanu, et al., Rev. Mod. Phys. 91, 025006 (2019)

→ the first measurement of the 1s level of kaonic deuterium (SIDDHARTA-2)

⬇

extract the **antikaon-nucleon isospin dependent scattering lengths**

Kaonic atom production

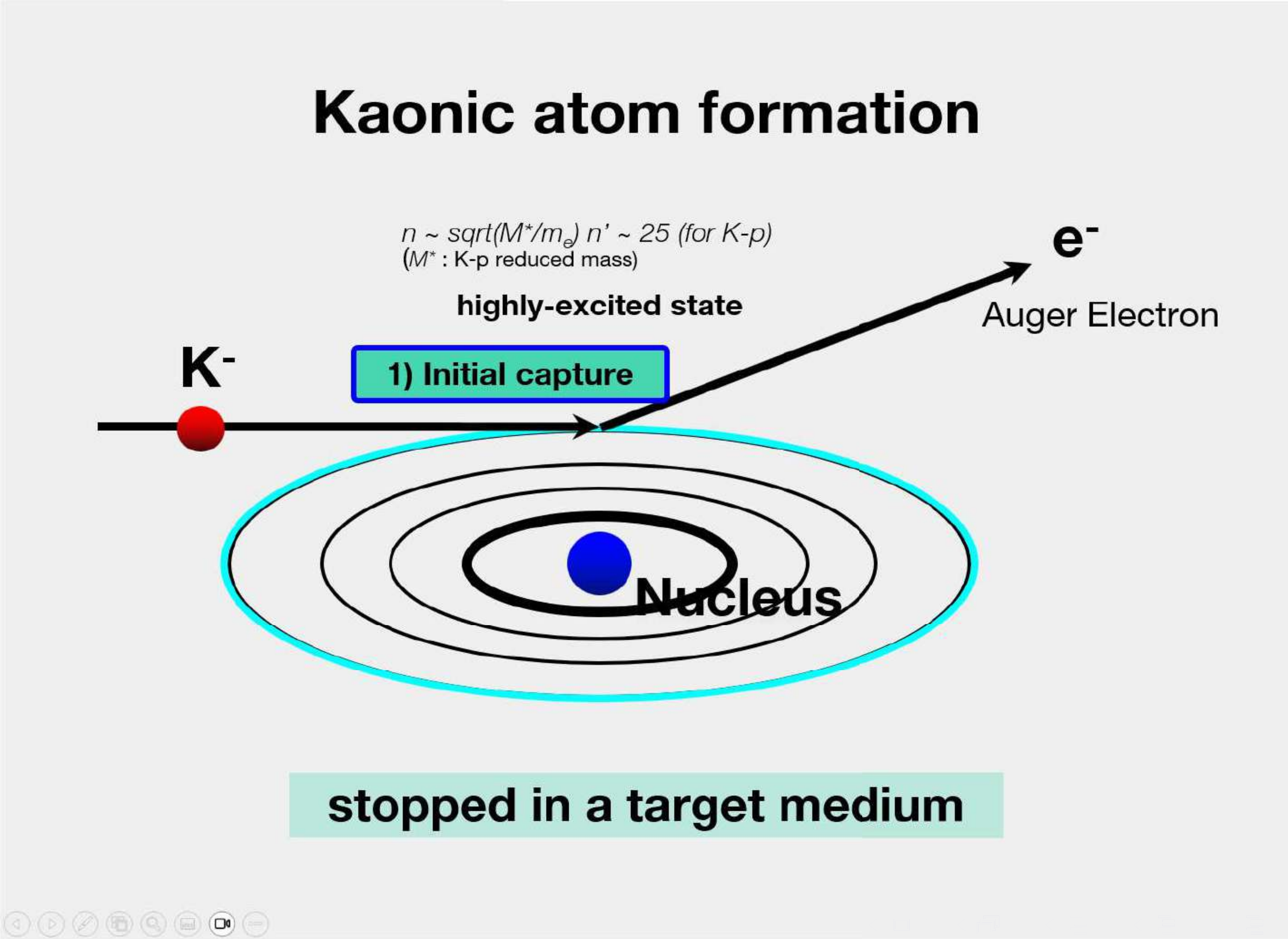

Kaonic atom production

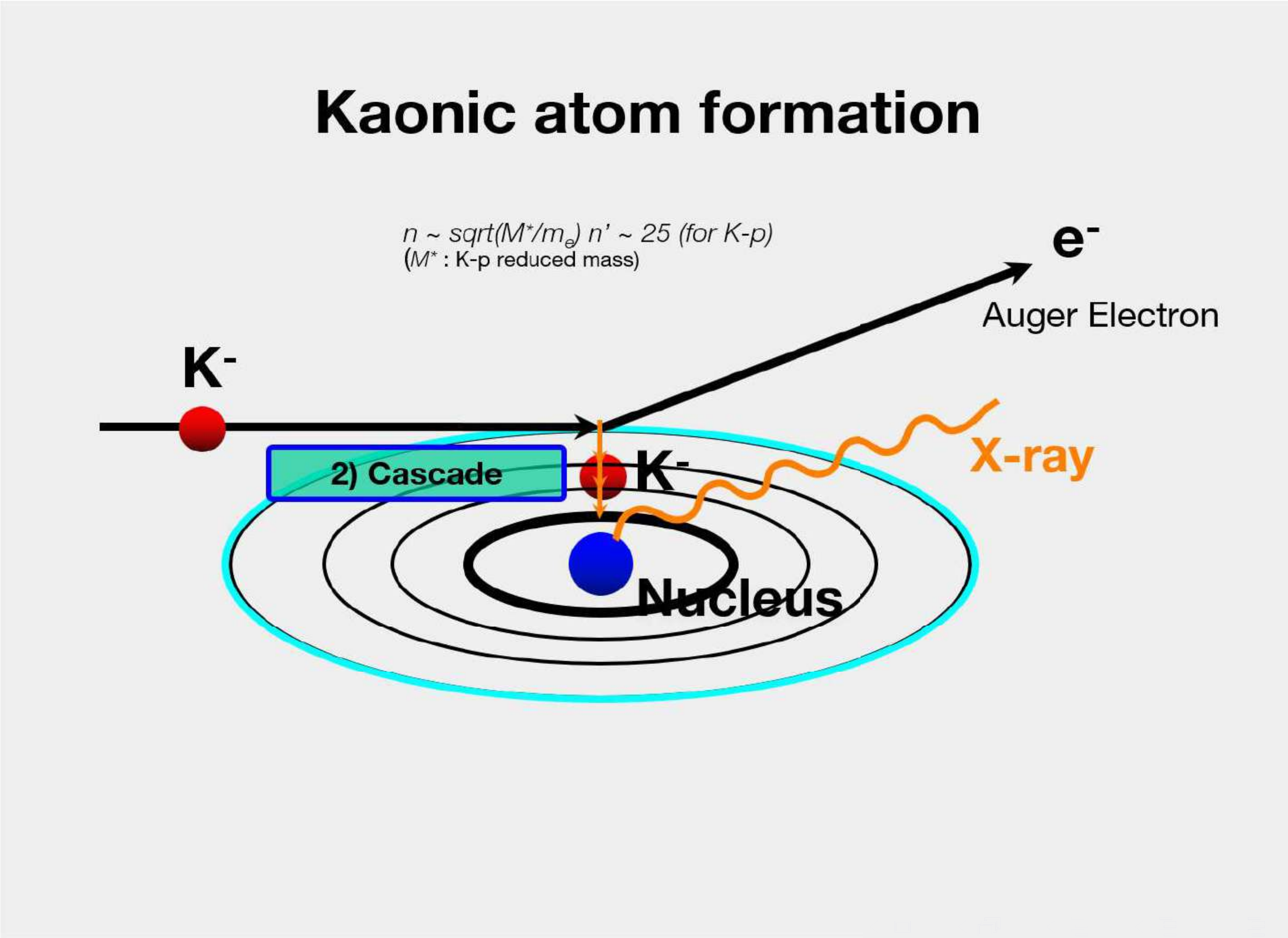

Kaonic atom production

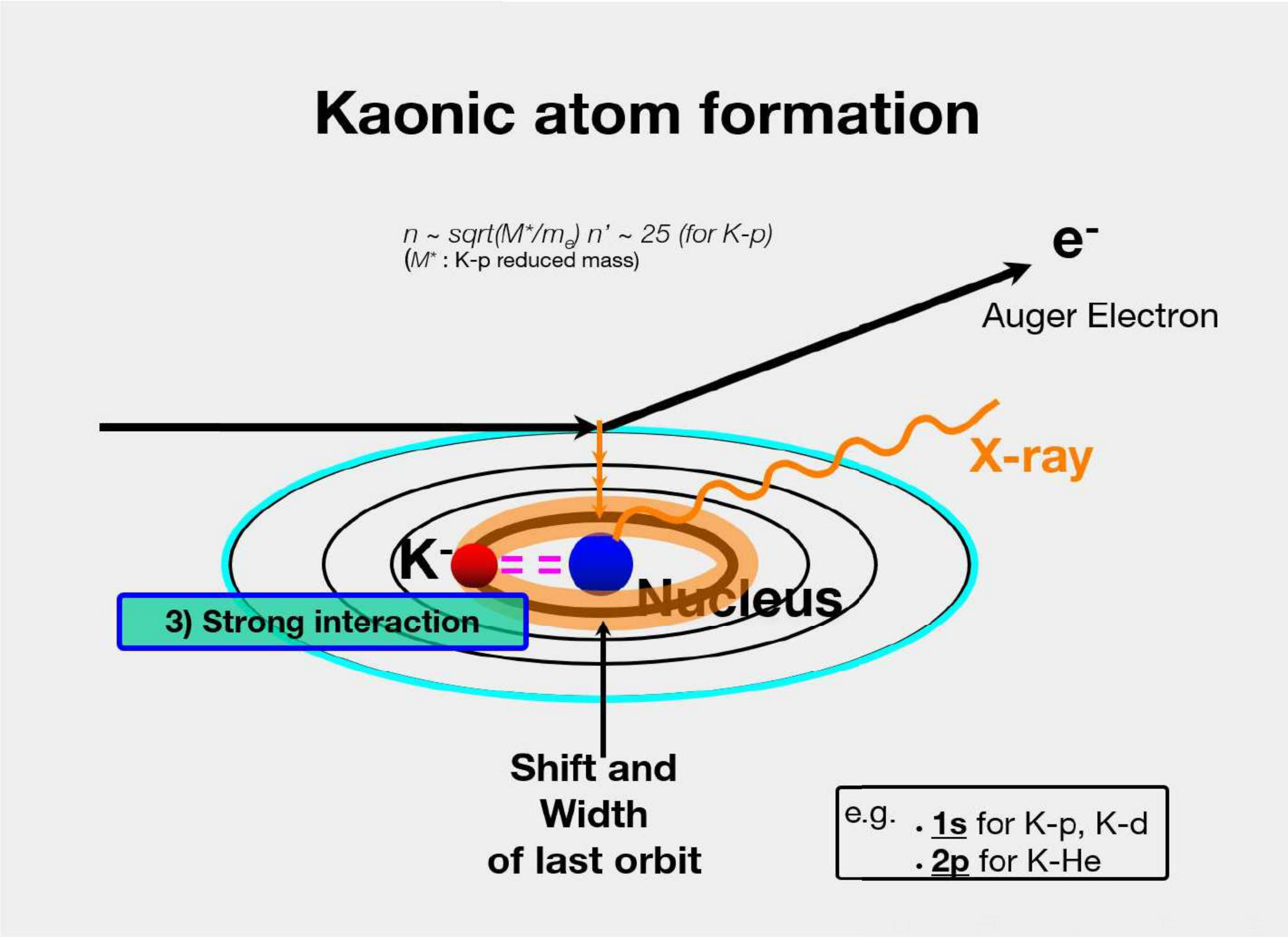

Kaonic atom production

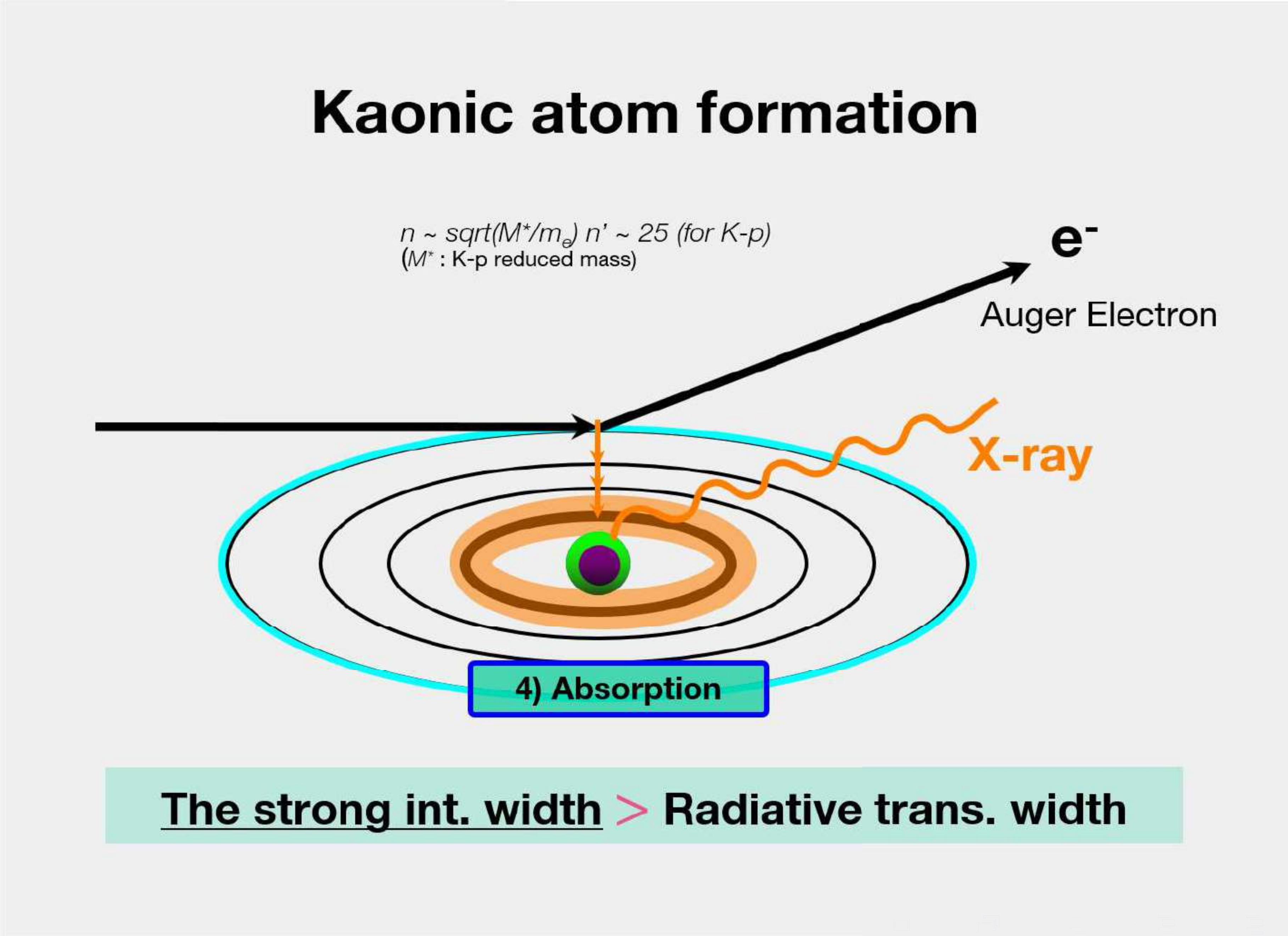

Kaonic atom production

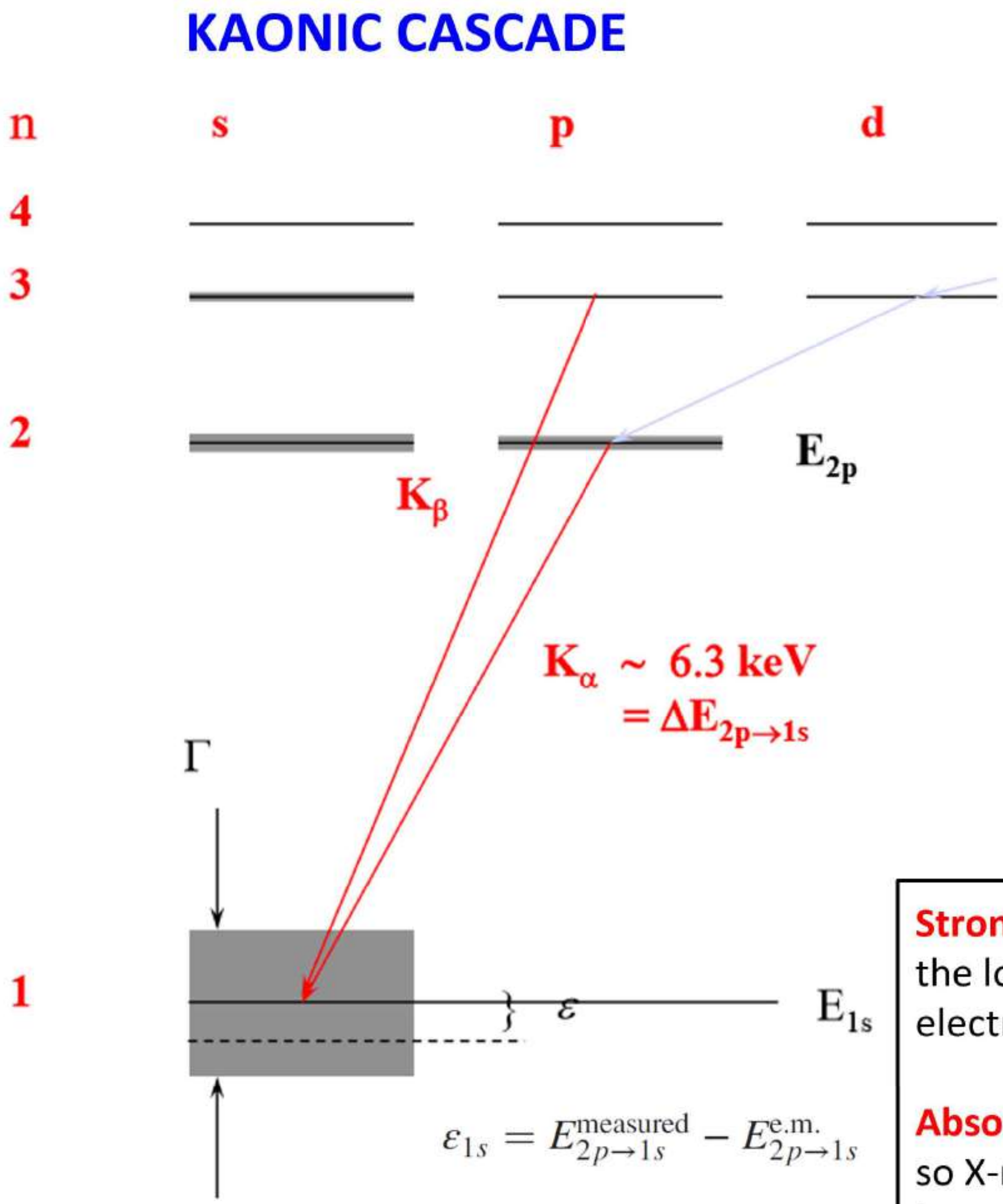

$$\varepsilon_{1s} = E^{\text{measured}}_{2p\to 1s} - E^{\text{e.m.}}_{2p\to 1s}$$

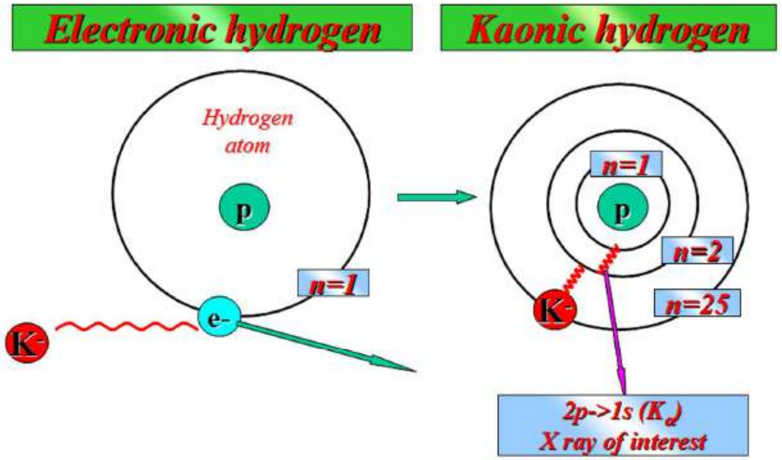

$$E_{1s} \simeq m_{red}c^2\frac{\alpha^2 Z^2}{2}$$

$$n \simeq \sqrt{\frac{m_{red}}{m_e}}n_e$$

Strong interaction -> shifting of the energy of the lowest atomic level from its purely electromagnetic value

Absorption -> reduces the lifetime of the state, so X-ray transitions to this final atomic level are broadened

SIDDHARTA-2 Scientific goal

To perform **precision measurements of the width** and **shift** for **kaonic hydrogen** and **deuterium**

Energy shift ε and **line width Γ of 1s state** are related to real and imaginary part of the S-wave scattering length (Deser-Trueman formula) :

$$\varepsilon_{1s} + \frac{i}{2}\Gamma_{1s} = 2\alpha^3\mu^2 a_{K-p}[1 - 2\alpha\mu(ln\alpha - 1)a_{K-p} + \ldots]$$

$$\varepsilon_{1s} + \frac{i}{2}\Gamma_{1s} = 2\alpha^3\mu^2 a_{K-d}[1 - 2\alpha\mu(ln\alpha - 1)a_{K-d} + \ldots]$$

Scattering lengths can be expressed in terms of $\bar{K}$N isospin dependent isoscalar a_0 and isovector a_1 scattering lengths:

$$a_{K-d} = \frac{4[m_N + m_K]}{[2m_N + m_K]}Q + C$$

$$a_{K-p} = \frac{1}{2}[a_0 + a_1]$$

$$Q = \frac{1}{2}[a_{K-p} + a_{K-n}] = \frac{1}{4}[a_0 + 3a_1]$$

$$a_{K-n} = a_1$$

⇓

the determination of the ***isospin dependent $\bar{K}$N scattering lengths*** with a ***precision of few %*** !

K^- deuterium predictions

To perform **precision measurements of the width** and **shift** for **kaonic hydrogen** and **deuterium**

Energy shift ε and **line width Γ of 1s state** are related to real and imaginary part of the S-wave scattering length (Deser-Trueman formula) :

$$\varepsilon_{1s} + \frac{i}{2}\Gamma_{1s} = 2$$

$$\varepsilon_{1s} + \frac{i}{2}\Gamma_{1s} =$$

Scattering lengths can b ... r

a_0 and isovector a_1 scat

$$a_{K-d} = \frac{4[m_N + m}{[2m_N + m}$$

$$Q = \frac{1}{2}\left[a_{K-p} + a_{K-n}\right] =$$

the determinati

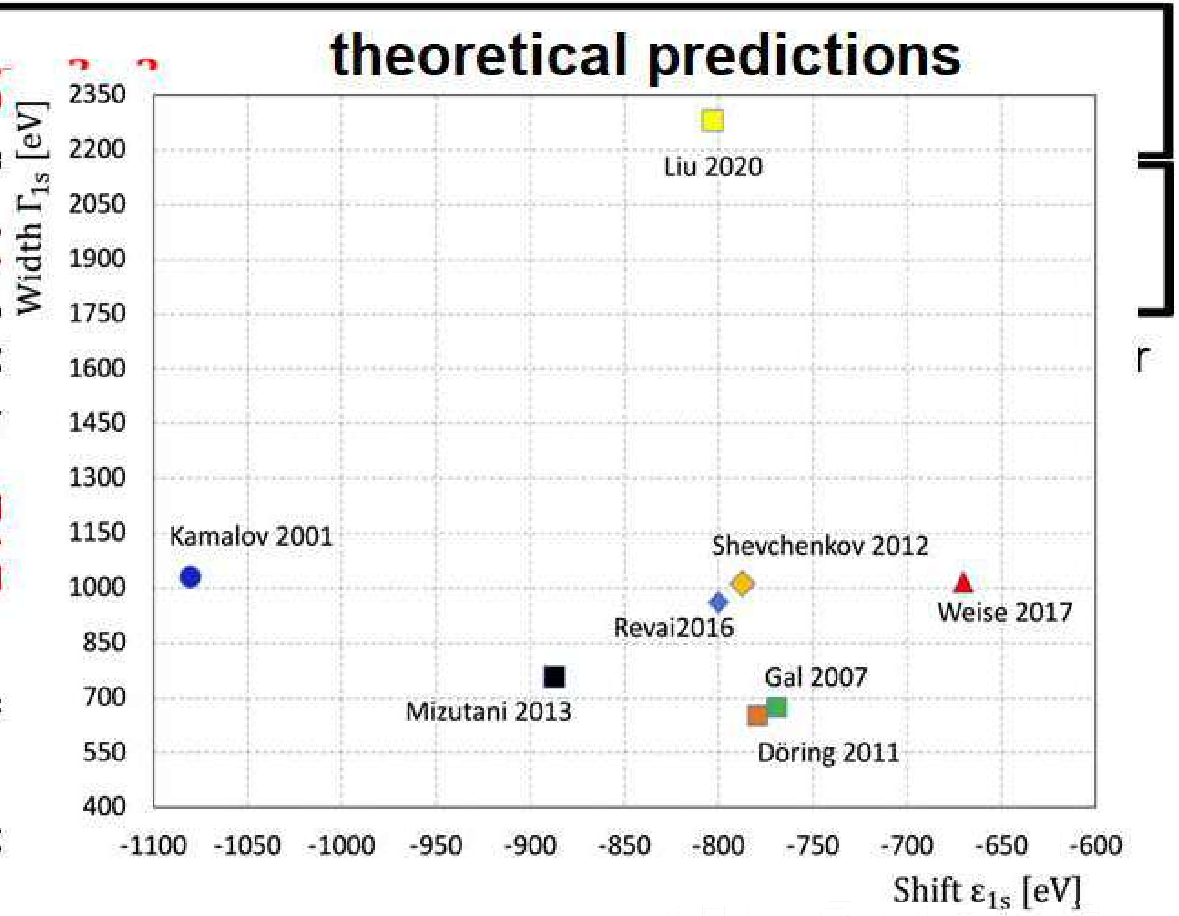

DAΦNE in LNF


DAΦNE, Laboratori Nazionali di Frascati
DAΦNE
Φ
LINAC
DAMPING RING

DAΦNE in LNF

DAΦNE @ LNF

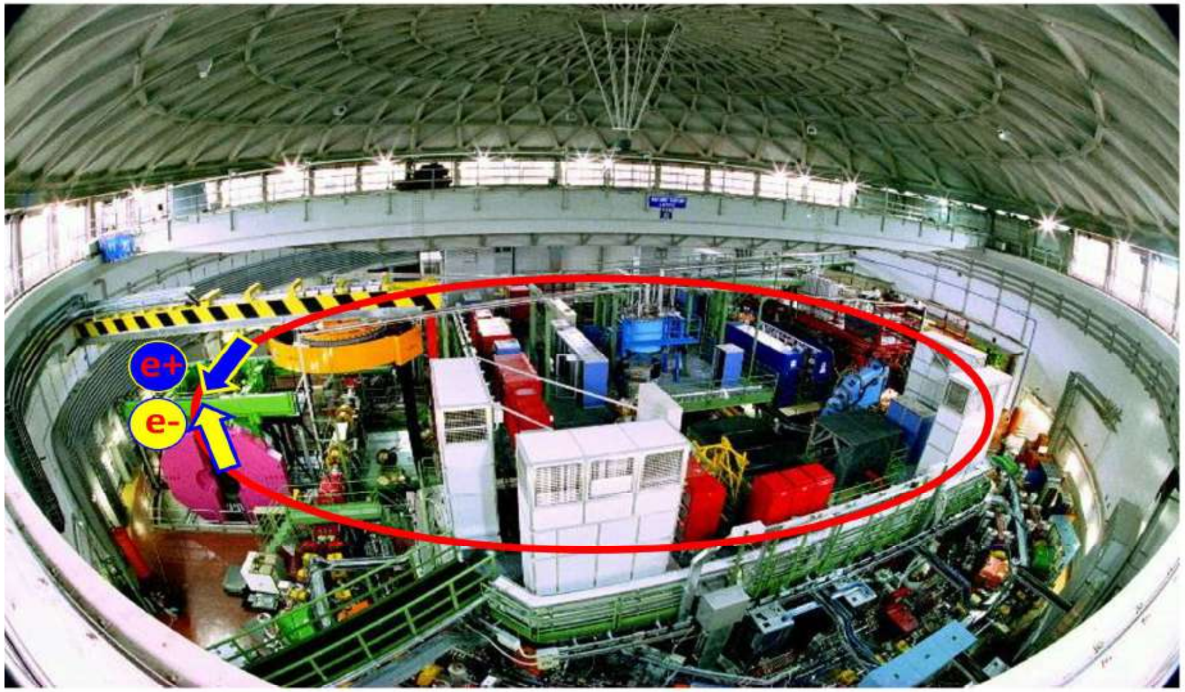

Best low momentum K-factory in the world

- **$\phi \to K^- K^+$** (49.2%), **≈1000 ϕ/s**
- monochromatic **low momentum** Kaons ≈127 Mev/c $\Delta p/p$=0.1%
- **back to back** $K^- K^+$ topology
- **small hadronic background** due to the beam

Suitable for low-energy kaon physics: kaonic atoms kaon-nucleons/nuclei interaction studies

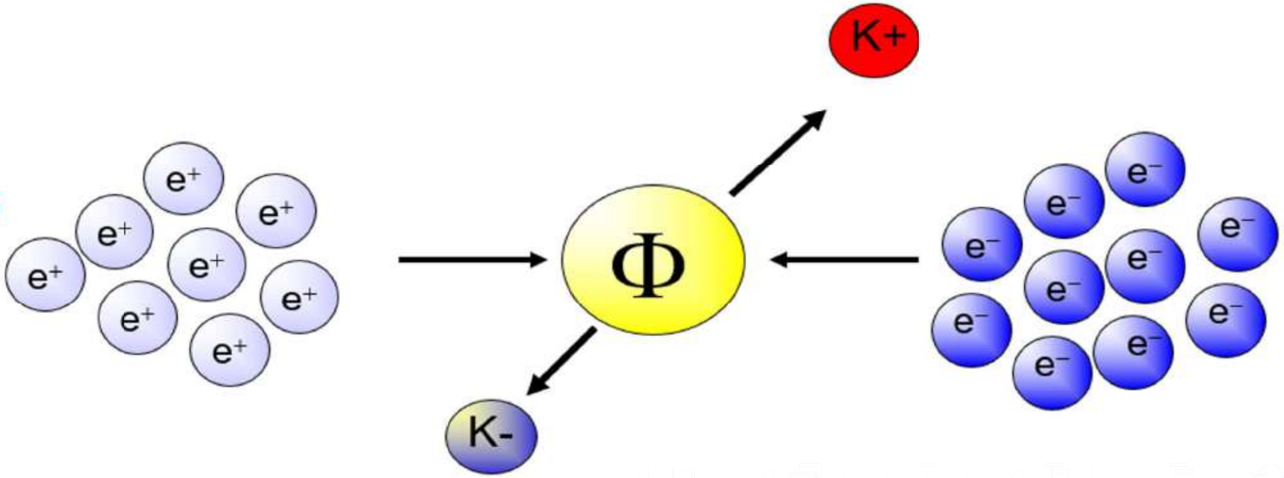

Kaonic atoms experiments at DAFNE LNF-INFN

The modern era of light kaonic atom experiments

Catalina Curceanu, Carlo Guaraldo, Mihail Iliescu, Michael Cargnelli, Ryugo Hayano, Johann Marton, Johann Zmeskal, Tomoichi Ishiwatari, Masa Iwasaki, Shinji Okada, Diana Laura Sirghi, and Hideyuki Tatsuno

Rev. Mod. Phys. **91**, 025006 – Published 20 June 2019

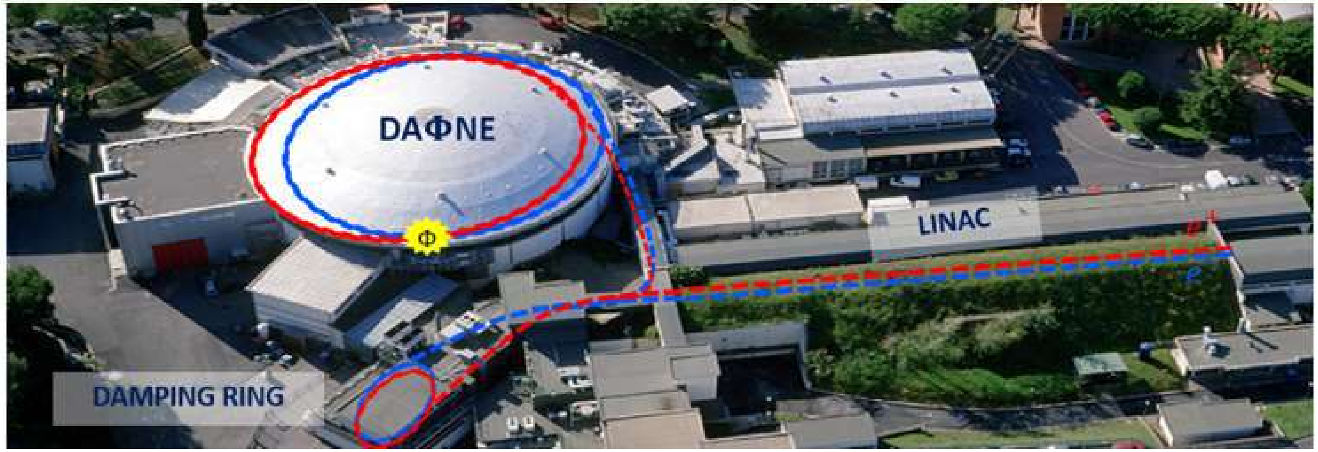

DEAR 2002	SIDDHARTA 2009	SIDDHARTA-2 2022

SIDDHARTA experiment

SIDDHARTA Setup

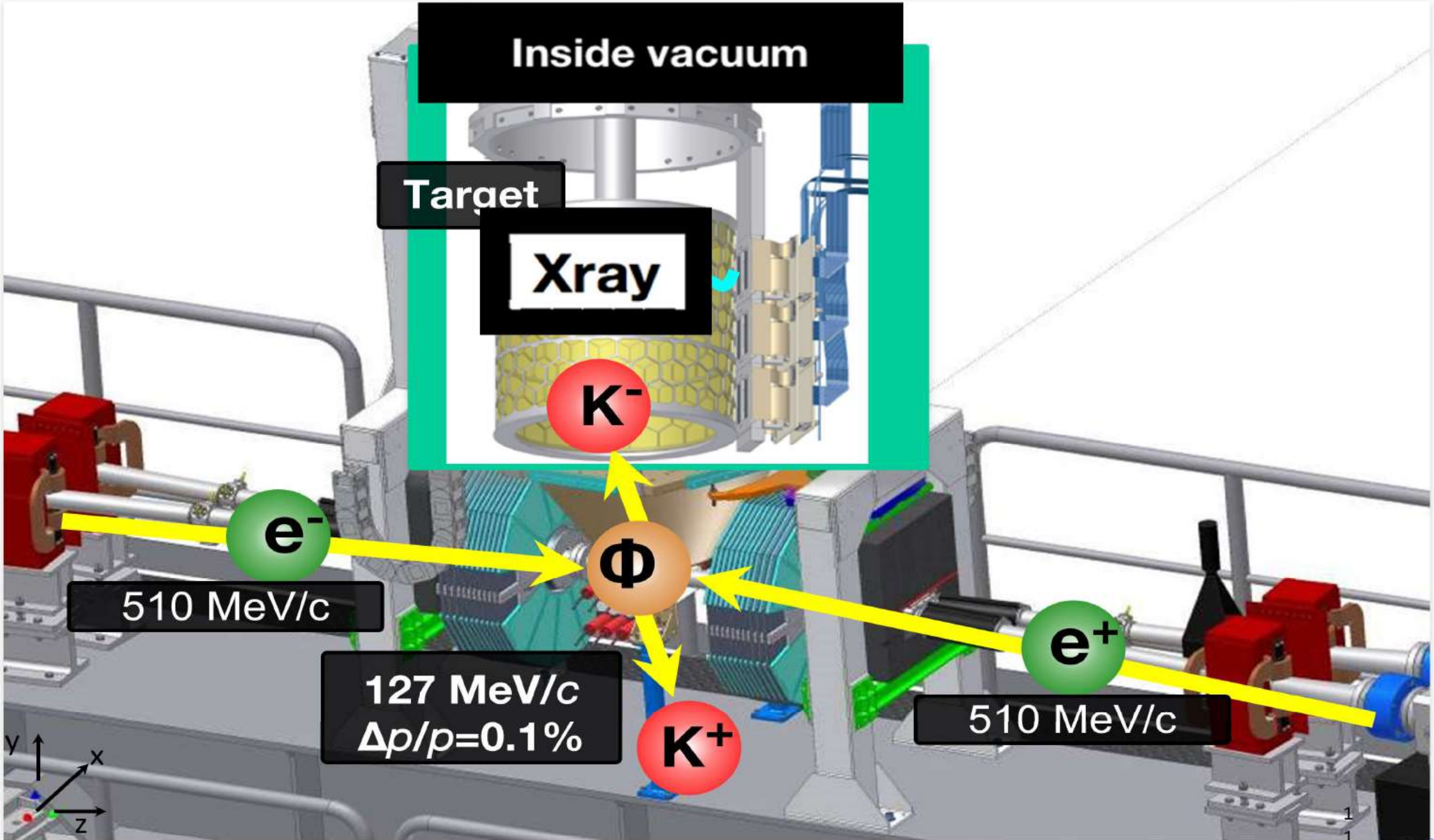

SIDDHARTA Setup

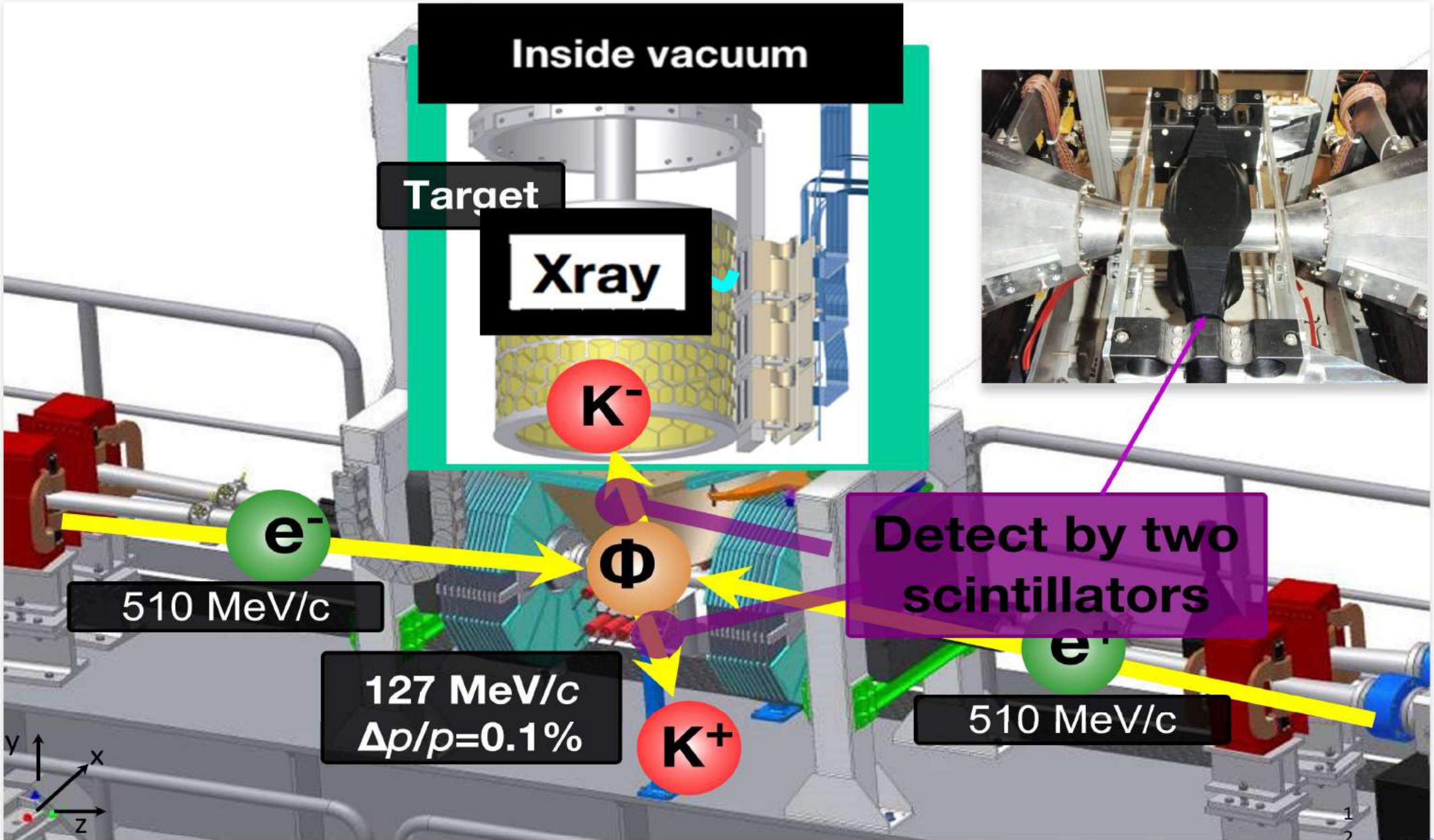

SIDDHARTA experiment

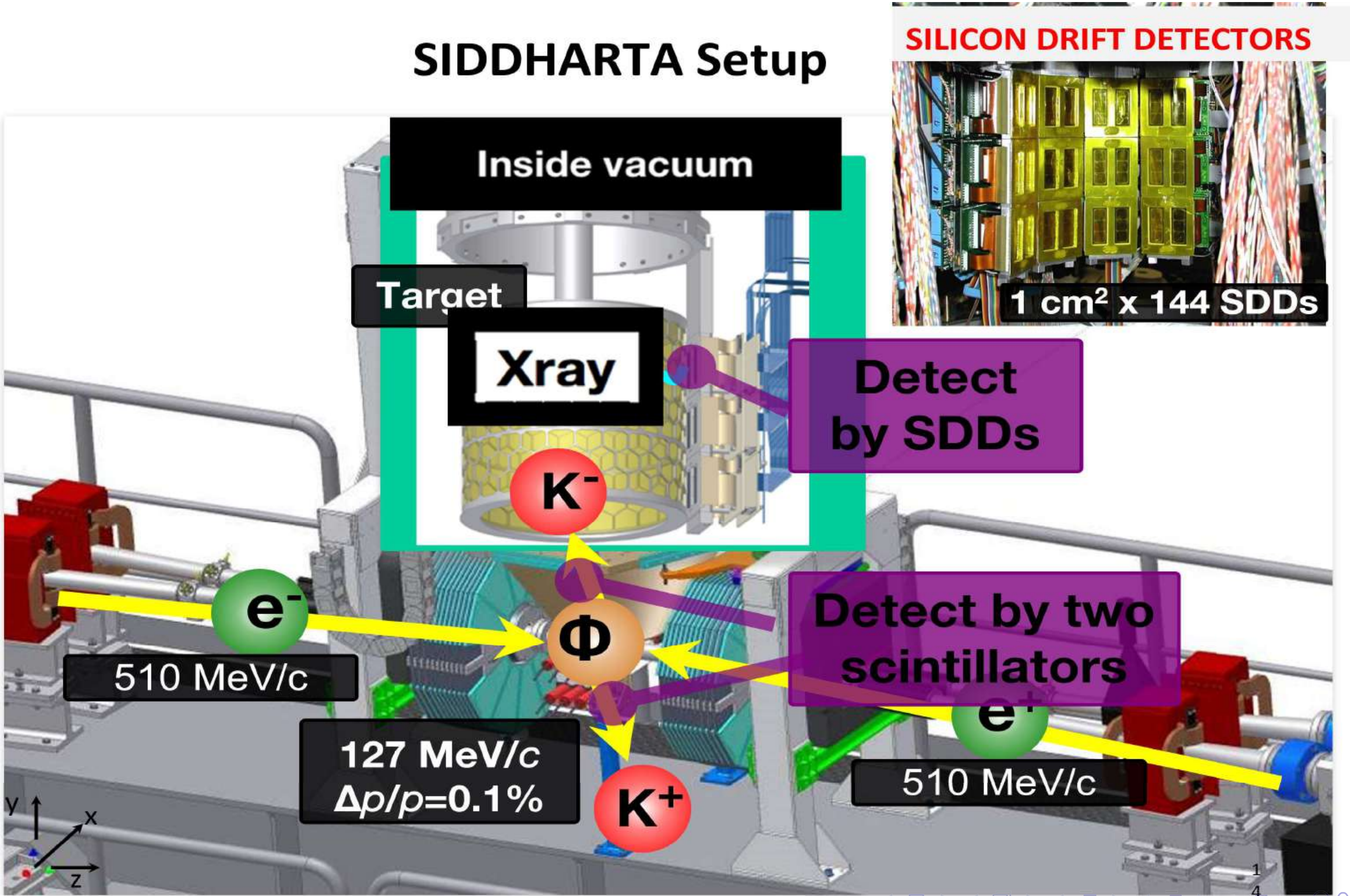

Silicon Drift Detector - SDD

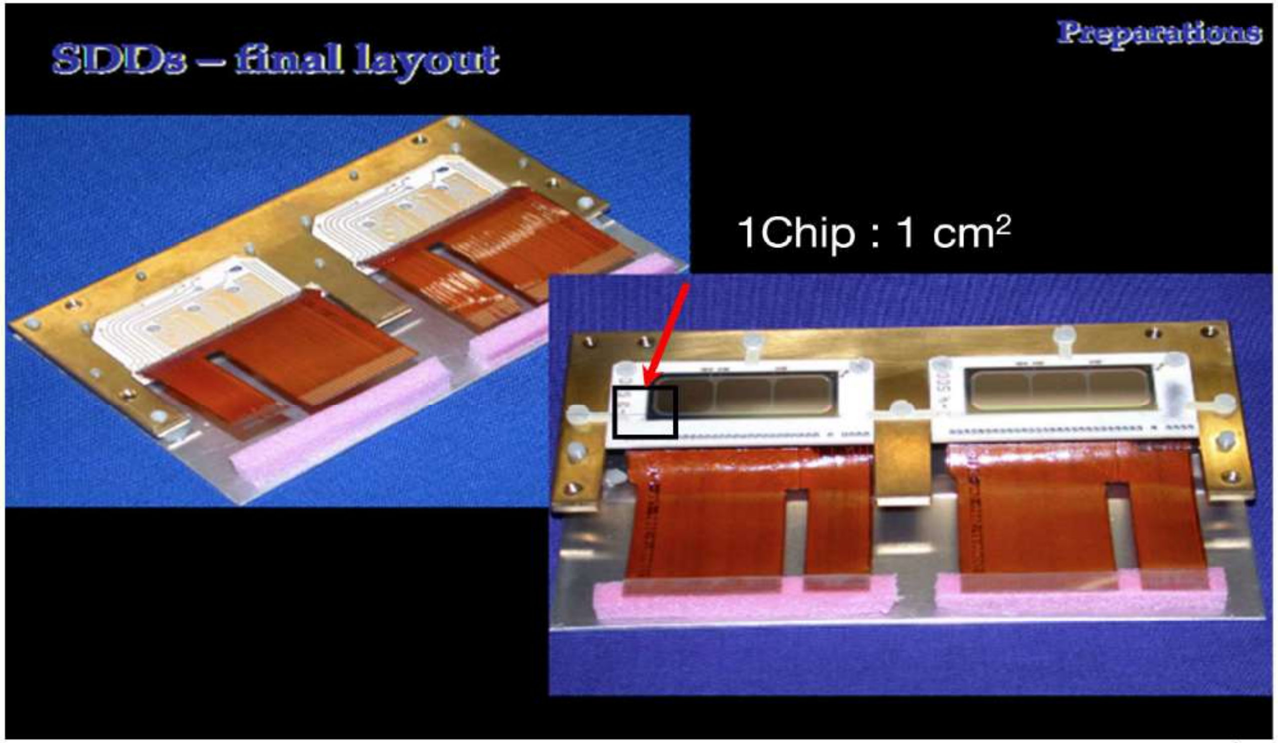

Used for the first time as energy detectors

- very fast and triggerable
- energy resolution of 160 eV (FWHM) at 6 keV
- drift time (timing resolution) below 1 μs
- 48 SDDs, each with 3 × 1 cm² cells
- thickness of 450 μm

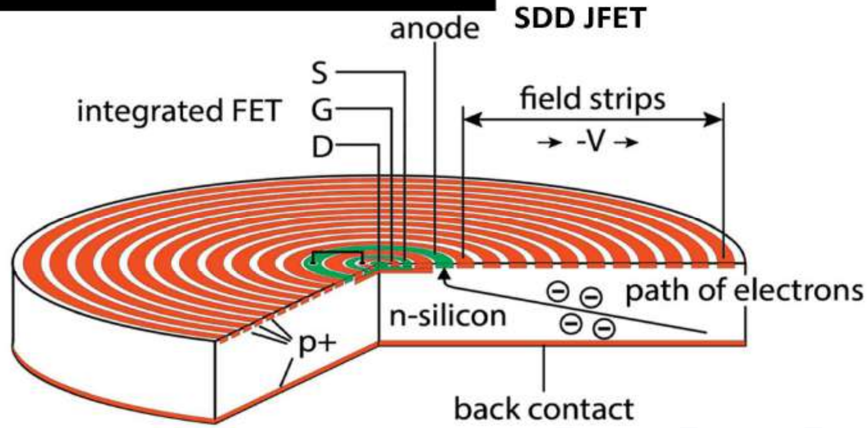

SIDDHARTA experiment

Results for Kaonic Hydrogen

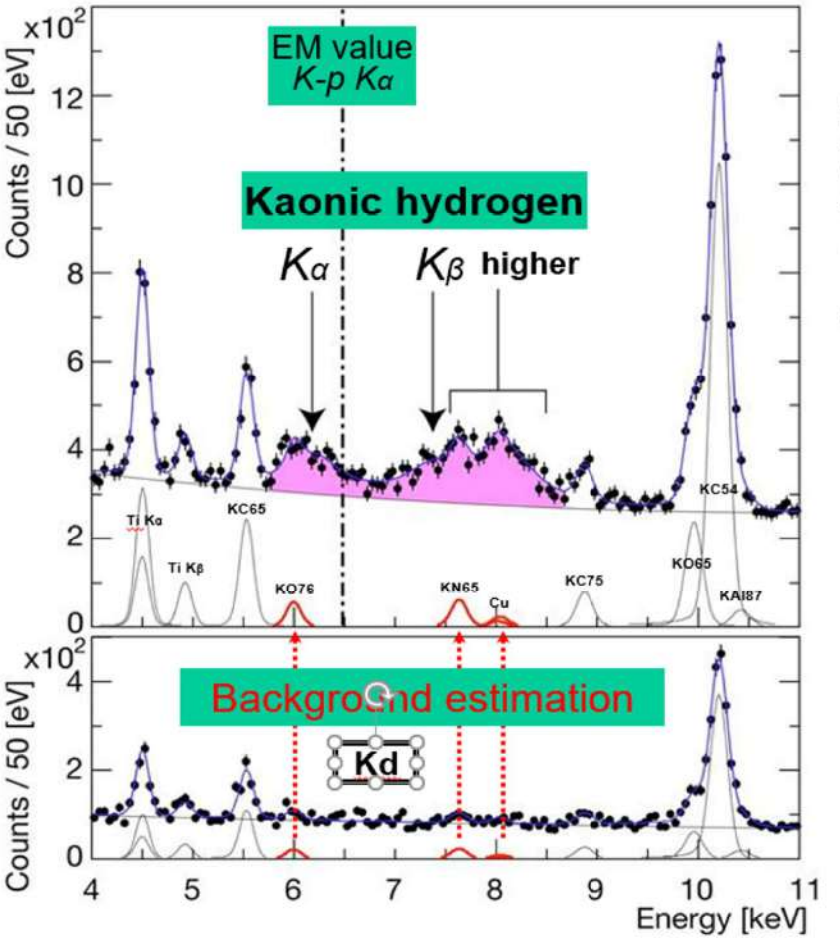

Only **exploratory first measurement for Kd**, no measured ε, Γ values obtained (100pb^{-1})

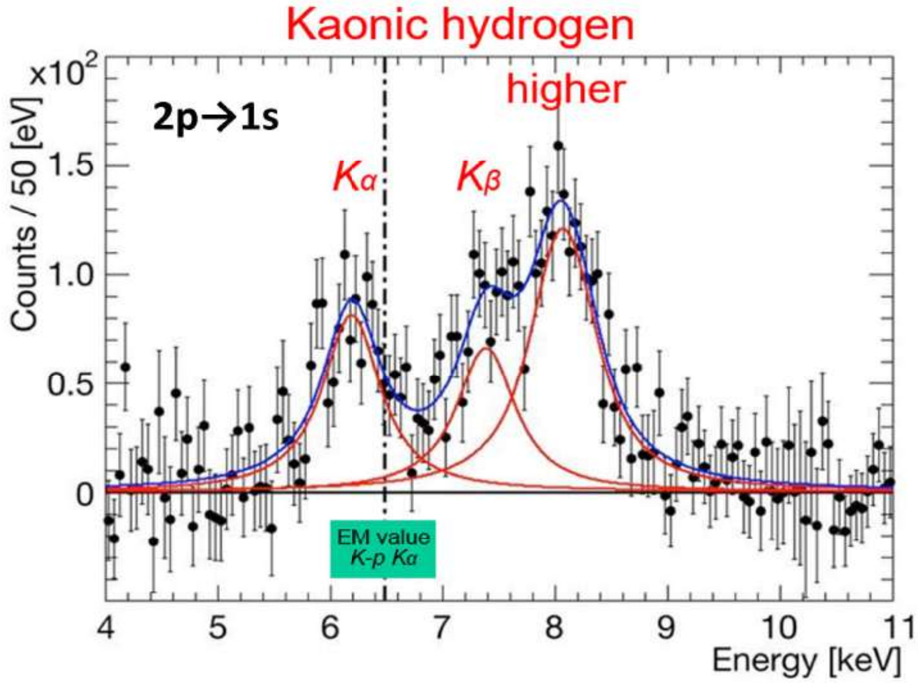

Residuals of K-p x-ray spectrum after subtraction of fitted background

$$\varepsilon_{1S} = -283 \pm 36(\text{stat}) \pm 6(\text{syst})\ \text{eV}$$

$$\Gamma_{1S} = 541 \pm 89(\text{stat}) \pm 22(\text{syst})\ \text{eV}$$

(400pb^{-1})

M. Bazzi et al.. 2011. (SIDDHARTA Coll.), Phys. Lett. B704, 113

Results for Kaonic Hydrogen

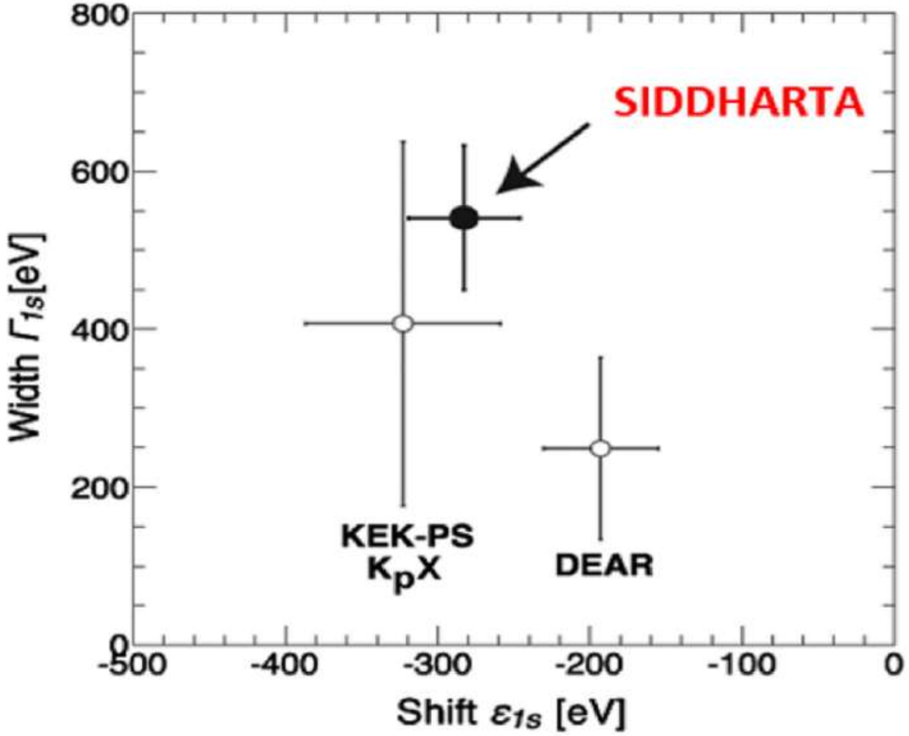

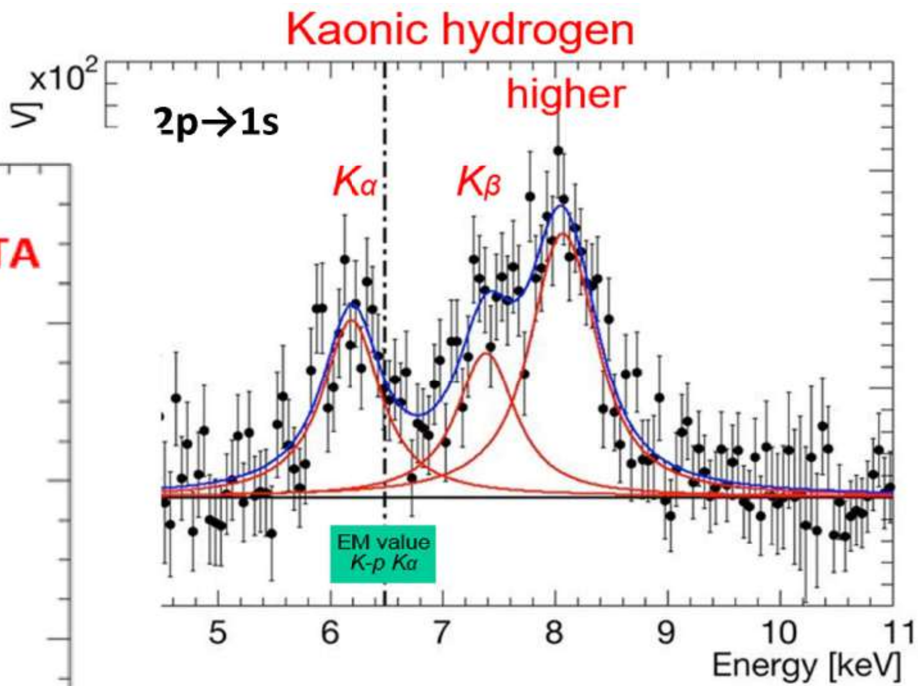

uals of K-p x-ray spectrum after subtraction of fitted background

$\varepsilon_{1S} = -283 \pm 36(\text{stat}) \pm 6(\text{syst})$ eV

$\Gamma_{1S} = 541 \pm 89(\text{stat}) \pm 22(\text{syst})$ eV

(400pb^{-1})

M. Bazzi et al.. 2011. (SIDDHARTA Coll.), Phys. Lett. B704, 113

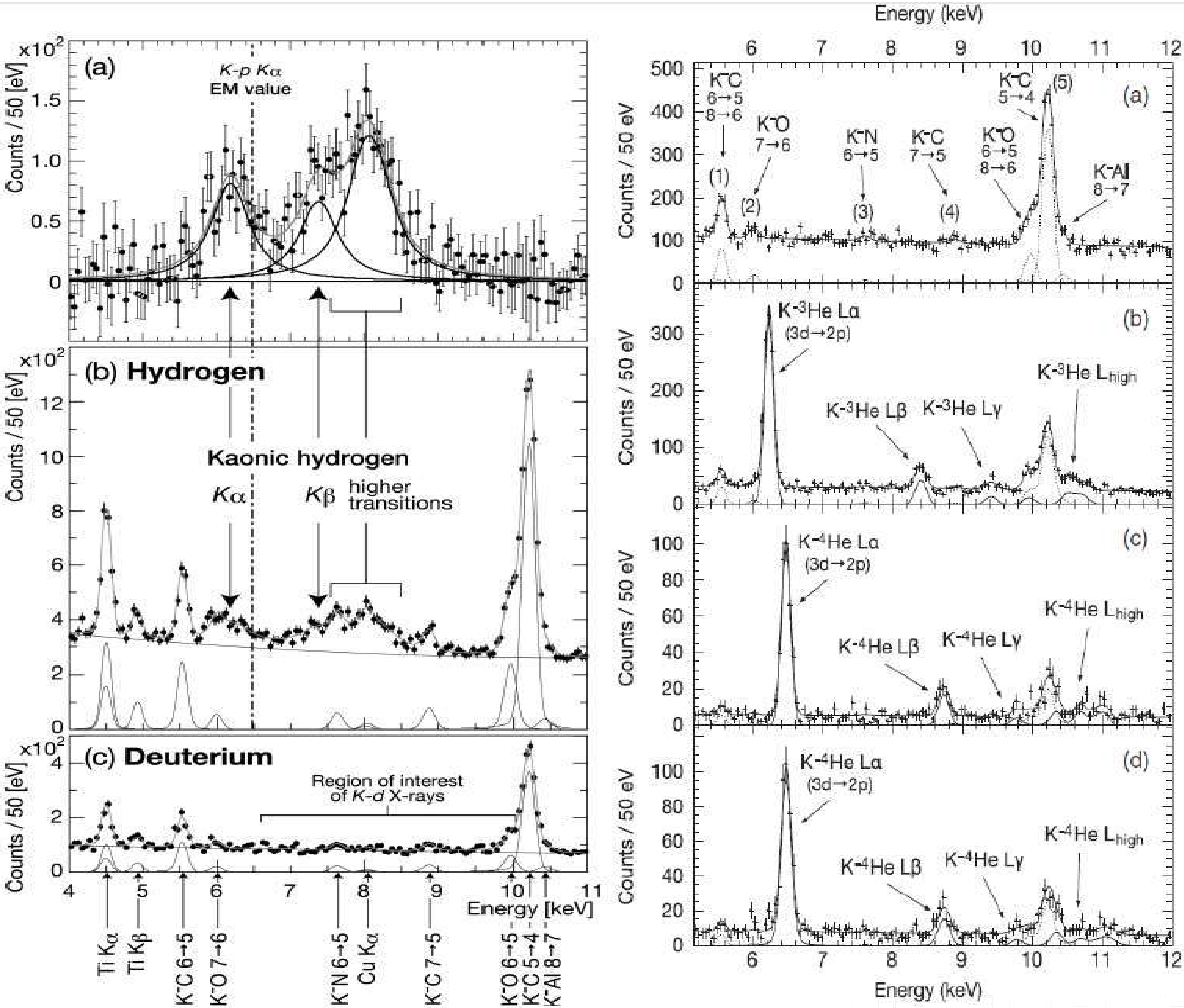
(a)
K-p Kα
EM value
Counts / 50 [eV]
(b) Hydrogen
Kaonic hydrogen
Kα
Kβ
higher transitions
(c) Deterium
Region of interest of K-d X-rays
Energy [keV]
Ti Kα
Ti Kβ
K⁻C 6→5
K⁻O 7→6
K⁻N 6→5
Cu Kα
K⁻C 7→5
K⁻O 6→5
K⁻C 5→4
K⁻Al 8→7
Energy (keV)
Counts / 50 eV
K⁻C 6→5 8→6
K⁻O 7→6
K⁻N 6→5
K⁻C 7→5
K⁻O 6→5 8→6
K⁻C 5→4
K⁻Al 8→7
K⁻³He Lα (3d→2p)
K⁻³He Lβ
K⁻³He Lγ
K⁻³He L_high
K⁻⁴He Lα (3d→2p)
K⁻⁴He Lβ
K⁻⁴He Lγ
K⁻⁴He L_high

M. Bazzi et al., Phys. Lett. B681, 310 (2009).

M. Bazzi et al., Phys. Lett. B697, 199 (2011).

M. Bazzi et al., Phys. Lett. B714, 40 (2012).

$$K^{-4}\text{He} : \epsilon_{2p} = 5 \pm 3(stat) \pm 4(syst)eV,$$

$$K^{-4}\text{He} : \Gamma_{2p} = 14 \pm 8(stat) \pm 5(syst)eV,$$

$$K^{-3}\text{He} : \epsilon_{2p} = -2 \pm 2(stat) \pm 4(syst)eV,$$

$$K^{-3}\text{He} : \Gamma_{2p} = 6 \pm 6(stat) \pm 7(syst)eV.$$

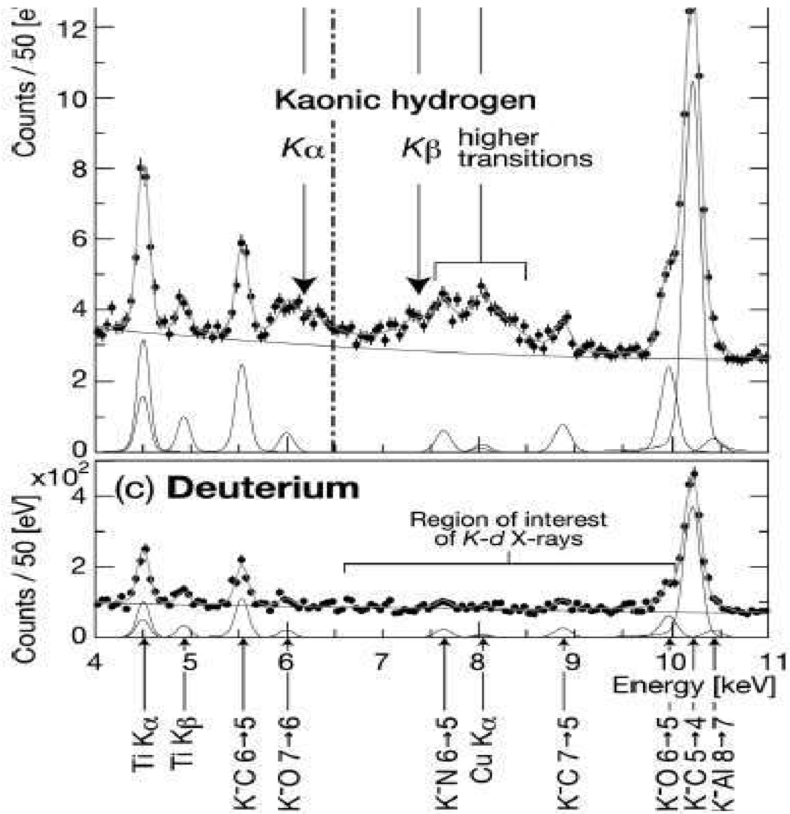

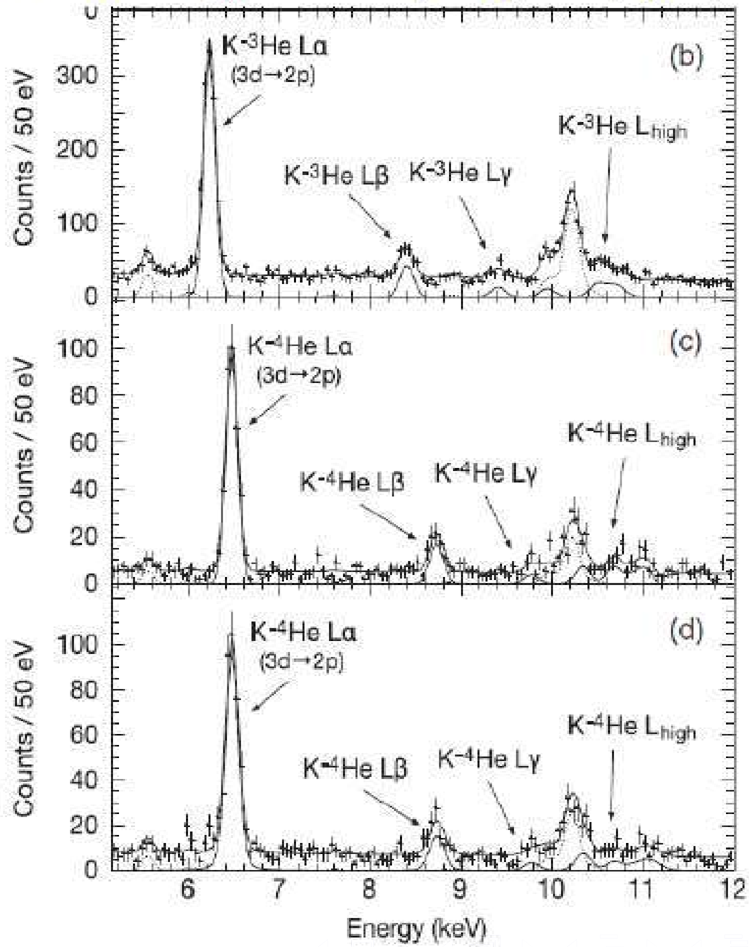

SIDDHARTA-2 experiment

LNF-INFN, Frascati, Italy
SMI-ÖAW, Vienna, Austria
Politecnico di Milano, Italy
IFIN –HH, Bucharest, Romania
TUM, Munich, Germany
RIKEN, Japan
Univ. Tokyo, Japan
Victoria Univ., Canada
Univ. Zagreb, Croatia
Univ. Jagiellonian Krakow, Poland
ELPH, Tohoku University

SIDDHARTA-2 facility

First exploratory measurement for Kd by SIDDHARTA (100pb^{-1})

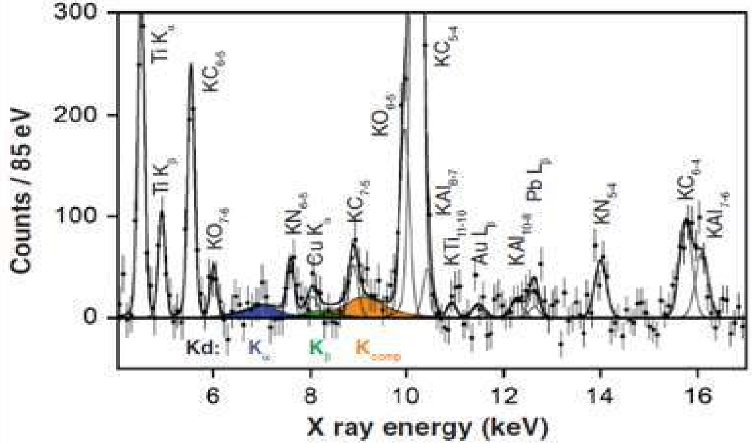

Upper limits of yields (90% C.L.):

Y(K_{tot}) <0.0143

Y(K_α) <0.0039

Yield of a factor about **10 times smaller** than for KH (estimated to be from **1 to 2%** for $\mathbf{K_\alpha}$)

SIDDHARTA-2: enhancement by one order of magnitude of the S/B ratio

upgrade of SIDDHARTA detector

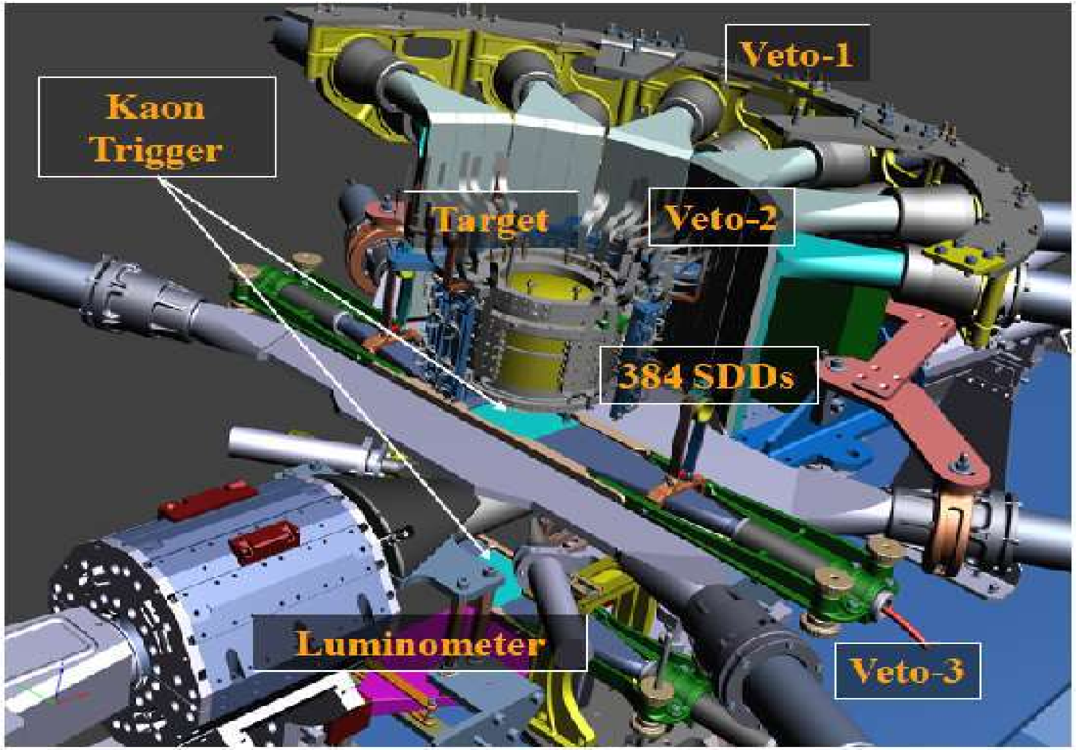

48 Silicon Drift Detector arrays with 8 SDD units (0.64 cm^2) for a total active area of 246 cm^2 The thickness of 450 µm ensures a high collection efficiency for X-rays of energy between 5 keV and 12 keV

details in: F. Sirghi, et al., JINST 19 (2024) P11006

Siddharta-2 setup details

SDD detectors

covering a solid angle for stopped kaons in the gaseous target of ~ 2π, 5mm from the target

48 monolithic SDD arrays will be around the target with a total area of about **246 cm^2**

the large active to total area of about 75% (compared to 20% for the SIDDHARTA SDDs)

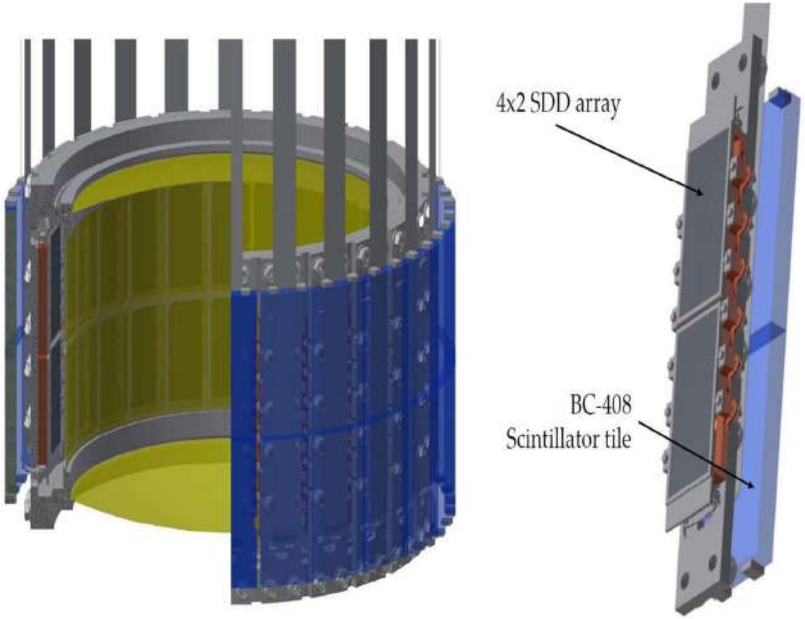

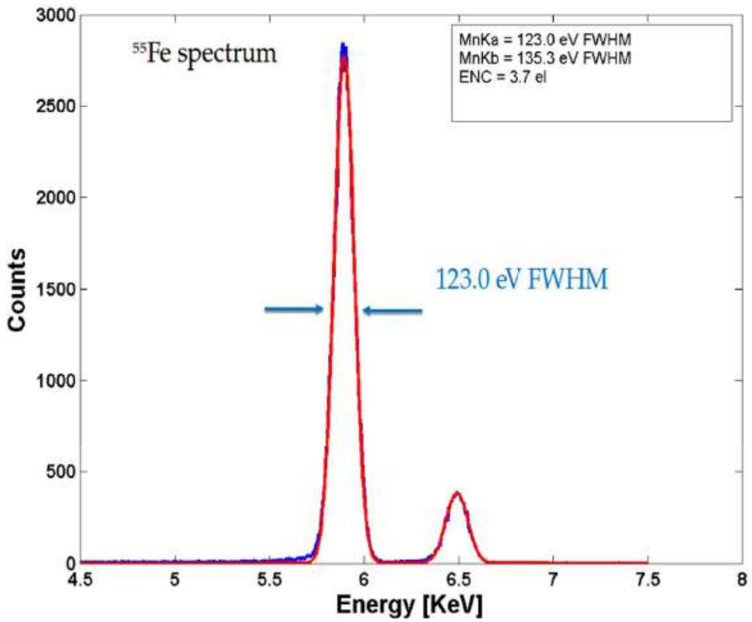

- single unit: 4x2 SDD array (48 units in total)
- SDD
  - external CUBE preamplifier (MOSFET input transistor)
  - larger total anode capacitance
  - better than FET performances
  - standard SDD technology
  - area/cell = 64mm^2
  - T=100 K
  - Thickness 0.45 mm
  - drift time<500ns

Siddharta-2 setup details

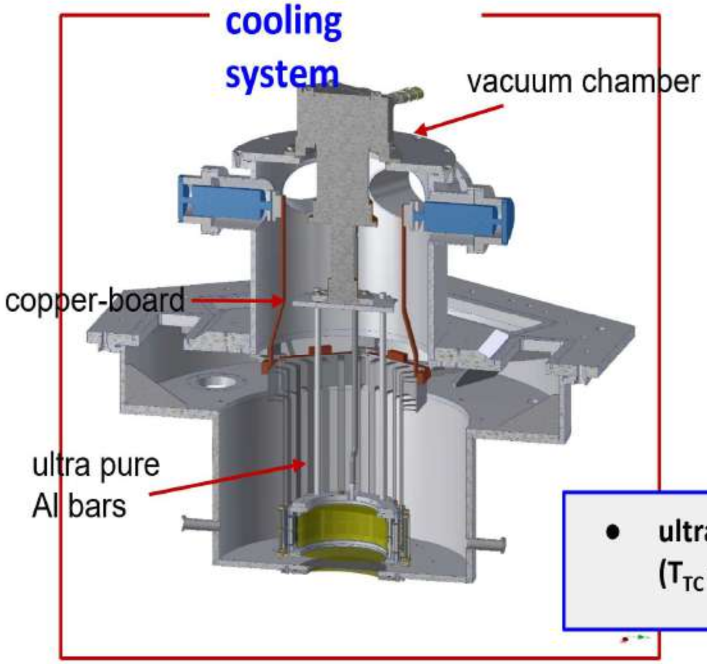

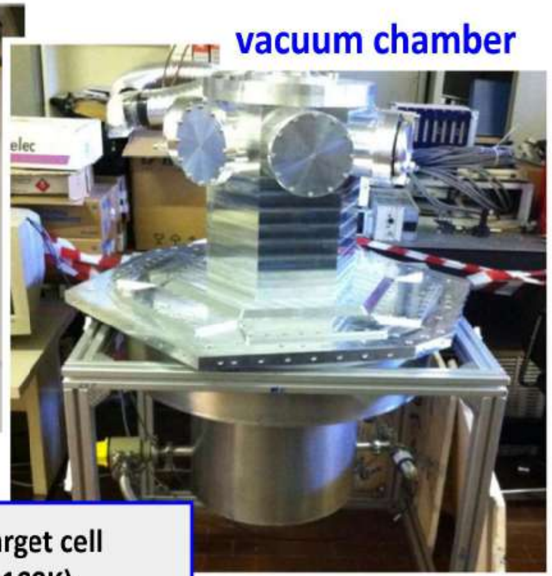

- ultra pure Al bars to cool target cell (T_{TC} = 30K) and SDDs (T_{SDD}= 100K)

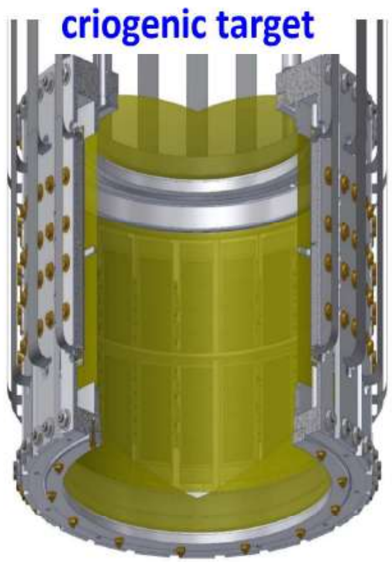

- Working temp. and pressure : 30 K and 0.3 MPa
- Target cell wall is made of a 2-Kapton layer structure (<100µm)
- HPH Deuterium generator and heavy water
- almost double gas density with respect to SIDDHARTA (3% LHD)
- X-ray transmission 85% at 7keV

Siddharta-2 setup details

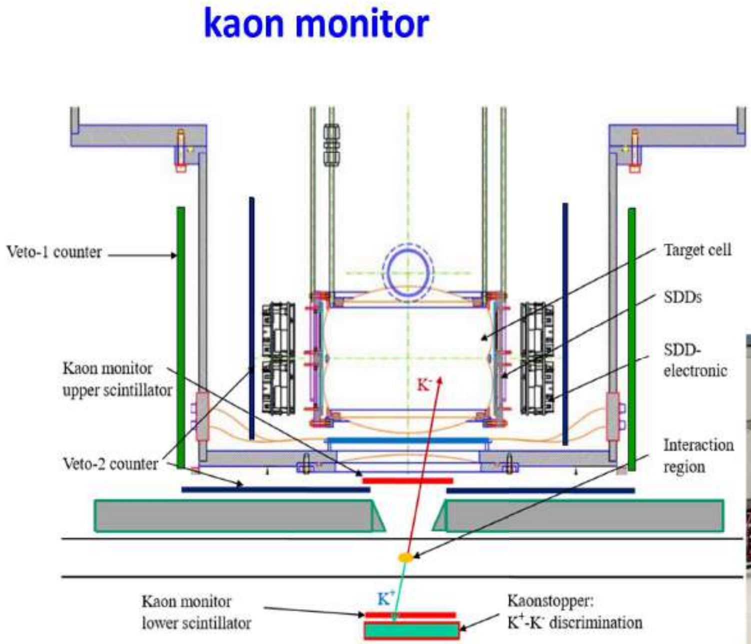

- with the new position only those kaons which are reaching directly the entrance flange of the vacuum chamber will be selected
- reduction of the hadronic and e. m. background is expected comparing to old geometry

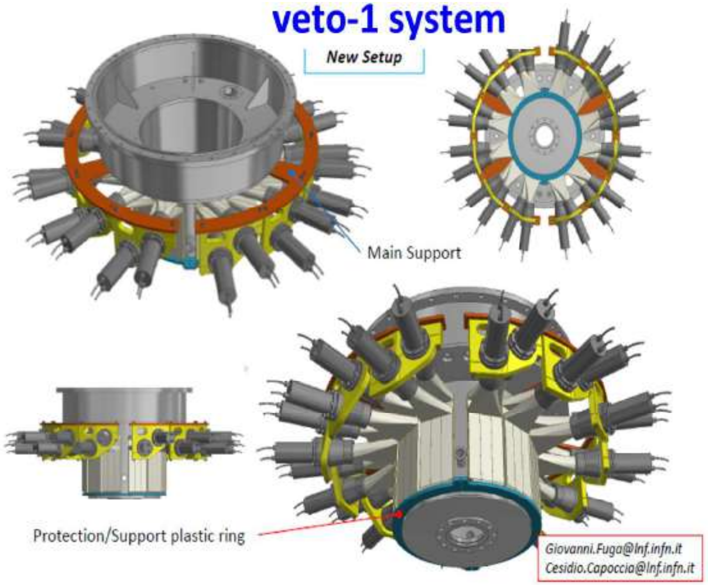

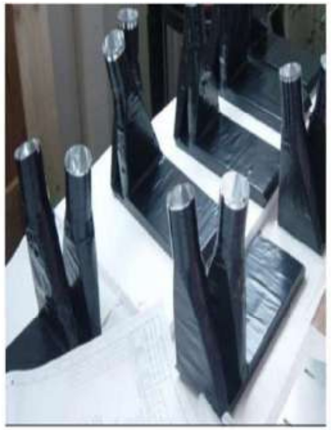

- outher barrel of scintillators
- to identify the products of K^- absorption on gas nuclei

Siddharta-2 setup details

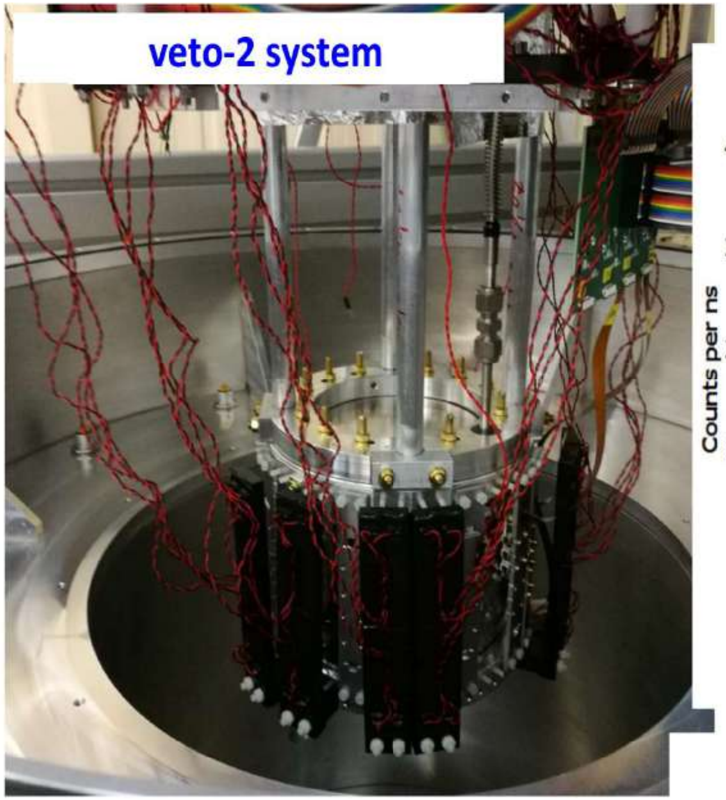

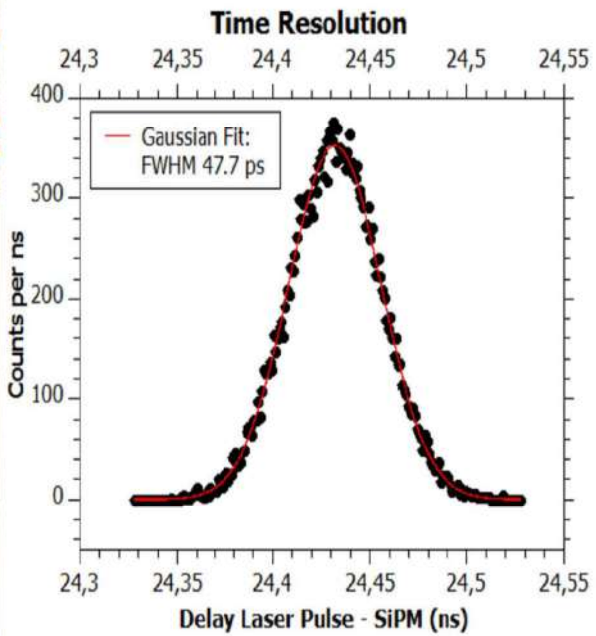

- an inner ring of scintillator tiles (SciTiles) placed as close as possible behind the SDDs
- for charge particle tracking

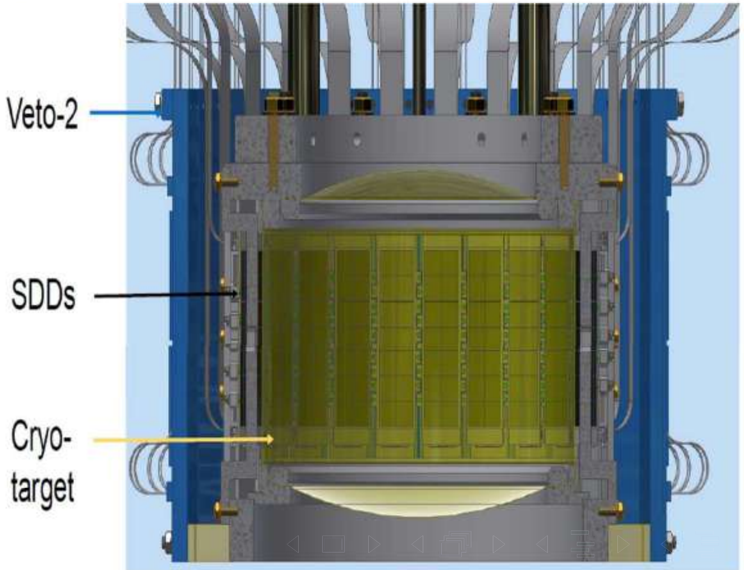

SIDDHARTA-2 way

SIDDHARTA-2 measurements

First kaonic deuterium measurement (2023 -2024)

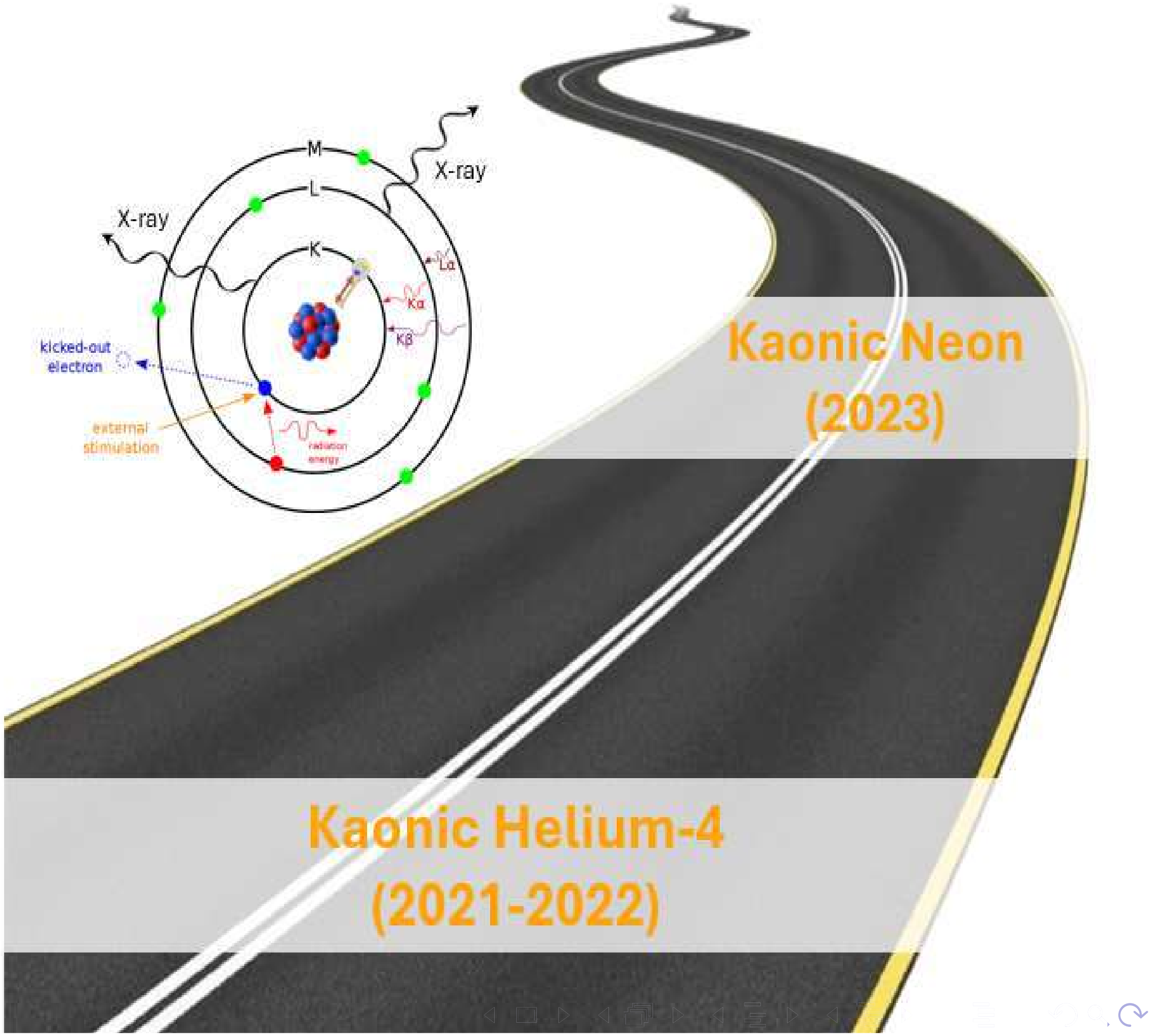

The Kaonic 4He measurement (2021-2022)

$$\varepsilon_{2p} = E^{exp}_{3d\to 2p} - E^{e.m}_{3d\to 2p} = -1.9 \pm 0.8\,(stat) \pm 2.0\,(sys)\ eV$$
$$\Gamma_{2p} = 0.01 \pm 1.60\,(stat) \pm 0.36\,(sys)\ eV$$

→ *no sharp effect of the strong interaction on the 2p level*

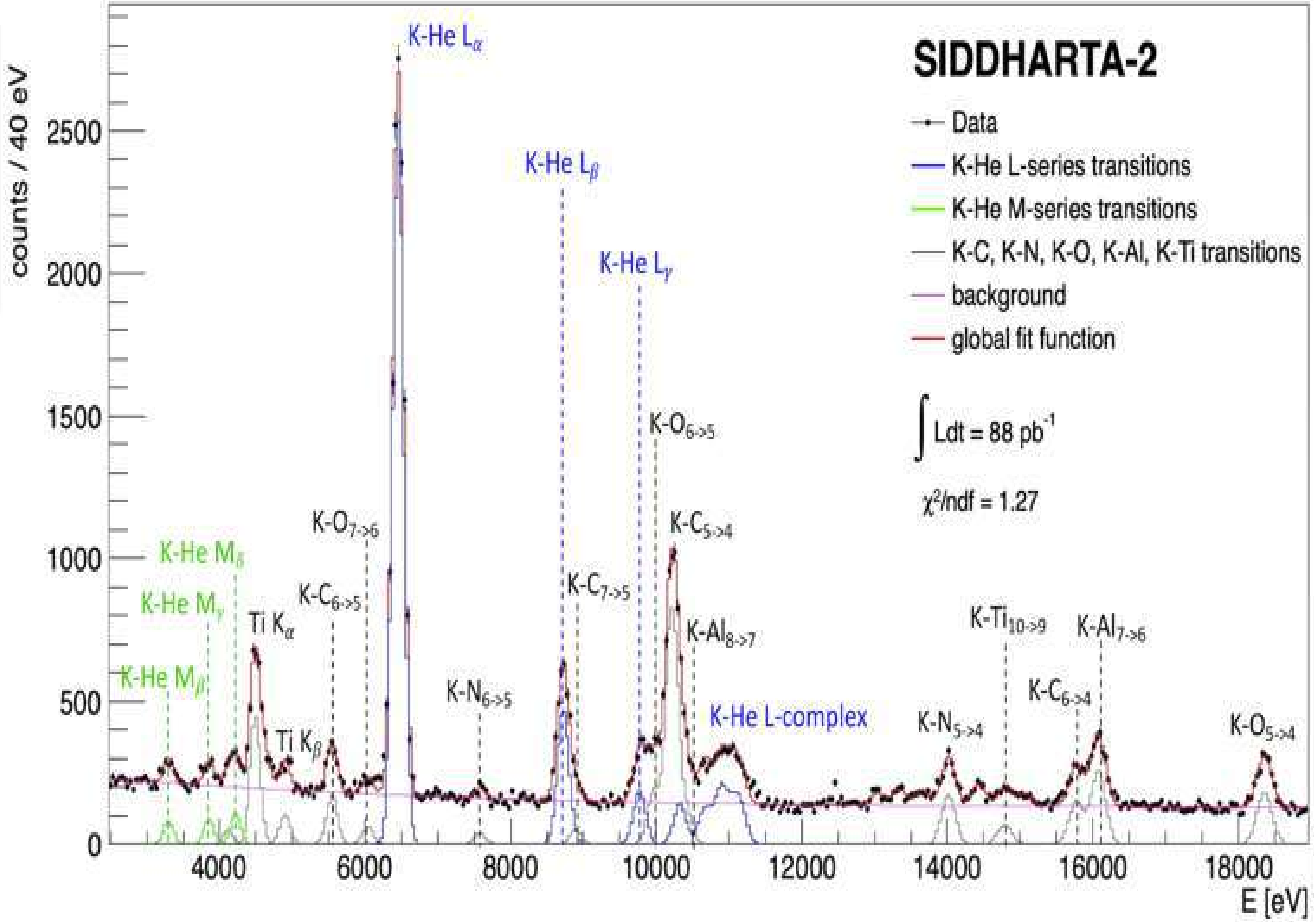

new data to enrich the kaonic atoms transitions database

Transition	Energy [eV]
K^-C (6→5)	5546.0 ± 5.4 (stat) ± 2.0 (syst)
K^-C (7→5)	8890.0 ± 13.0 (stat) ± 2.0 (syst)
K^-C (5→4)	10216.6 ± 1.8 (stat) ± 3.0 (syst)
K^-C (6→4)	15760.3 ± 4.7 (stat) ± 12.0 (syst)
K^-O (7→6)	6014.8 ± 8.4 (stat) ± 2.0 (syst)
K^-O (6→5)	9965.1 ± 6.9 (stat) ± 2.0 (syst)
K^-O (5→4)	18361.1 ± 5.4 (stat) ± 12.0 (syst)
K^-N (6→5)	7581.1 ± 16.0 (stat) ± 2.0 (syst)
K^-N (5→4)	14008.0 ± 6.0 (stat) ± 9.0 (syst)
K^-Al (8→7)	10441.0 ± 8.5 (stat) ± 3.0 (syst)
K^-Al (7→6)	16083.4 ± 3.8 (stat) ± 12.0 (syst)
K^-Ti (10→9)	14790.3 ± 16.6 (stat) ± 9.0 (syst)

Sgaramella F., et al., 2023, Eur. Phys. J. A, 59 (3) 56

The Kaonic 4He measurement (2021-2022)

Density	2.25 ± 0.11 g/l
L_α yield	$0.075 \pm 0.003\,(stat)^{+0.006\,(syst)}_{-0.009\,(syst)}$
L_β / L_α	$0.190 \pm 0.027\,(stat)$
L_γ / L_α	$0.082 \pm 0.012\,(stat)$

Density	1.90 ± 0.10 g/l	0.82 ± 0.08 g/l
L_α yield	$0.148 \pm 0.027\,(stat)^{+0.006\,(syst)}_{-0.009\,(syst)}$	$0.126 \pm 0.023\,(stat)^{+0.006\,(syst)}_{-0.009\,(syst)}$
L_β / L_α	$0.193 \pm 0.042\,(stat)$	$0.133 \pm 0.037\,(stat)$
L_γ / L_α	$0.0035 \pm 0.015\,(stat)$	not detected

Study of yield density dependence for the K-^{4}He Lα transition

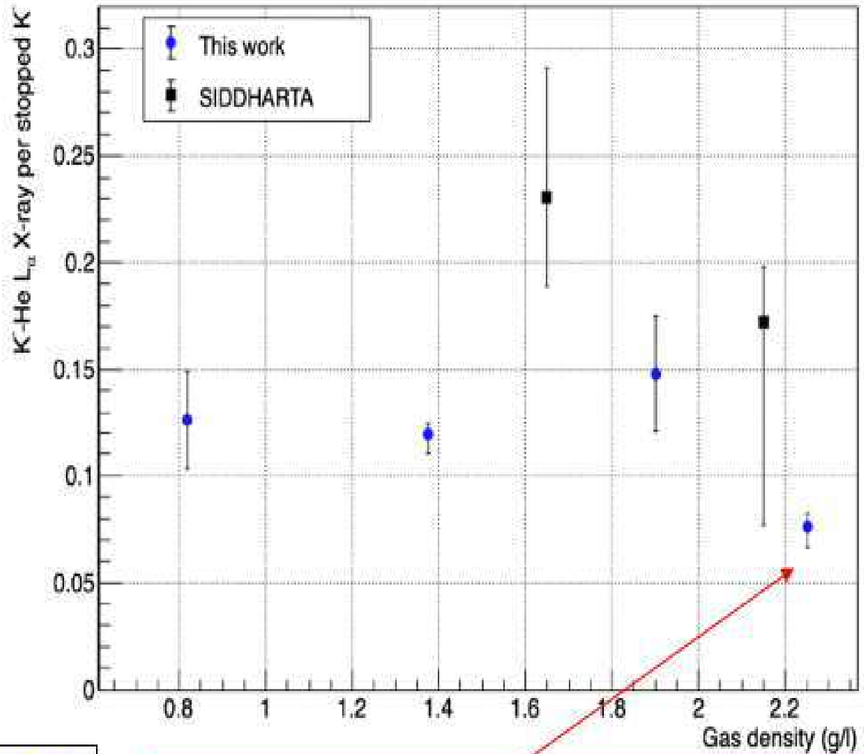

First observation of the stark effect in kaonic helium-4

Sgaramella F., et al., 2024, Acta Phys. Pol.B Proc. Suppl. 17, 1-A8

Sirghi D.L., Shi H., Guaraldo C., Sgaramella F., et al., 2023, Nucl. Phys. A,1029 122567

The Kaonic Ne measurement (2023)

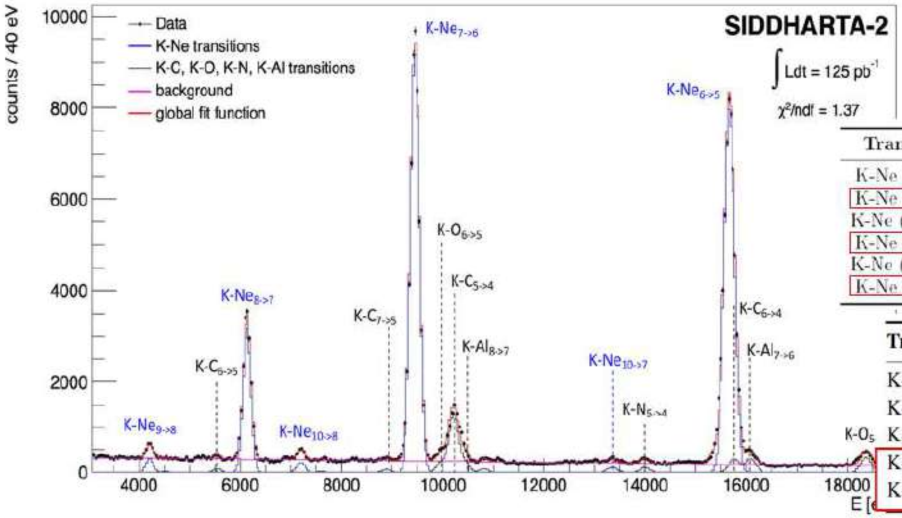

Ne density: 3.60+-0.18 g/l

Transition	Energy [eV]
K-Ne (9 → 8)	4206.35 ± 3.75 (stat) ±2.00 (syst) eV
K-Ne (8 → 7)	6130.86 ± 0.71 (stat) ±1.50 (syst) eV
K-Ne (10 → 8)	7191.21 ± 4.91 (stat) ±2.00 (syst) eV
K-Ne (7 → 6)	9450.08 ± 0.41 (stat) ±1.50 (syst) eV
K-Ne (10 → 7)	13352.20 ± 10.07 (stat) ±3.00 (syst) eV
K-Ne (6 → 5)	15673.30 ± 0.52 (stat) ±9.00 (syst) eV

Transition	Yield
K-Ne (10 → 8)	0.010 ± 0.001 (stat) ± 0.001 (sys)
K-Ne (9 → 8)	0.137 ± 0.012 (stat) ± 0.010 (sys)
K-Ne (8 → 7)	0.228 ± 0.004 (stat) ± 0.011 (sys)
K-Ne (7 → 6)	0.277 ± 0.002 (stat) ± 0.014 (sys)
K-Ne (6 → 5)	0.308 ± 0.003 (stat) ± 0.015 (sys)

$$K-Ne(8\to 7) = \frac{A_G}{\sqrt{2\pi}\sigma}\cdot e^{\frac{-(E-E_0)^2}{2\sigma^2}} \quad E_0 = (m_{8\to 7}\cdot K_{mass} + q_{8\to 7})$$

$$K-Ne(7\to 6) = \frac{A_G}{\sqrt{2\pi}\sigma}\cdot e^{\frac{-(E-E_0)^2}{2\sigma^2}} \quad E_0 = (m_{7\to 6}\cdot K_{mass} + q_{7\to 6})$$

Kaonic Ne energy transition as function of kaon mass (MCDFGME code)

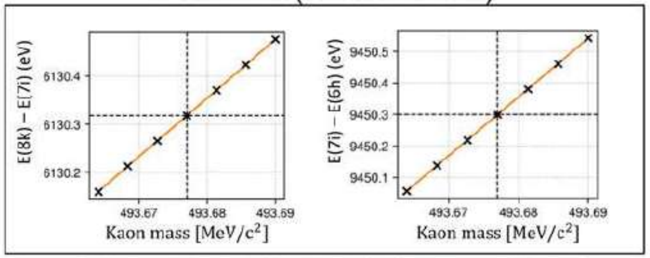

Santos, J. & Parente, F. & Indelicato, Paul & Desclaux, J. (2005). X-ray energies of circular transitions and electron screening in kaonic atoms. Physical Review A. 71.10.1103/PhysRevA.71.032501.

Measurement	Kaon mass [MeV]
DENISOV 91 [23]	493.696 ± 0.007
GALL 88 [22]	493.636 ± 0.011
LUM 81 [114]	493.640 ± 0.054
BARKOV 79 [115]	493.670 ± 0.029
CHENG 75 [116]	493.657 ± 0.020
BACKENSTOSS 73 [117]	493.691 ± 0.040
This work	493.694 ± 0.015 (stat) ± 0.060 (syst)

PRELIMINARY

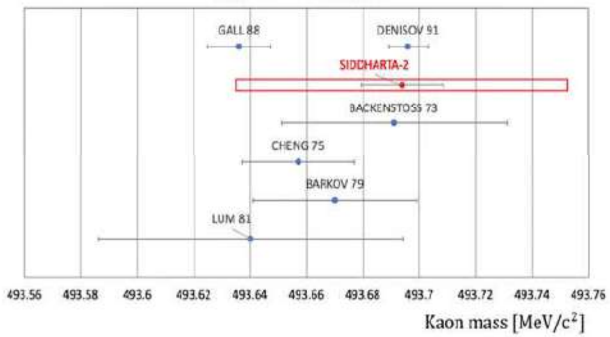

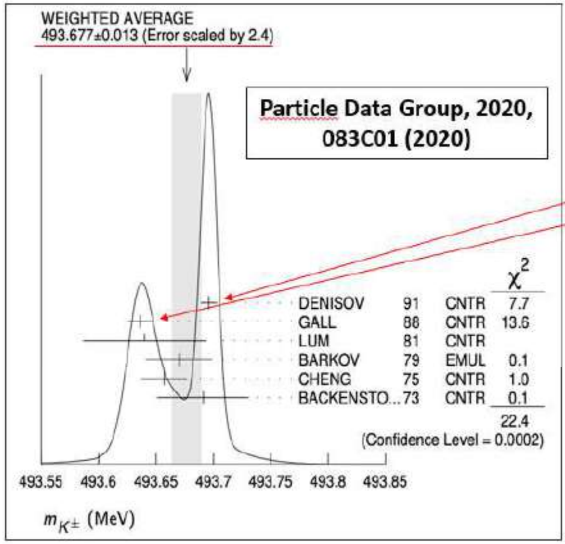

Particle Data Group, 2020, 083C01 (2020)

VALUE (MeV)	DOCUMENT ID		TECN	CHG	COMMENT
493.677±0.016 OUR FIT	Error includes scale factor of 2.8.				
493.677±0.013 OUR AVERAGE	Error includes scale factor of 2.4. See the ideogram below.				
493.696±0.007	[1] DENISOV	91	CNTR	−	Kaonic atoms
493.636±0.011	[2] GALL	88	CNTR	−	Kaonic atoms
493.640±0.054	LUM	81	CNTR	−	Kaonic atoms
493.670±0.029	BARKOV	79	EMUL	±	$e^+e^- \to K^+K^-$
493.657±0.020	[2] CHENG	75	CNTR	−	Kaonic atoms
493.691±0.040	BACKENSTO...	73	CNTR	−	Kaonic atoms

Large uncertainty → 26 p.p.m, compared to charged pion:
$m_\pi = 139.57061 \pm 0.00023$ MeV, 1.6 p.p.m

The first kaonic deuterium measurement (2023-2024)

The SIDDHARTA-2 collaboration aims **to perform the first measurement of the strong interaction induced energy shift and width of the kaonic deuterium ground state with similar precision as K-p !**

- **First run** with SIDDHARTA-2 optimized setup for **200 pb^{-1}** integrated luminosity: May – July 2023
- **Second run** - October – December 2023: **345 pb^{-1}** **Fourth run** - May - July 2024: **200 pb^{-1}**
- **Third run** 2024 - February – April 2024: **435 pb^{-1}**

Total integrated luminosity of 1200 pb^{-1}

Kaonic deuterium Run1 — May – July 2023

Kaonic deuterium Run2 — October – December 2023

Kaonic deuterium Run3 — February – April 2024

Run1 data analysis and preliminary results

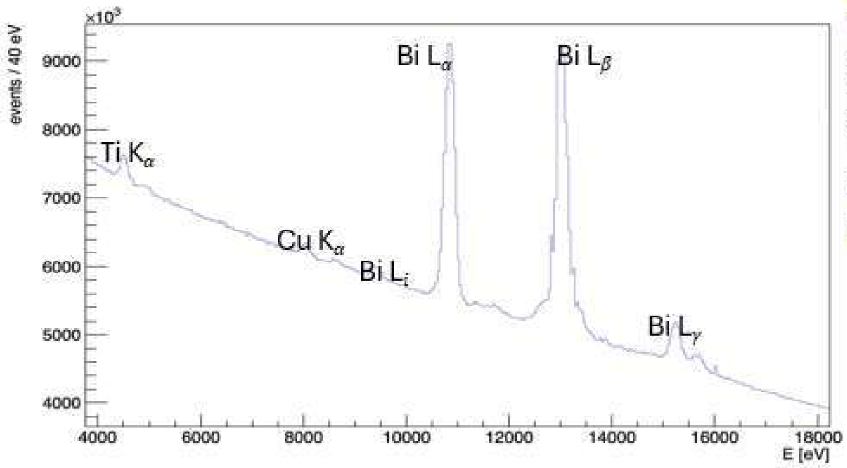

-Asynchronous background: the EM shower produced in the accelerator pipe invested by e-/e+ lost from the beam overlaps the signal; the loss rate in the interaction region reaches few MHz. The main contribution comes from Touschek effect. → Kaon Trigger and SDDs drift time

-Synchronous background, hadronic background from kaon absorption on materials nuclei, or other Φ decay channels and from X-rays produced in higher transitions of other kaonic atoms, formed in the setup materials;
→ Veto systems

Kaonic atoms measurements at DAFNE perspectives

Present status: old and very old measurements with low precision

We propose to do precision measurements along the periodic table at DAFNE for:

- Selected light kaonic atoms
- Selected intermediate mass kaonic atoms
- Selected heavy kaonic atoms

charting the periodic table

E. Friedman et al. / Nuclear Physics A579 (1994) 518–538 521

Table 1
Compilation of K^- atomic data

Nucleus	Transition	ϵ (keV)	Γ (keV)	Y	Γ_u (eV)	Ref.
He	$3\to2$	-0.04 ± 0.03	–	–	–	[15]
		-0.035 ± 0.012	0.03 ± 0.03	–	–	[16]
Li	$3\to2$	0.002 ± 0.026	0.055 ± 0.029	0.95 ± 0.30	–	[17]
Be	$3\to2$	-0.079 ± 0.021	0.172 ± 0.58	0.25 ± 0.09	0.04 ± 0.02	[17]
^{10}B	$3\to2$	-0.208 ± 0.035	0.810 ± 0.100	–	–	[18]
^{11}B	$3\to2$	-0.167 ± 0.035	0.700 ± 0.080	–	–	[18]
C	$3\to2$	-0.590 ± 0.080	1.730 ± 0.150	0.07 ± 0.013	0.99 ± 0.20	[18]
O	$4\to3$	-0.025 ± 0.018	0.017 ± 0.014	–	–	[19]
Mg	$4\to3$	-0.027 ± 0.015	0.214 ± 0.015	0.78 ± 0.06	0.08 ± 0.03	[19]
Al	$4\to3$	-0.130 ± 0.050	0.490 ± 0.160	–	–	[20]
		-0.076 ± 0.014	0.442 ± 0.022	0.55 ± 0.03	0.30 ± 0.04	[19]
Si	$4\to3$	-0.240 ± 0.050	0.810 ± 0.120	–	–	[20]
		-0.130 ± 0.015	0.800 ± 0.033	0.49 ± 0.03	0.53 ± 0.06	[19]
P	$4\to3$	-0.330 ± 0.08	1.440 ± 0.120	0.26 ± 0.03	1.89 ± 0.30	[18]
S	$4\to3$	-0.550 ± 0.06	2.330 ± 0.200	0.22 ± 0.02	3.10 ± 0.36	[18]
		-0.43 ± 0.12	2.310 ± 0.170	–	–	[21]
		-0.462 ± 0.054	1.96 ± 0.17	0.23 ± 0.03	2.9 ± 0.5	[19]
Cl	$4\to3$	-0.770 ± 0.40	3.80 ± 1.0	0.16 ± 0.04	5.8 ± 1.7	[18]
		-0.94 ± 0.40	3.92 ± 0.99	–	–	[22]
		-1.08 ± 0.22	2.79 ± 0.25	–	–	[21]
Co	$5\to4$	-0.099 ± 0.106	0.64 ± 0.25	–	–	[19]
Ni	$5\to4$	-0.180 ± 0.070	0.59 ± 0.21	0.30 ± 0.08	5.9 ± 2.3	[20]
		-0.246 ± 0.052	1.23 ± 0.14	–	–	[19]
Cu	$5\to4$	-0.240 ± 0.220	1.650 ± 0.72	0.29 ± 0.11	7.0 ± 3.8	[20]
		-0.377 ± 0.048	1.35 ± 0.17	0.36 ± 0.05	5.1 ± 1.1	[19]
Ag	$6\to5$	-0.18 ± 0.12	1.54 ± 0.58	0.51 ± 0.16	7.3 ± 4.7	[19]
Cd	$6\to5$	-0.40 ± 0.10	2.01 ± 0.44	0.57 ± 0.11	6.2 ± 2.8	[19]
In	$6\to5$	-0.53 ± 0.15	2.38 ± 0.57	0.44 ± 0.08	11.4 ± 3.7	[19]
Sn	$6\to5$	-0.41 ± 0.18	3.18 ± 0.64	0.39 ± 0.07	15.1 ± 4.4	[19]
Ho	$7\to6$	-0.30 ± 0.13	2.14 ± 0.31	–	–	[23]
Yb	$7\to6$	-0.12 ± 0.10	2.39 ± 0.30	–	–	[23]
Ta	$7\to6$	-0.27 ± 0.50	3.76 ± 1.15	–	–	[23]
Pb	$8\to7$	–	0.37 ± 0.15	0.79 ± 0.08	4.1 ± 2.0	[24]
		-0.020 ± 0.012	–	–	–	[25]
U	$8\to7$	-0.26 ± 0.4	1.50 ± 0.75	0.35 ± 0.12	45 ± 24	[24]

SDDs (4-15 keV) - Light Kaonic Atoms

HPGe
(0,1-1 MeV)
Heavy Kaonic Atoms

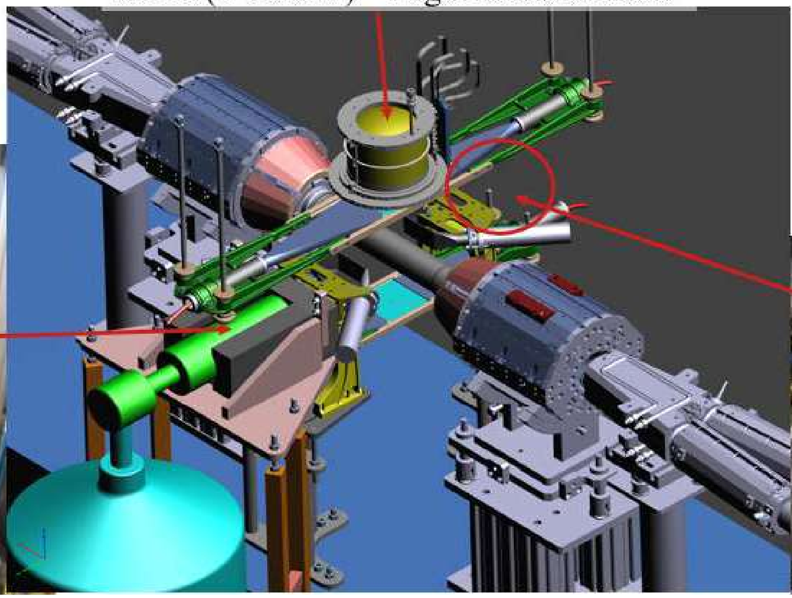

CdZnTe
(30-300 keV)
Intermediate Kaonic Atoms

Two modules (8 CdZnTe) installed

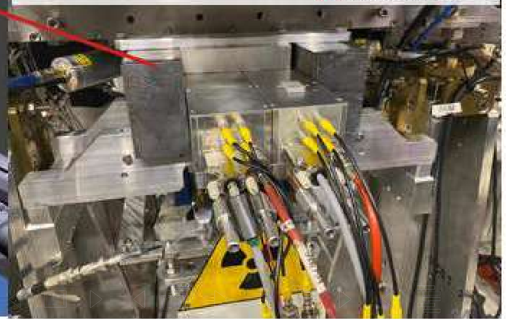

Kaonic atoms measurements at DAFNE perspectives

Present status: old and very old measurements with low precision

We propose to do precision measurements along the periodic table at DAFNE for:

- Selected light kaonic atoms
- Selected intermediate mass kaonic atoms
- Selected heavy kaonic atoms

charting the periodic table

E. Friedman et al. / Nuclear Physics A579 (1994) 518–538 521

Table 1
Compilation of K^- atomic data

Nucleus	Transition	ϵ (keV)	Γ (keV)	Y	Γ_u (eV)	Ref.
He	3 → 2	−0.04 ± 0.03	–	–	–	[15]
		−0.035 ± 0.012	0.03 ± 0.03	–	–	[16]
Li	3 → 2	0.002 ± 0.026	0.055 ± 0.029	0.95 ± 0.30	–	[17]
Be	3 → 2	−0.079 ± 0.021	0.172 ± 0.58	0.25 ± 0.09	0.04 ± 0.02	[17]
^{10}B	3 → 2	−0.208 ± 0.035	0.810 ± 0.100	–	–	[18]
^{11}B	3 → 2	−0.167 ± 0.035	0.700 ± 0.080	–	–	[18]
C	3 → 2	−0.590 ± 0.080	1.730 ± 0.150	0.07 ± 0.013	0.99 ± 0.20	[18]
O	4 → 3	−0.025 ± 0.018	0.017 ± 0.014	–	–	[19]
Mg	4 → 3	−0.027 ± 0.015	0.214 ± 0.015	0.78 ± 0.06	0.08 ± 0.03	[19]
Al	4 → 3	−0.130 ± 0.050	0.490 ± 0.160	–	–	[20]
		−0.076 ± 0.014	0.442 ± 0.022	0.55 ± 0.03	0.30 ± 0.04	[19]
Si	4 → 3	−0.240 ± 0.050	0.810 ± 0.120	–	–	[20]
		−0.130 ± 0.015	0.800 ± 0.033	0.49 ± 0.03	0.53 ± 0.06	[19]
P	4 → 3	−0.330 ± 0.08	1.440 ± 0.120	0.26 ± 0.03	1.89 ± 0.30	[18]
S	4 → 3	−0.550 ± 0.06	2.330 ± 0.200	0.22 ± 0.02	3.10 ± 0.36	[18]
		−0.43 ± 0.12	2.310 ± 0.170	–	–	[21]
		−0.462 ± 0.054	1.96 ± 0.17	0.23 ± 0.03	2.9 ± 0.5	[19]
Cl	4 → 3	−0.770 ± 0.40	3.80 ± 1.0	0.16 ± 0.04	5.8 ± 1.7	[18]
		−0.94 ± 0.40	3.92 ± 0.99	–	–	[22]
		−1.08 ± 0.22	2.79 ± 0.25	–	–	[21]
Co	5 → 4	−0.099 ± 0.106	0.64 ± 0.25	–	–	[19]
Ni	5 → 4	−0.180 ± 0.070	0.59 ± 0.21	0.30 ± 0.08	5.9 ± 2.3	[20]
		−0.246 ± 0.052	1.23 ± 0.14	–	–	[19]
Cu	5 → 4	−0.240 ± 0.220	1.650 ± 0.72	0.29 ± 0.11	7.0 ± 3.8	[20]
		−0.377 ± 0.048	1.35 ± 0.17	0.36 ± 0.05	5.1 ± 1.1	[19]
Ag	6 → 5	−0.18 ± 0.12	1.54 ± 0.58	0.51 ± 0.16	7.3 ± 4.7	[19]
Cd	6 → 5	−0.40 ± 0.10	2.01 ± 0.44	0.57 ± 0.11	6.2 ± 2.8	[19]
In	6 → 5	−0.53 ± 0.15	2.38 ± 0.57	0.44 ± 0.08	11.4 ± 3.7	[19]
Sn	6 → 5	−0.41 ± 0.18	3.18 ± 0.64	0.39 ± 0.07	15.1 ± 4.4	[19]
Ho	7 → 6	−0.30 ± 0.13	2.14 ± 0.31	–	–	[23]
Yb	7 → 6	−0.12 ± 0.10	2.39 ± 0.30	–	–	[23]
Ta	7 → 6	−0.27 ± 0.50	3.76 ± 1.15	–	–	[23]
Pb	8 → 7	–	0.37 ± 0.15	0.79 ± 0.08	4.1 ± 2.0	[24]
		−0.020 ± 0.012	–	–	–	[25]
U	8 → 7	−0.26 ± 0.4	1.50 ± 0.75	0.35 ± 0.12	45 ± 24	[24]

Nucl. Instrum. Meth. A 1069 (2024) 169966

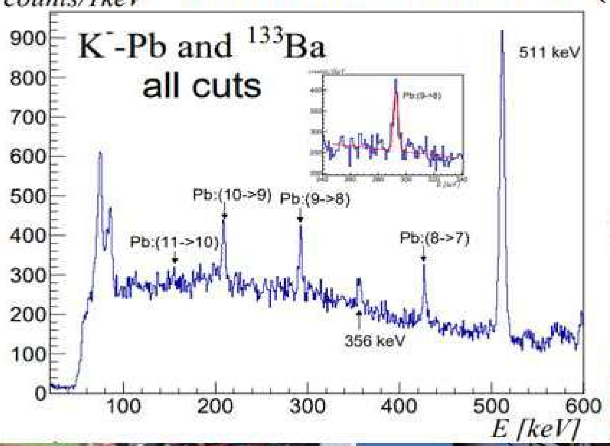

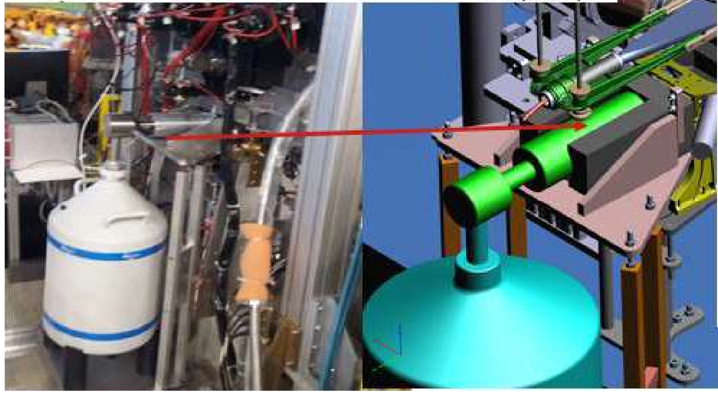

~ 60 pb^{-1} of data with a 2,2 mm Al target

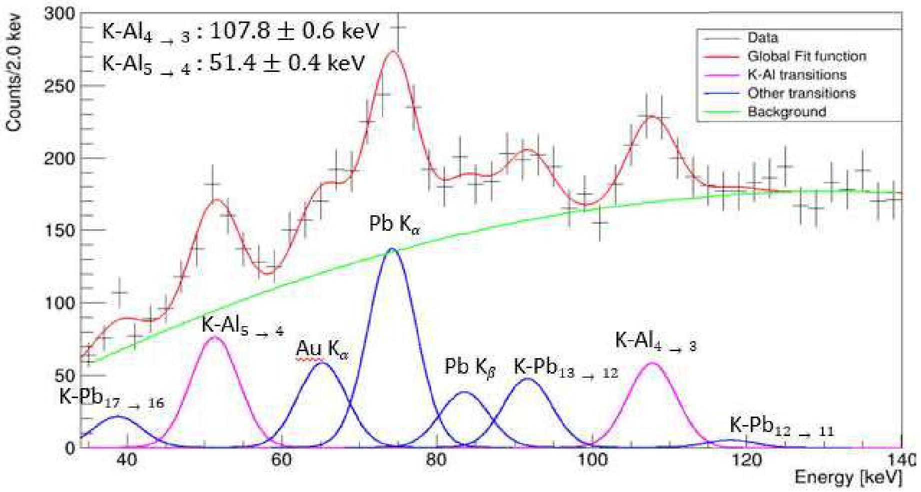

Summary and Conclusions

- study of exotic systems in the form of mesic nuclei and kaonic atoms is extremely important for a deeper understanding of elementary meson-nucleon interactions at low energies
- Investigations of exotic bound states: η-mesic helium search using the ramped beam technique at WASA-at-COSY and kaonic atoms measurements with SIDDHARTA-2.
- The upper limits for η-mesic helium production in pd/dd collisions and decays into different channels obtained **few - order of 20 nb**!
- Kaonic He, Ne, deuterium measurements in SIDDHARTA-2 experiment: new data for kaonic atoms transition database, **first result for kaonic deuterium 1s level shift and width**

Thank you for attention